IGS

SESSION 5

ORBIT DETERMINATION

Results of CODE as an Analysis Center of the IGEX-98 Campaign

Daniel Ineichen, Markus Rothacher, Tim Springer, and Gerhard Beutler
Astronomical Institute, University of Berne,
Sidlerstrasse 5, CH-3012 Berne, Switzerland

Abstract

On October 19, 1998, at the beginning of the International GLONASS Experiment (IGEX-98), the Center for Orbit Determination in Europe (CODE) has started to compute precise orbits for all active GLONASS satellites. The campaign was initially scheduled for three months, but the activities still continue in September, 1999. One of the main reasons for this extension was the launch of three new GLONASS satellites at the end of the year 1998.

The processing of the IGEX network is done on a routine basis at CODE and precise ephemerides are made available through the global IGEX Data Centers. The improved GLONASS orbits are referred to the International Terrestrial Reference System (ITRF96) and to GPS system time. They are therefore fully compatible with GPS orbits and allow a combined processing of both satellite systems.

All GLONASS satellites are equipped with a laser reflector array and the SLR ground network is tracking most of the GLONASS satellites. Comparisons of the GLONASS orbits computed by CODE with the SLR measurements show that the orbit accuracy is of the order of 20 cm.

Introduction

The main purpose of the IGEX-98 campaign was to conduct the first global GLONASS observation campaign for geodetic and geodynamic applications. Since the beginning of the campaign CODE participated as an Analysis Center. The main reasons for CODE's participation in the IGEX-98 campaign - in accordance with the objectives formulated by the Steering Committee (Willis et al., 1998) - are

- to enhance and test the GLONASS processing capabilities of the Bernese GPS Software,
- to determine GLONASS orbits with an accuracy of 1 meter or below, realized in a well defined Earth-fixed reference frame,
- to determine transformation parameters between the GLONASS reference frame (PZ-90) and the GPS reference frame (WGS84/ITRF96),
- to investigate the system time difference between GLONASS and GPS, and
- to collaborate with the SLR community to evaluate the accuracy of the computed GLONASS orbits.

Figure 1. IGEX observation network as used by the CODE Analysis Center.

A map of the IGEX-98 network as used by CODE for orbit determination processing may be found in Figure 1. Only the sites providing dual-frequency GLONASS data are shown on the map (and only those sites were used for the processing). Most of the sites are located in Europe. The connection to the receivers located in other parts of the World is quite weak (using observations on the double-difference level). The map shows all sites used during the campaign (about 35 sites). For some weeks, however, the number of available sites decreased to 20.

The measurement data of these sites are collected and made available at five Regional and two Global Data Centers (Noll, 1998). As of today, six Analysis Centers were or are making use of the data for computing improved GLONASS orbits and delivering their products to the CDDIS Global Data Center (CDDIS, 1999).

Determination of Precise GLONASS Orbits

Processing Strategies

For the combined processing of GLONASS and GPS data the enhanced Version 4.1 of the Bernese GPS Software is used; see Rothacher and Mervart (1996), Habrich (1999). The analysis is done by fixing both, the GPS orbits and Earth rotation parameters to CODE's final IGS solutions. The orbital parameters for the GLONASS satellites are estimated using double difference phase observations (including double differences

between GLONASS and GPS satellites). The processing of the IGEX network is done without fixing the ambiguities to their integer values.

Six initial conditions and nine radiation pressure parameters are determined for each satellite and arc (Springer, 1999). Pseudo-stochastic pulses have been set up every 12 hours for test purposes, but have been constrained to zero for the official CODE solution. Only receivers providing dual-frequency GPS and GLONASS data or dual-frequency GLONASS data are included in the processing procedure. The final precise orbits stem from the middle day of a 5-day arc. The satellite clock values included in the precise orbit files are broadcast clock values for the GLONASS satellites, because no satellite clock estimation is performed so far. In order to align the IGEX network to the terrestrial reference frame the coordinates of seven sites (Brisbane (Australia), Greenbelt (USA), Kiruna (Sweden), Metsahovi (Finland), Onsala (Sweden), Yaragadee (Australia), and Zimmerwald (Switzerland)), are constrained to their ITRF96 coordinates.

Quality Assessment

Long-Arc Fits

In order to check the internal consistency of our precise GLONASS orbits, we perform a long-arc fit for each processed week. For each satellite, one orbital arc is fitted through the seven consecutive daily solutions of the week. As an example, the result of such a long-arc fit is given in Table 1 for GPS week 1002. The table shows the rms of this fit for each satellite and day. In the last line ("Week") the rms of the entire 7-day fit is included for each satellite.

Table 1. Orbit Repeatability from a 7-Day Fit through Daily Orbit Solutions Days 80-86, 1999, RMS Values (cm)

Slot No.	1	3	4	6	7	8	9	10	11	13	16	17	20	22
DOY 80	5	6	10	11	8	8	7	18	11	8	15	8	10	8
DOY 81	5	4	5	6	7	7	7	9	6	7	9	5	5	6
DOY 82	6	5	3	8	5	6	7	9	9	8	7	7	8	6
DOY 83	5	3	6	7	6	6	4	6	7	11	10	5	5	6
DOY 84	6	6	5	6	5	6	6	6	12	9	7	5	6	4
DOY 85	6	4	6	6	6	4	7	9	7	7	5	4	4	5
DOY 86	6	4	5	9	6	5	10	18	16	11	14	7	5	6
Week	6	5	6	8	6	6	7	12	10	9	10	6	7	6

These weekly rms values of all GLONASS satellites are plotted in Figure 2 over a time period of 30 weeks. The values are in general between 5 and 20 cm. The improvement of the rms values after the first four weeks is caused by the transition from 3-day arcs to 5-

day arcs, the improvement of the processing strategies, and the increasing number of available IGEX sites. On the one hand it must be stated that these values might be too optimistic because we fit the middle days of 5-day arcs with a 7-day arc. On the other hand, the small values indicate that the adopted orbit model is well suited to describe the motion of the GLONASS satellites over a time period of several days.

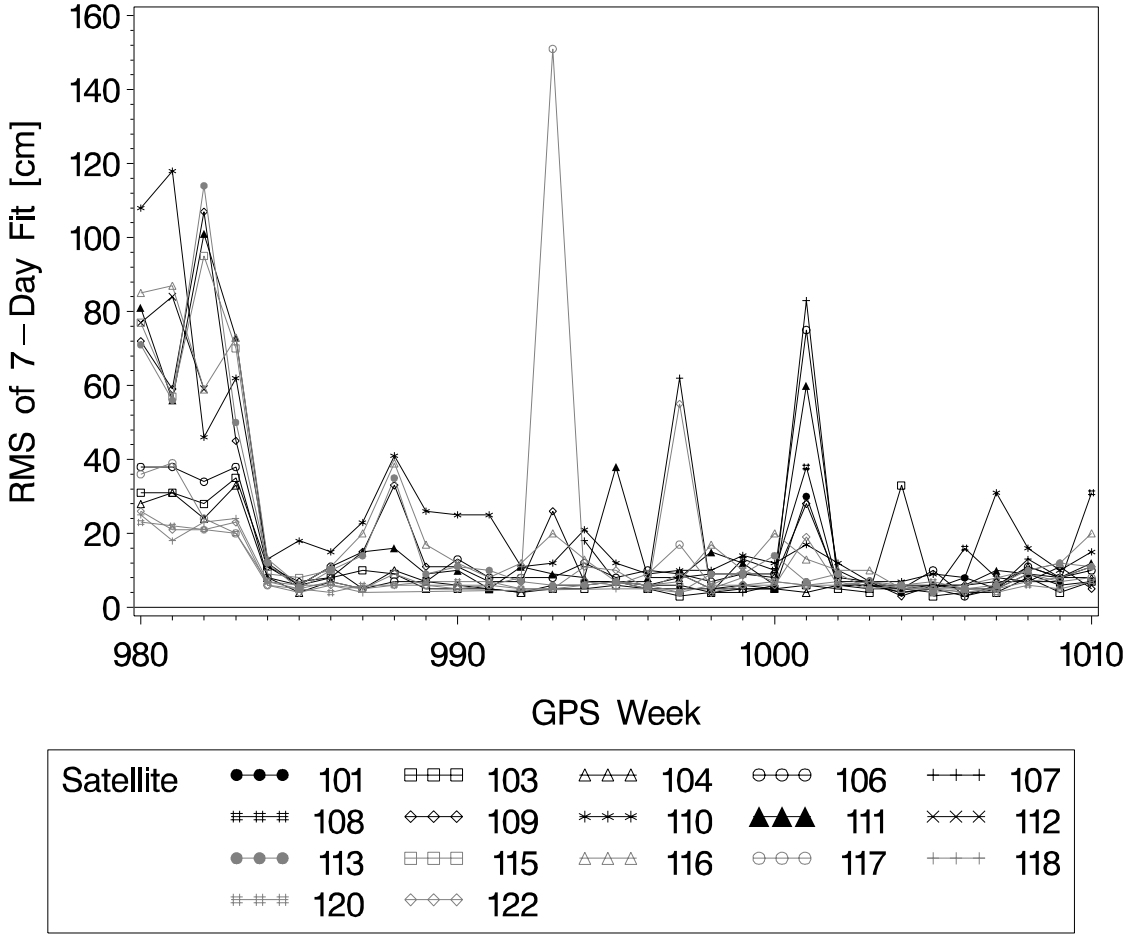

Figure 2. RMS of 7-day orbit fits for GPS Weeks 980-1010.

Comparison with the Precise Orbits of Other IGEX Analysis Centers

The IGEX Analysis Center Coordinator R. Weber (Technical University of Vienna) is in charge of comparing the precise GLONASS orbits stemming from the six IGEX-98 Analysis Centers providing precise GLONASS orbits. In addition, he combines the Analysis Centers' precise GLONASS orbits into one official IGEX orbit product. The results of this combination procedure are distributed via IGEX mail and can be found on the following Web page:

http://lareg.ensg.ign.fr/IGEX/IGEXMAIL/

At present, combined orbits of twenty weeks (0980-0999) are made available at the Global IGEX Data Center at CDDIS. The results of the first ten weeks of orbit comparison confirm that the achieved orbit quality is of the order of 20 cm.

Comparison with SLR Measurements

The comparison of CODE's precise GLONASS orbits with SLR measurements is a fully independent quality check and therefore very valuable for checking the quality of GLONASS orbits determined by means of microwave signals. This method of quality assessment also shows that the precise GLONASS orbits of CODE are on a 10-20 cm accuracy level. More details are given later in this paper.

System Time Difference Between GLONASS and GPS

When processing GLONASS and GPS data we are setting up one additional parameter for each station and session in our pseudorange pre-processing step: the difference between GLONASS and GPS system time. The estimation is done in the following way: we use broadcast orbits for both systems, estimate the site coordinates and the time offset between GPS and GLONASS once per session and, as usual, one receiver clock correction for each epoch. In order to account for the different reference systems, the GLONASS broadcast orbits are rotated around the z-axis by -330 mas (Habrich, 1999).

What kind of components are contributing to the estimated system time difference? On the one hand we have the difference between the national realizations of UTC (Universal Time Coordinated) on which the GLONASS and GPS system times are based: UTC(USNO, Washington DC) and UTC(SU, Moscow).

Values for the difference between these national time references and UTC are published in the Circular T of the Bureau International des Poids et Mesures (BIPM, 1999). In July 1999, the difference between UTC(USNO) and UTC is below 10 nanoseconds and the difference between UTC(SU) and UTC below 100 nanoseconds. On the other hand we have to take into account the differences between GPS system time and UTC(USNO) and GLONASS system time and UTC(SU).

When comparing the time offsets resulting from the IGEX network processing, it becomes clear that we do not have direct access to the pure difference between GPS and GLONASS system time, but that receiver type specific offsets have to be taken into consideration as well. Figure 3 shows the estimated system time differences for different receiver types covering a time span from September 20, 1998 to June 6, 1999 (260 days). Each line represents a different receiver type. Starting from bottom to top:

- ESA/ISN GNSS (about -900 ns)
- JPS receivers (about -50 ns)
- Ashtech Z18 receivers (about 50 ns)
- 3S Navigation receivers (about 1000 ns)
- Ashtech GG24 receiver (about 2100 ns)

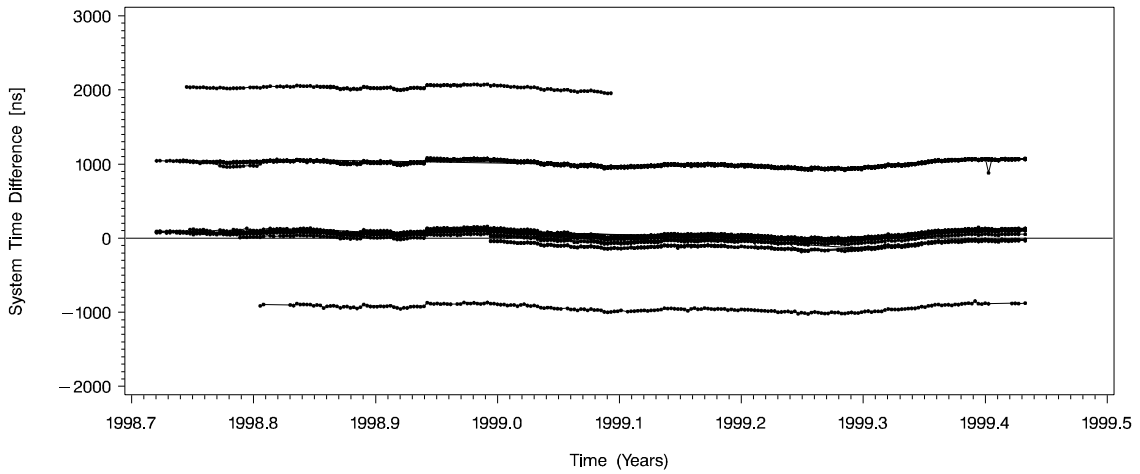

Figure 3. System time difference estimated with different receiver types.

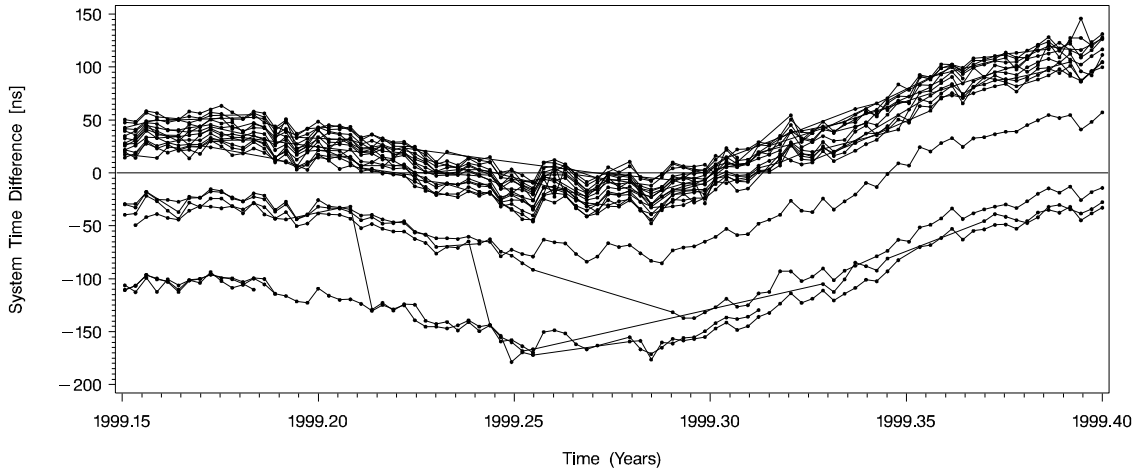

Figure 4. Detail of Figure 3: system time differences derived from Ashtech Z18 and JPS Legacy data.

The differences between different receiver types are of the order of one microsecond. Figure 4 shows a detail of Figure 3: the time differences of the Z18 and JPS receivers during a time period of three months. The lower two bands represent the JPS receivers, the upper one the Z18 receivers. The time series of the individual stations are highly correlated. It is interesting to note the jumps of three JPS receivers from the medium level to the lower level. These jumps are correlated with software upgrades. The firmware of the JPS receiver at Zimmerwald, Switzerland for example, was upgraded from Version 1.4 to Version 1.5 and the RINEX converter software from Version 1.01 to Version 1.02. At that time, the estimated system time differences show a jump of -40 ns (between doy 093 and doy 106, 1999).

Transformation Parameters Between the Two Reference Systems

In principle, there are two possibilities for the determination of transformation parameters between the GLONASS and the GPS reference system: One is based on coordinate sets which are determined in both systems, and the other is based on the comparison of satellite orbits available in both systems. Here, we present results stemming from the orbit comparison method.

Seven Helmert transformation parameters were determined using precise GLONASS orbits in the ITRF96 reference frame and the broadcast GLONASS orbits in the PZ-90 reference frame. For each day one set of parameters (three translations, three rotations, and one scale factor) was established. Figure 5 shows the time series of the rms values, the translation parameters, and the rotation parameters. Using the described method, the accuracy of the transformation parameters is limited by the quality of the GLONASS broadcast orbits. The rms of the daily Helmert transformations (between 3 m and 6 m) may be interpreted as indicators of the broadcast orbit quality.

Mean values and standard deviations for each of the seven Helmert parameters and for the entire time series are summarized in Table 2. The rotation around the z-axis definitely has to be taken into account when processing combined GLONASS and GPS data using broadcast orbits. A rotation of -350 mas around the z-axis is determined highly significant and corresponds to a satellite position offset of up to 45 m (if the satellite is close to the equatorial plane). The three translations and the rotation around the y-axis are not significantly different from zero. The influence of the x-rotation and the scale value on the GLONASS broadcast orbits is of the order of the broadcast orbit accuracy itself and may therefore be neglected.

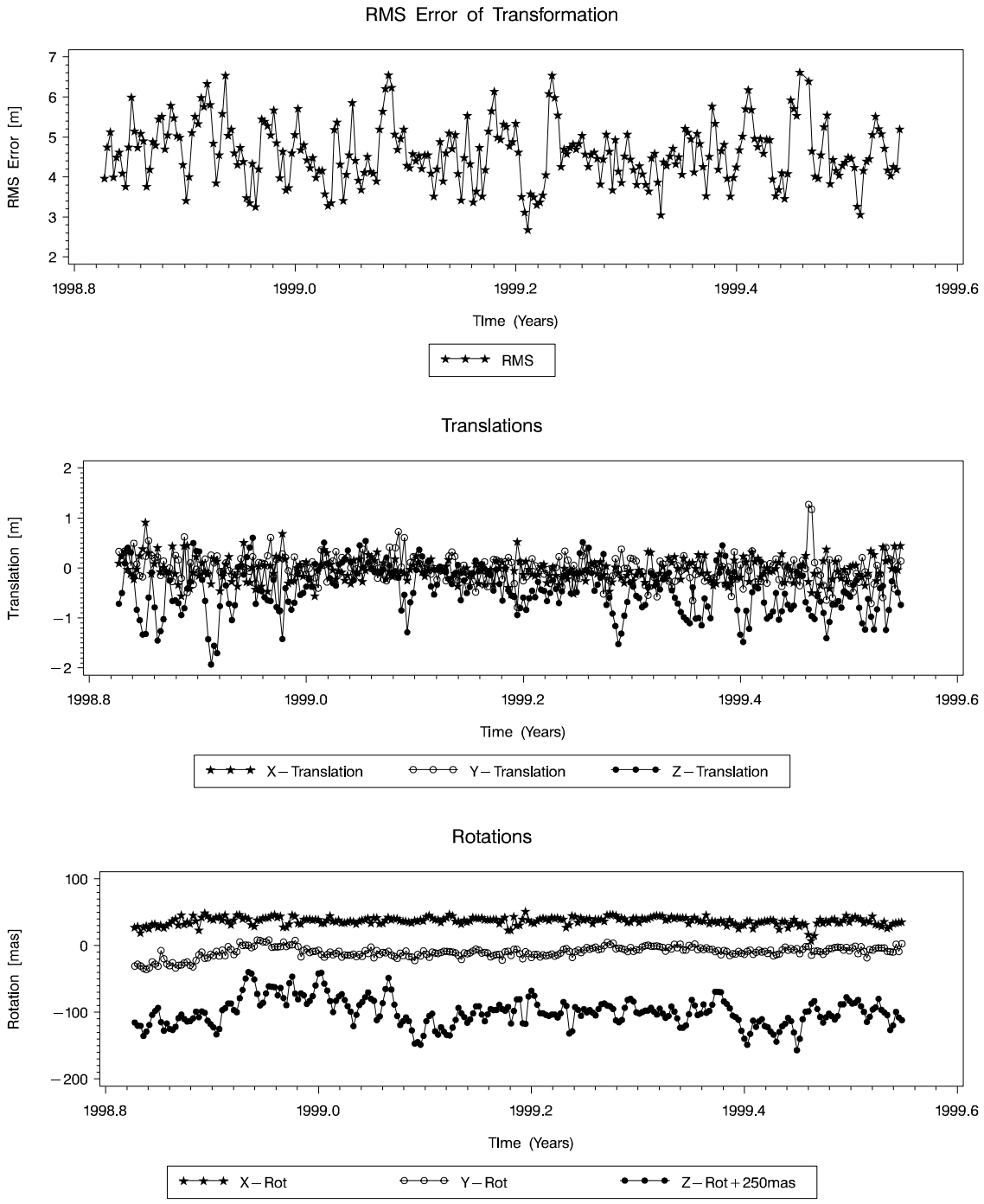

Figure 5. RMS, translation parameters, and rotation parameters of the Helmert transformation between broadcast orbits in the PZ-90 system and CODE's precise orbits in the ITRF96 system.

Table 2. Mean Values and RMS of the Daily Helmert Transformation Parameters for the Transition from PZ-90 to ITRF96

Parameter	Mean	RMS
X--Translation [m]	-0.03	0.23
Y--Translation [m]	-0.02	0.27
Z--Translation [m]	-0.45	0.47
X--Rotation [mas]	37	6
Y--Rotation [mas]	-10	8
Z--Rotation [mas]	-350	21
Scale Value [ppb]	13	3

Comparison of Precise GLONASS Orbits with SLR Measurements

All GLONASS satellites are equipped with a laser retroreflector array. It is an interesting and important aspect of the IGEX-98 campaign that the SLR community was and still is very active in observing the GLONASS satellites: measurements to nine GLONASS satellites were performed during the first six months of the IGEX-98 campaign. At present, during the extended phase of the test campaign, three GLONASS satellites are still tracked by the SLR community. The SLR measurements are completely independent of the orbit determination process based on microwave signals. Comparisons between SLR measurements and improved orbits are therefore an important measure for the achieved quality of the precise GLONASS orbit determination using the microwave observations.

For the comparison of GLONASS orbits with SLR measurements, the residuals between SLR measurements and computed distances (derived from our GLONASS precise orbits and the SLR site coordinates) are analyzed. In addition, one constant offset is estimated for all SLR distances and removed from the residuals.

Figure 6 shows the residuals of the SLR measurements with respect to the GLONASS broadcast orbits and with respect to the CODE final IGEX orbits (middle day of a 5-day arc) over a time span of 230 days (October 10, 1998 to May 29, 1999). The rms decreases from 1.67 m (broadcast orbits) to 0.16 m (precise orbits), which proves that we are not only changing the orbits, but actually improve them. An offset of 39 mm between improved orbits and SLR measurements was determined (SLR distances are shorter than the distances derived from the CODE orbits). It is interesting to note that this offset agrees well with the offset found for SLR measurements with respect to the GPS orbits (55 mm). The reason for this offset is not yet fully understood and subject of discussions between the SLR and the GPS/GLONASS community.

A comparison of SLR measurements was also done with respect to daily orbits stemming from the mid day of a 3-day arc. The smaller rms of our 5-day solution compared to the 3-day solution is the reason for submitting the mid day of a 5-day arc as CODE's official IGEX orbit product.

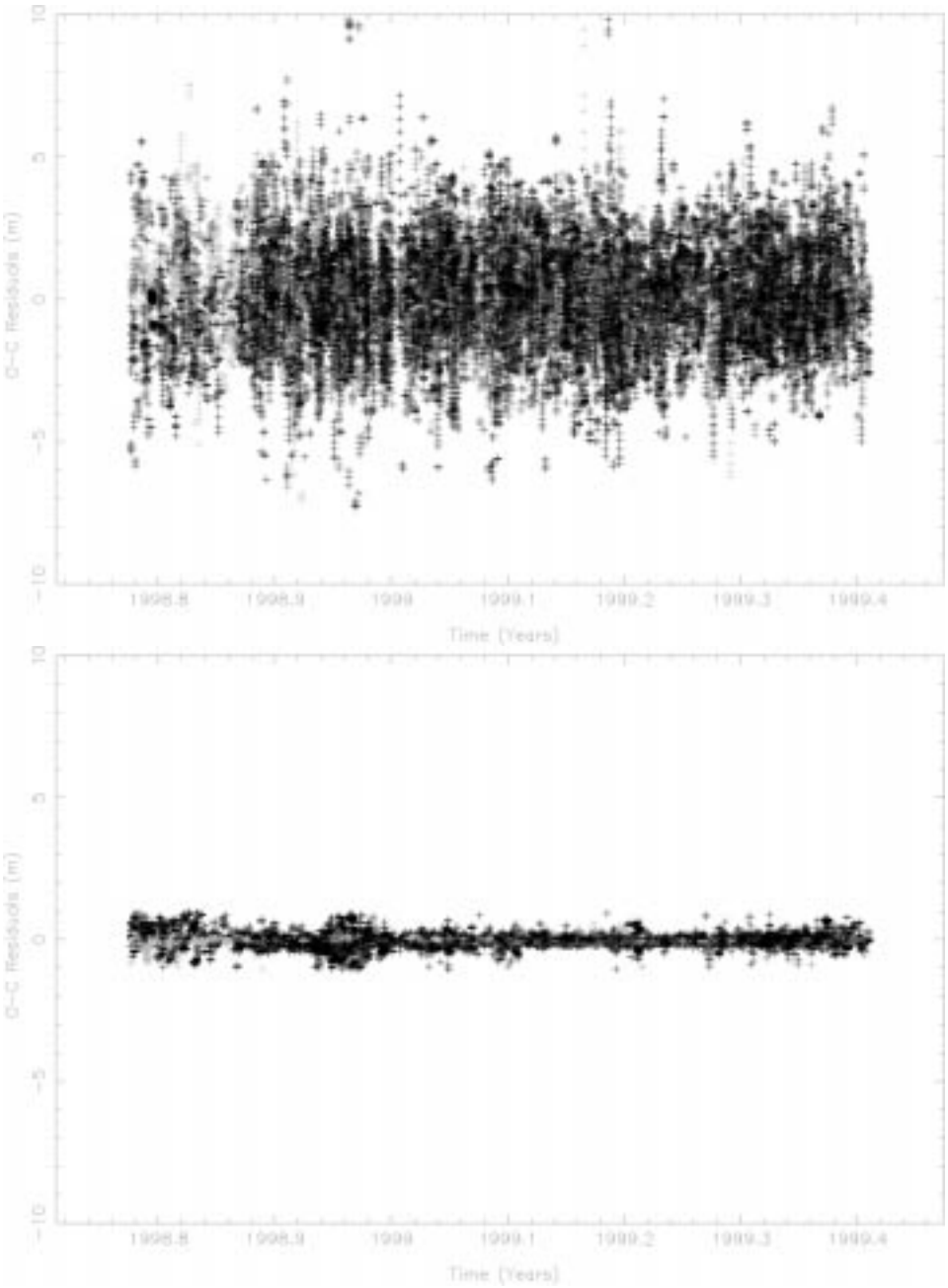

Figure 6. Comparison of broadcast GLONASS orbits (on the top) and CODE's precise orbits (on the bottom) with SLR measurements.

Outlook

CODE intends to continue with its activities in GLONASS data processing. Of course, these activities are dependent on the future of the GLONASS system itself and the continuous data availability of a globally distributed tracking network. It is an encouraging fact, however, that several institutions expressed their willingness to participate in a GLONASS pilot service, following the IGEX-98 test campaign.

On the technical side, there are several issues waiting for investigation, such as:

- Tests concerning the parameterization of GLONASS orbits (reduction of the number of estimated radiation pressure parameters, estimation of stochastic pulses).

- Processing IGEX and IGS data in one step. Study of the impact of GLONASS data on estimated global parameters like, e.g., Earth rotation parameters (different orbit inclinations of GPS and GLONASS, no 2:1 resonance of GLONASS revolution period with Earth rotation).

- Introduction of ambiguity fixing for GLONASS phase measurements within the IGEX network.

A densification of the global dual-frequency receiver network would certainly significantly contribute to the improvement of the accuracy of the estimated GLONASS orbits.

References

BIPM (1999). Bureau International des Poids et Mesures, Sevres, France; http://www.bipm.fr/enus/5_Scientific.

CDDIS (1999). Crustal Dynamics Data Information System, NASA Goddard Space Flight Center, Greenbelt, USA; http://cddisa.gsfc.nasa.gov/glonass_datasum.html.

Habrich, H. (1999). Geodetic Applications of the Global Navigation Satellite System (GLONASS). Ph. D. thesis, Astronomical Institute, University of Berne.

Noll, C. (1998). IGEX98 Data Center Information; http://lareg.ensg.ign.fr/IGEX/ix_datac.html.

Rothacher, M., L. Mervart (1996). Bernese GPS Software, Version 4.0, Printing Office of the University of Berne.

Springer, T., G. Beutler, M. Rothacher (1999). Improving the Orbit Estimates of GPS Satellites, *Journal of Geodesy*, Vol. 73, pp. 147-157.

Willis, P., G. Beutler, W. Gurtner, G. Hein, R. Neilan, J. Slater (1998). The International GLONASS Experiment IGEX-98; http://lareg.ensg.ign.fr/IGEX/goals.html.

IGEX Analysis at BKG

Heinz Habrich
Bundesamt fuer Kartographie und Geodaesie
Richard-Strauss-Allee 11, D-60598 Frankfurt, Germany

Abstract

The Bundesamt fuer Kartographie und Geodaesie (BKG) has been processing combined GPS/GLONASS observations of IGEX-98 since the beginning of the campaign in October 1998. The Bernese GPS Software is used in all processing steps. A routine processing scheme has been established in order to generate improved orbits for GLONASS satellites, receiver-specific estimates of the system time difference between GPS and GLONASS and daily estimates of the transformation parameters between PZ−90 and ITRF 96. The processing results are summarised in a report for each GPS week and submitted by "IGEX-Mail".

Introduction

In collaboration with the Astronomical Institute University of Berne (AIUB) the Bernese GPS Software was modified for combined GPS/GLONASS processing. GLONASS observations can be processed similarly to GPS data, if the differences in the reference frame, the system time and in the frequencies of the satellite signals are taken into consideration. In order to process GPS/GLONASS observations a *unique time scale* for all observations and satellite ephemerides and a *unique reference frame* for all satellite and receiver positions is required. Therefore, we transform the GLONASS satellite positions from PZ-90 as given in the broadcast navigation messages into the ITRF 96 reference frame and use the GPS time scale as reference time for the generation of the initial GLONASS satellite orbits. The GLONASS orbit files are then merged with precise GPS orbit files provided by the IGS service and referred to the ITRF 96 reference frame and the GPS time scale, too.

Because the system time difference between GPS and GLONASS is not exactly known, we solve for an additional parameter in the code single point positioning of combined GPS/GLONASS observations. This parameter could be meaningfully determined. However, we found biases between the estimates of different receiver types.

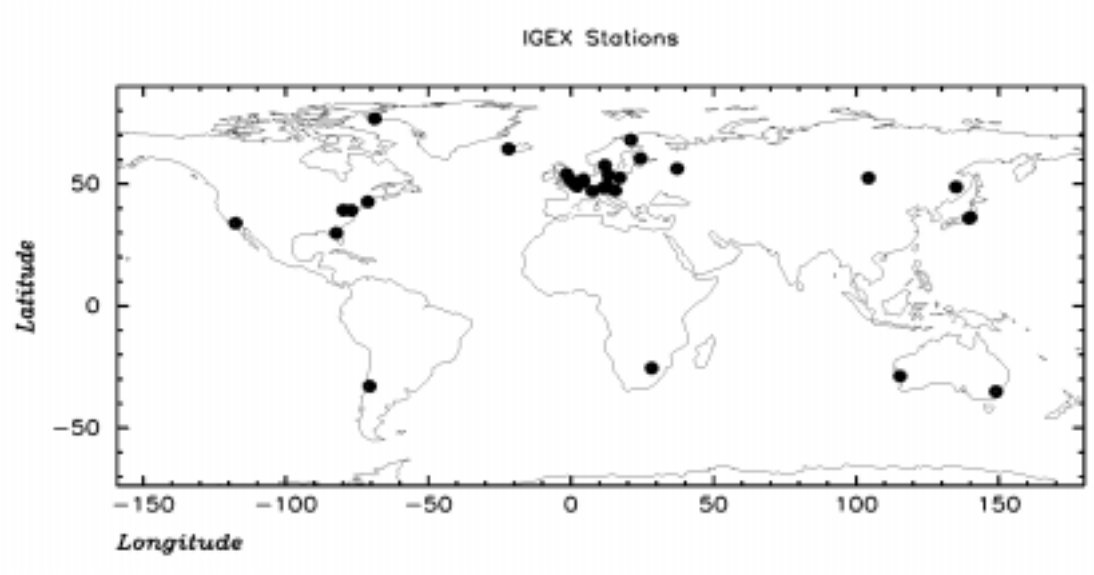

Figure 1. IGEX stations with dual-frequency receivers processed at BKG in December 1998.

The satellite-specific frequencies of GLONASS satellite signals have to be considered in the phase processing. In our processing a baseline by baseline pre-processing of the phase observations determines the relative receiver clock errors of the two receivers for each epoch. After the correction of those determined receiver clock errors to the single difference (between stations) observations, the cycle slips of the corresponding wavelength of the satellite could be detected and corrected on the single difference level. A new ambiguity parameter is set up, if a cycle slip cannot be corrected.

In order to compute improved orbit parameters for GLONASS satellites we process the double difference phase observations of GPS and GLONASS satellites. This leads to double differences between GPS and GLONASS satellites, too. For selected stations the corresponding ITRF 96 coordinates are tightly constrained. Because the coordinates of the reference stations as well as the GPS satellite positions are “fixed” to their ITRF 96 values, the improved positions of the GLONASS satellites refer to ITRF 96, too. A Helmert transformation between the GLONASS broadcast orbits given in PZ-90 and the improved GLONASS satellite orbits provide a set of transformation parameters between PZ-90 and ITRF 96 which is calculated for every day.

Processing Scheme

Observations of *dual-frequency combined GPS/GLONASS* receivers have been used in the processing, only. A map of the 28 IGEX observation stations which were included in the processing at BKG in December 1998 is given in Figure 1. The processing scheme is given in Figure 2. For the GPS satellites the final precise orbits as provided by the IGS are used. No attempt is made to improve the orbits of the GPS satellites. The GPS orbit files are merged with broadcast GLONASS orbits to a common GLONASS/GPS orbit

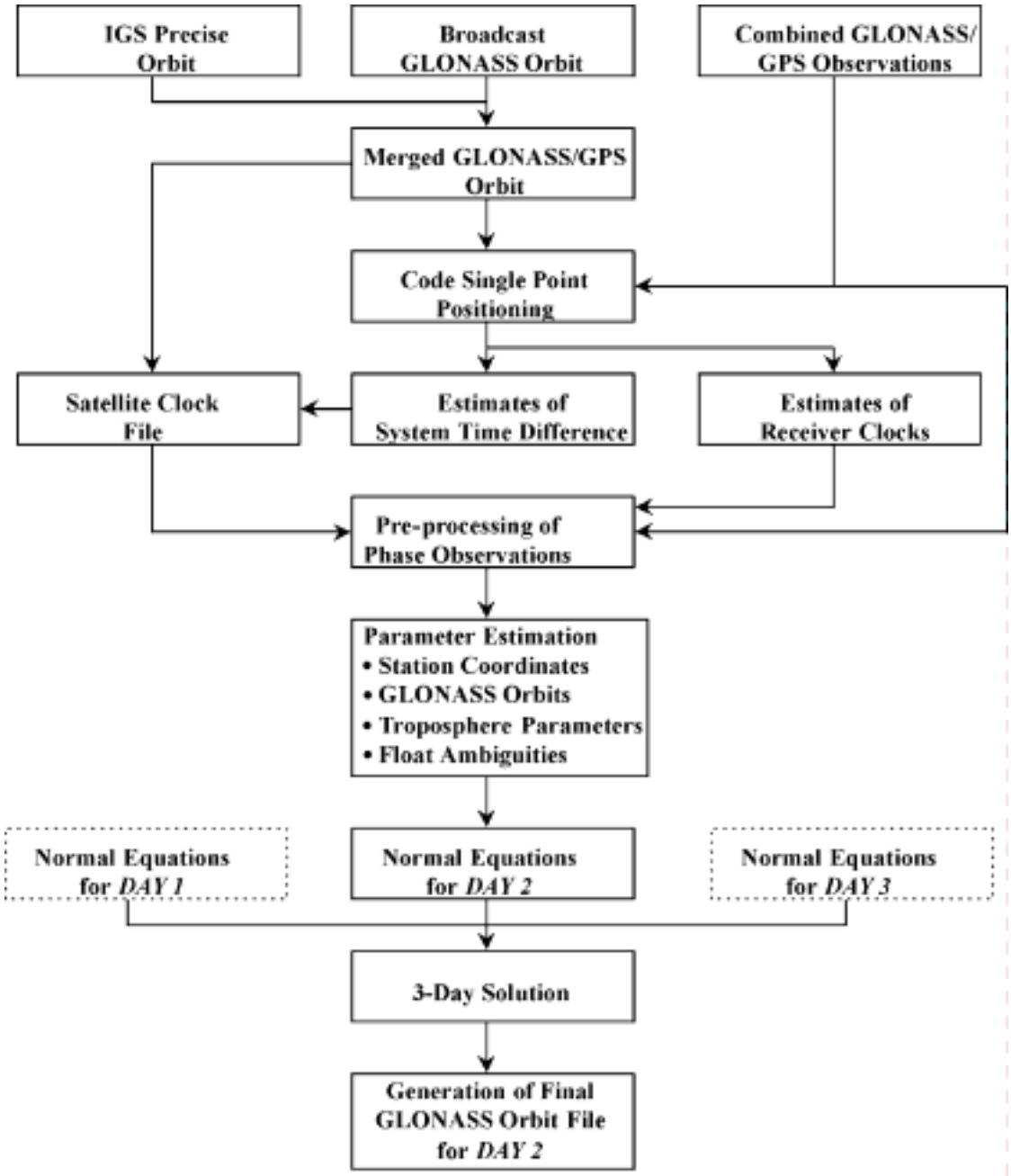

Figure 2. Processing scheme for the computation of improved GLONASS orbits.

file in the ITRF 96 reference system and referred to the GPS system time scale. A code single point positioning is performed for each station solving for station coordinates and receiver clock corrections. If both, GLONASS and GPS observations are available for a station also the system time difference is estimated.

The estimates of the system time difference are introduced into the phase observations by applying one common system time correction (the average from all stations) to all GLONASS satellite clock offsets. It has to be mentioned that the average value cannot be

Table 1. Orbit Repeatability of Improved GLONASS Orbits for GPS Week 981, Daily Solutions Compared to 7-Day Arc

Day of	GLONASS Satellite Numbers													Units: cm
Year	103	104	106	109	110	111	112	113	115	116	117	118	120	122
298	13	22	25	14	67	16	17	17	19	25	48	15	11	11
299	22	16	23	11	43	8	37	13	17	52	27	10	7	6
300	28	32	16	23	41	12	34	16	10	35	39	21	6	16
301	26	32	18	17	59	9	49	24	13	36	37	14	11	12
302	14	29	29	14	50	29	12	14	9	28	29	18	12	7
303	7	10	45	9	66	26	60	17	8	17	43	8	20	9
302	11	16	26	8	86	19	46	12	22	48	14	11	11	8
ALL	19	24	27	15	61	19	40	17	15	36	35	14	12	10

in accordance with the correct system time difference, as long as different receiver types lead to different estimates of the system time difference.

A first orbit improvement for the GLONASS satellites is calculated after performing the phase pre-processing and the results are stored into normal equations. Six initial conditions and nine radiation pressure parameters per satellite are determined. Finally, the normal equations of three days are combined in order to generate a 3-day arc for each GLONASS satellite. The middle day of each arc is saved into the resulting orbit file.

Results of Orbit Improvement

To monitor the precision of the orbits obtained, a 7-day arc for each GLONASS satellite is fitted through the satellite positions of seven individual days (one GPS week). The RMS error of the differences between the daily orbits and the 7-day arc are used to indicate the quality of the improved GLONASS orbits. Table 1 shows these RMS errors for GPS week 0981. An overall precision of 20 to 30 cm for the satellite positions was found. This is much better than the RMS error of the broadcast ephemerides which is given in (ICD, 1995) to be of the order of 20 m, 10 m and 5 m for the along track, cross track and radial direction, respectively.

System Time Difference Between GPS and GLONASS

For each IGEX station processed the system time difference between GLONASS and GPS is estimated in the code single point positioning, provided observations from both systems are available. Figure 3 shows the estimates of the system time difference for 20 IGEX stations. Nearly identical estimates were found for identical receiver types. However, discrepancies of up to 2 μsec occur between different receiver types. For all Ashtech Z-18 receivers the system time difference was determined to be approximately 50 $n$sec. The 3S Navigation receivers show values of about 1 μsec with the exception of one receiver of this type, located in Wettzell, Germany. The estimates for Wettzell were determined to about -700 $n$sec. It has to be mentioned, that this receiver was one of the first produced by the manufacturer and may include different hardware components. One JPS receiver was included in the processing and shows less stable estimates of the system time difference compared to other receivers. The estimates of the ESA/ISN receiver in Leeds, UK, amount to approximately -900 $n$sec.

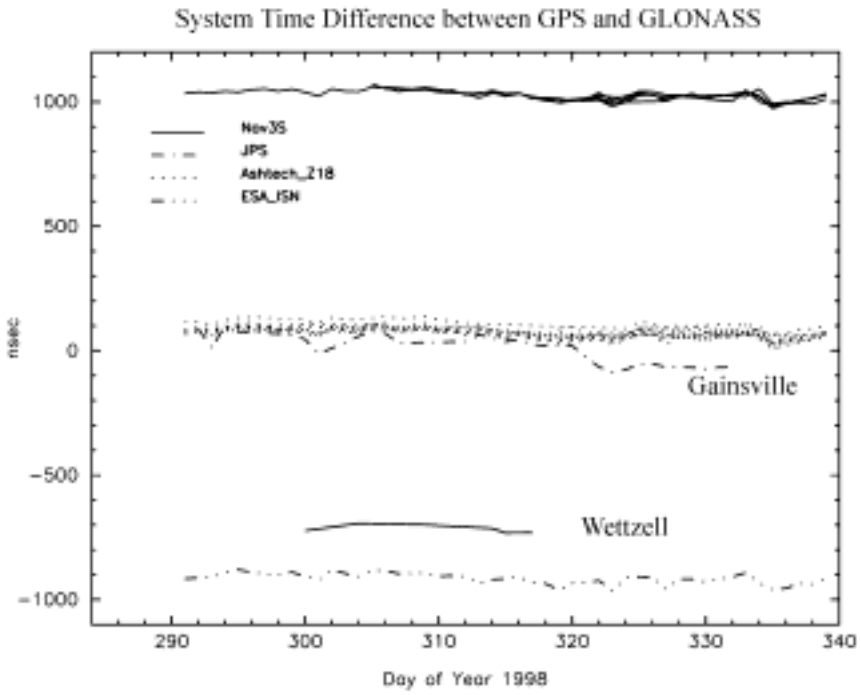

Figure 3. Results of code single point positioning.

GLONASS/GPS Receiver Biases for Ashtech Z-18 Receivers

In order to look at the estimates of the GLONASS/GPS system time difference of Ashtech Z-18 receivers in more detail, these estimates of Figure 3 are printed in Figure 4 separately. Almost identical day to day variations of all Ashtech Z-18 receivers involved can be seen in Figure 4. However, biases of up to 50 *nsec* between the receiver specific curves show up. We may use the difference between two curves of the corresponding receivers to compute a receiver-dependent part of the system time difference of the specified receiver pair (called "differential receiver bias"). A more efficient computation of the differential receiver biases may be performed, if we compute mean day to day changes of the GLONASS/GPS system time differences and correct the receiver-dependent estimates for those changes. The mean day to day changes could be computed in two steps. In the first step the difference of the receiver-specific system time difference estimates between two successive observation days is computed. The mean values of those differences of all receivers involved may be computed in the second step.

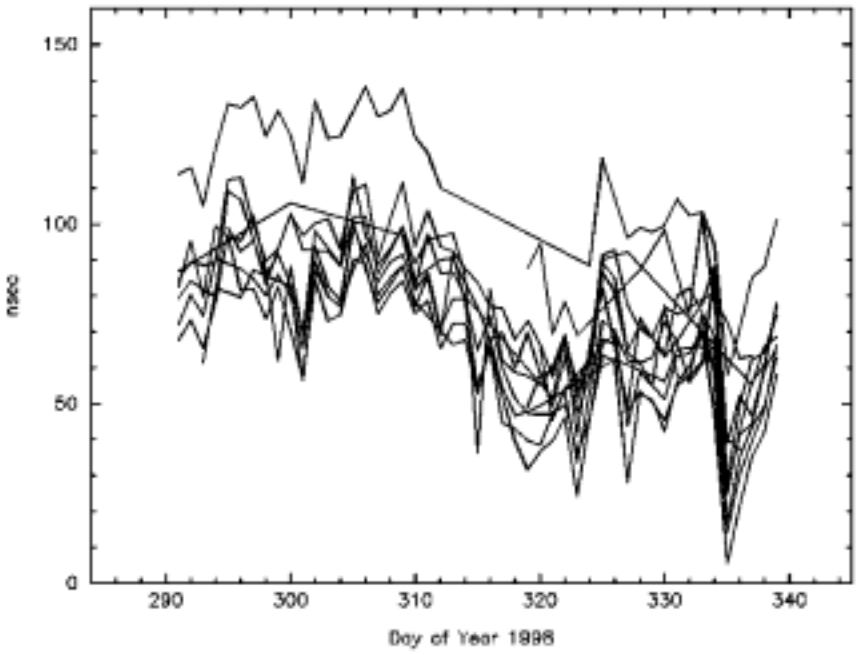

Figure 4. Ashtech Z-18 GLONASS/GPS system time difference.

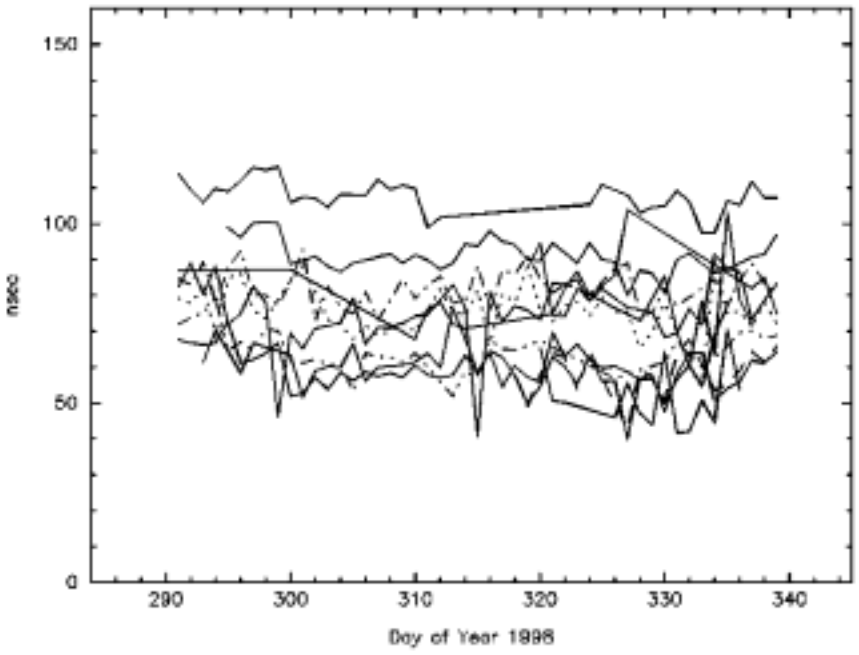

Figure 5. Ashtech Z-18 GLONASS/GPS system time difference, mean changes removed.

Figure 6. Ashtech Z-18 GLONASS/GPS receiver biases.

Table 2. Mean Values of Corrected System Time Differences

Ashtech Z-18	3S-Navigation		
Station Name	**GLONASS/GPS Receiver Bias [nsec]**	**Station Name**	**GLONASS/GPS Receiver Bias [nsec]**
REYZ	107.60	BORG	1033.64
GODZ	75.86	CSIR	1049.92
GRAB	58.40	3SNA (IRVI)	1064.23
IRKZ	82.25	NPLC	1006.61
KHAB	75.24	SANG	998.78
MTKA	80.34		
OS0G	91.06		
SL1X	61.35		
YARR	78.35		
ZIMZ	58.96		

Thus computed mean changes of the system time difference for the Ashtech Z-18 receivers of Figure 4 are printed in Figure 6 (lowest curve in each picture).

The receiver-specific estimates of the system time difference after the correction of their mean changes are given in Figure 5. Systematic effects between the curves of the different receivers are no longer present in Figure 5. Some outliers show up, for example, days 299 and 314, but the corresponding estimates of the system time difference were not used in the computation of the mean day to day changes by the usage of a majority voting.

Figure 6 shows 4 curves for each receiver. These are the original estimates of the GLONASS/GPS system time difference, the mean day to day changes of those and the estimates of the system time difference corrected for their mean changes. Those corrected system time differences were used to compute mean values for each receiver, which are given in Figure 6, also. Thus computed mean values of all Ashtech Z-18 receivers involved are summarized in Table 2 and may be used to compute the differential receiver biases of all possible receiver combinations. These computations were performed for the 3S Navigation receivers, also, and the corresponding mean values of the receiver biases are given in Table 2.

The receiver-specific estimates of the system time difference of the station OS0G in Figure 6 are very similar to the mean changes of the estimates. Therefore, the corrected estimates of the system time difference of station OS0G show very small variations around its mean value. Much larger variations of the corrected system time difference around its mean value were found for station GODZ in Figure 6. These are caused by the discrepancy between the receiver-specific estimates and the mean changes of the estimates. The small number of observations that were used in the code single point processing of some particular days could be responsible for the outliers in the daily estimates because the resulting station coordinates are affected by the number of observations.

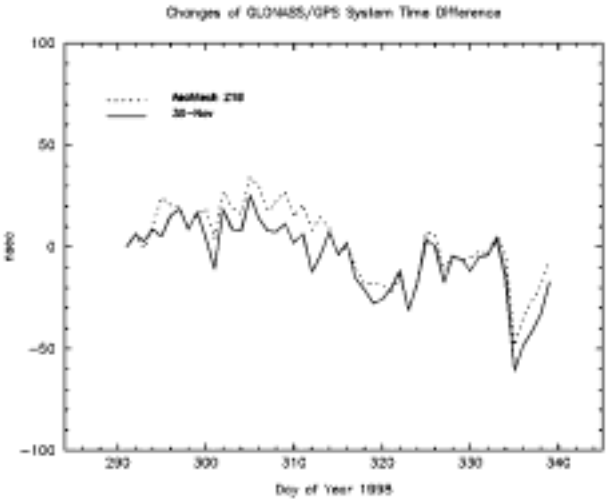

Figure 7. Mean changes of GLONASS/GPS system time difference from different receiver types.

The mean changes of the system time difference as computed from Ashtech Z-18 and 3S Navigation receivers separately are given in Figure 7. Both receiver types lead to nearly identical results for the changes of the system time difference. The discrepancy between the two curves in Figure 7 for the period day 291 to 312 may be caused by the small number of 3S Navigation receivers, that were available during this period.

Transformation Parameters between PZ-90 and ITRF 96

The orbit improvement for the GLONASS satellites, as shown in Figure 2, yields the satellite positions in ITRF 96, since the ITRF 96 coordinates of the reference stations are held fixed and since the orbits of the GPS satellites are given in the ITRF 96. Thus, two coordinate sets for the satellite positions are available, one in each system, and may be used in order to estimate the parameters of a seven parameter Helmert transformation. The expected accuracy of the resulting transformation parameters mainly depends on the accuracy of the broadcast orbits, assuming that the improved GLONASS orbits have an accuracy level of about a few decimeters.

The transformation parameters were calculated on a daily basis for the period from day of year 291 to 346, 1998. The results are shown in Figure 8. For each transformation parameter linear approximations and the corresponding RMS errors were computed and are given in Figure 8. The translation parameters show a scatter of about 0.5 m, which is a consequence of the broadcast orbit quality. On the average the translation parameters in direction of the X- and Z-axis are equal to zero, if the corresponding RMS errors of the linear approximation of 0.37 m and 0.62 m are taken into account. The translation in direction of the Y-axis shows a significant drift of 0.48 m for the period of 56 days.

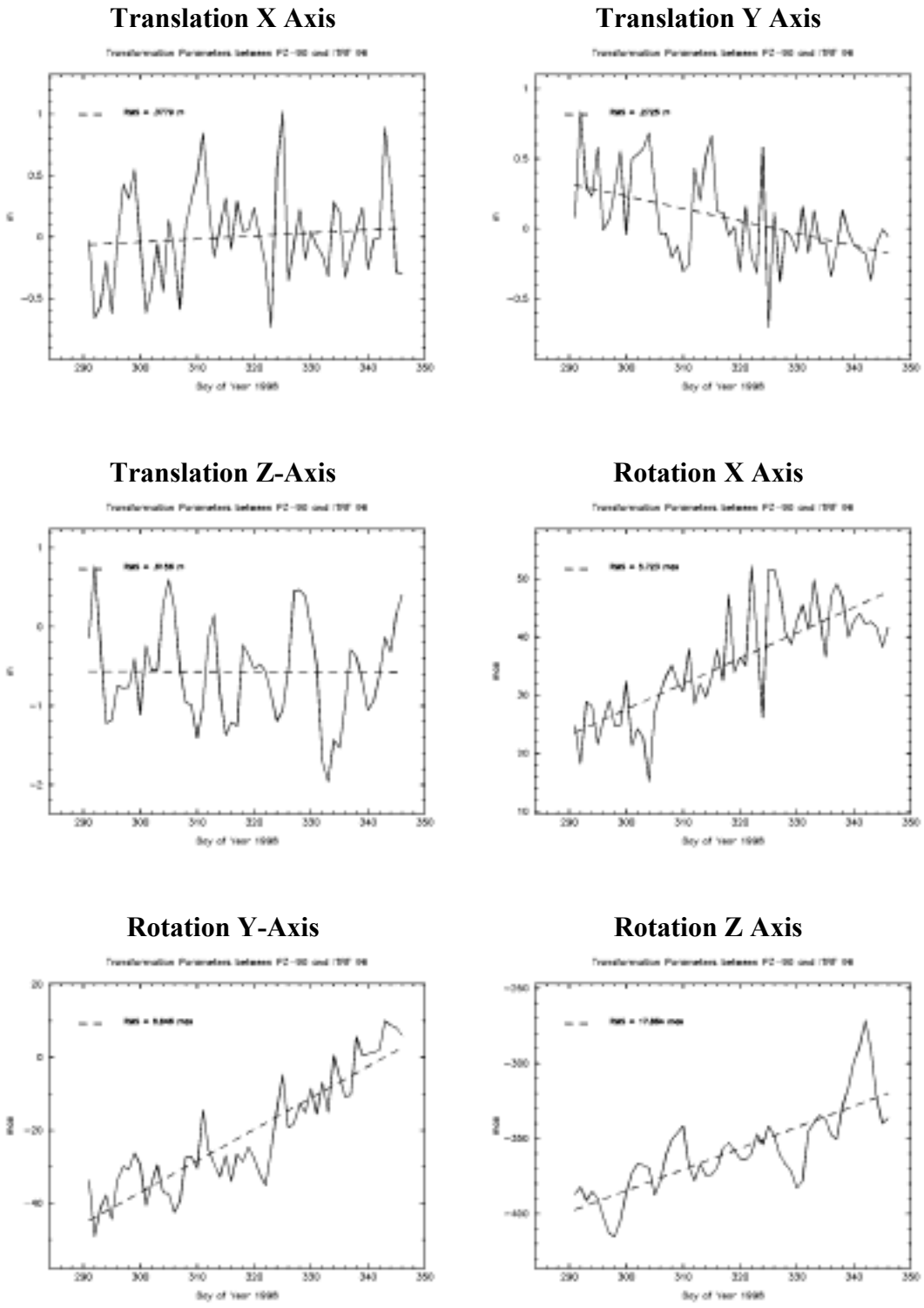

Figure 8a. Daily transformation parameters between PZ-90 and ITRF 96.

Scale

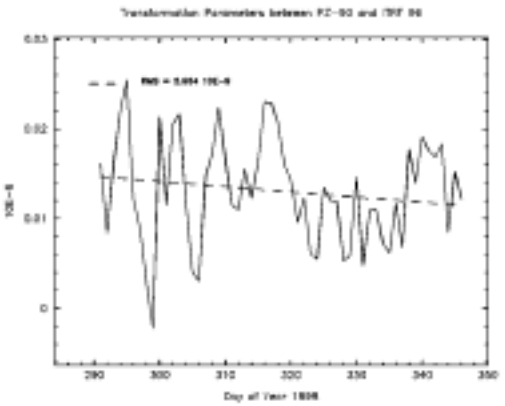

Figure 8b. Daily transformation parameters between PZ-90 and ITRF 96.

All rotation parameters show a significant drift for the period given in Figure 8, also. This confirms the changing of the transformation parameters in time, as found in (Mitrikas et al., 1998). The most significant parameter is the rotation parameter around the Z-axis, which is determined to a mean value of -358 mas. The scatter of the scale factor estimates decreases with the beginning of day 312, because of the increased number of stations that were used in the processing. The scale parameter shows no linear drift, if we exclude the results of the period before day 312 and is determined to a mean value of $1 \cdot 10^{-8}$.

The mean values of the transformation parameters over the period mentioned above are given in Table 3. The RMS errors of each of the 7 parameters are derived from the residuals of the daily transformation parameter estimates. Those RMS errors of the mean values are much larger than the RMS errors in Figure 8, because no linear drift is accounted for. The total RMS error of the IGEX-98 results in the last column in Table 3 was computed from the residuals of the transformed satellite positions. It is a measure of the overall quality of the broadcast orbits. The RMS of about 5 m indicates, that the broadcast orbits are in general much better, than specified in (ICD, 1995).

(Bazlov et al., 1999) determined transformation parameters between PZ-90 and WGS-84 using the coordinates of eight reference sites in Russia with known coordinates in both systems. If we compare the RMS error of the two approaches in Table 3 we must take into consideration, that an RMS error of 5.07 m for the satellite positions corresponds to approximately 1.2 m on the Earth's surface. But even after applying this conversion the RMS error of the transformation by Bazlov et al. is still smaller by a factor of 3 than that of the IGEX results, with the important disadvantage, however, that all participating stations were located on the Russian territory.

Table 3. Mean Value of Transformation Parameters between PZ-90 and ITRF 96

$$\begin{vmatrix} X \\ Y \\ Z \end{vmatrix}_{ITRF-96} = \begin{vmatrix} X \\ Y \\ Z \end{vmatrix}_{PZ-90} + \begin{vmatrix} DX \\ DY \\ DZ \end{vmatrix} + \begin{vmatrix} Scale & RZ & -RY \\ -RZ & Scale & RX \\ RY & -RX & Scale \end{vmatrix} \cdot \begin{vmatrix} X \\ Y \\ Z \end{vmatrix}_{PZ-90}$$

	DX RMS [m]	**DY** RMS [m]	**DZ** RMS [m]	**RX** RMS [mas]	**RY** RMS [mas]	**RZ** RMS [mas]	**Scale** RMS [10^{-6}]	**Total** RMS [m]
IGEX-98	0.06 ± 0.38	0.07 ± 0.32	-0.57 ± 0.62	35 ± 9.17	-21 ± 15.56	-358 ± 29.12	0.01 ± 0.006	5.07
Bazlov 1999	-1.08 -	-0.27 -	-0.90 -	- -	- -	-160 -	-0.12 -	0.38

Conclusion

Combined GPS/GLONASS observations of the IGEX-98 campaign have been processed at BKG and weekly reports of the processing results have been submitted by IGEX-Mail. Improved orbits for GLONASS satellites are now available with an accuracy level of about a few decimeters. The estimates of the system time between GPS and GLONASS show up receiver-specific biases. As shown in (Habrich, 1999), those receiver-specific biases would prevent the ambiguity resolution for double difference observations between GPS and GLONASS satellites. We have seen that the transformation parameters between PZ-90 and ITRF 96 are changing in time. However, since the beginning of IGEX-98 daily transformation parameters are available and may be used to account for the changes of the parameters.

References

BKG (1999). Processing Results of the Bundesamt fuer Kartographie und Geodaesie of the IGEX-98 Campaign, IGEXmail, http://lareg.insg.fr/IGEX/.

Bazlov, Y.A., V.F. Galazin, B.L. Kaplan, V.G. Maksimov, V.P. Rogozin (1999). GLONASS to GPS, A New Coordinate Transformation, *GPS World*, Vol. 10, No. 1.

Habrich, H. (1998). Experiences of the BKG in Processing GLONASS and Combined GLONASS/GPS Observations, *Proceedings IGS Analysis Center Workshop*, Darmstadt, Feb. 9-11, 1998.

Habrich, H. (1999). Geodetic Applications of the Global Navigation Satellite System (GLONASS) and GLONASS/GPS Combinations, Ph.D. Dissertation, Astronomical Institute, University of Berne, Switzerland.

Habrich, H., W. Gurtner, M. Rothacher (1998). Processing of GLONASS and Combined GLONASS/GPS Observations, 32nd COSPAR Scientific Assembly, Nagoya, Japan, Jul.12-19, 1998.

ICD (1995). GLONASS Interface Control Document, Coordinational Scientific Information Center of Russian Space Forces, Moscow, Russia.

Mitrikas, V.V., S.G. Revnivykh, E.V. Bykhanov (1998). WGS 84/PZ 90 /Transformation Parameters Determination Based on Laser and Ephemerides Long-Term GLONASS Orbital Data Processing, *Proceedings ION GPS-98*, Nashville, Sept. 15-18, 1998, pp. 1625-1635, Inst. of Navigation.

GLONASS Data Analysis at ESA/ESOC

Carlos García[1], Tomas Martin-Mur, John Dow, and Ignacio Romero[1]
ESA/European Space Operations Centre
Robert Bosch Strasse 5, 64923 Darmstadt, Germany

[1]GMV at ESOC

Introduction

This paper presents the GLONASS Analysis activities performed at ESOC in the context of the IGEX campaign. ESOC has been for a long time committed to the processing and analysis of GNSS data for precise orbit determination. Our GNSS activities started in 1991 with the analysis of the data from the GPS CIGNET-91 campaign and the software for automated processing of GNSS data has been almost constantly improved and extended since then. The processing of GLONASS data has benefited from ESOC experience as an IGS Analysis Centre but has needed a number of GLONASS specific adaptations for the software.

The present paper will analyze the current ESOC IGEX processing along with an evaluation of the results from the first months of processing.

Processing Strategy

The strategy for the processing of GLONASS data was derived from the current set up that is used for the IGS products. In this way the IGEX processing can take advantage of the high system automation that makes possible the processing of big amounts of data with limited human and computer resources. The introduction of GLONASS processing capabilities in our software was not straight forward. A number of changes have been necessary in the preprocessing and orbit determination stages. The main ones are the following:

- The use of the GLONASS frequencies in the preprocessing program GPSOBS
- The use of undifferenced measurements as basic observable has been the main change. Previously the processing was based on phase double-differences and satellite clock biases were estimated using the pseudoranges in a second step. The use of undifferenced data is advantageous in three ways:

  1. Clocks and orbits are estimated at the same time and are consistent with each other.
  2. More observations can be used. The limitation of the use of only the measurements which can be combined in a double difference link disappears. This approach was developed for IGEX processing and was also later adopted for our IGS processing.
  3. The assessment of the GLONASS receivers can be more accurately characterized with this approach.

- The lack of a priori solar radiation pressure force models for the GLONASS satellites triggered the implementation of empirical models in our orbit determination package BAHN.
- The orbit determination program BAHN was modified to allow for the estimation of time dependent parameters, typically receiver and satellite clock biases.

The final strategy was fine-tuned taking into account our limited computer resources. GPS orbits and clocks that have already been estimated for IGS are used as input data.

Processing Description

RINEX observation and navigation files are retrieved from CDDIS and stored in our computer. A reduced number of IGS ITRF core stations are downloaded from our internal archive. The role of the IGS stations is to fix the solution to the ITRF in the way that GLONASS orbits and station coordinates are represented in ITRF96. Seven well distributed stations are selected. Every station has a back-up that is used in case of unavailability.

All GLONASS observation files are re-formatted with teqc (UNAVCO RINEX formatter) to correct for phase overflow problems that have been detected in some receivers.

Three days of data constitute the data arc and are available on the disk for the preprocessing program GPSOBS. IGS GPS orbits and clocks from the ESA final solution are also input to GPSOBS. The ionospheric free combination is formed. Cycle slip detection is based on a propagated orbit from the previous day.

Satellite antenna corrections are applied. The output is an observation file which contains the ionospheric free phase combination plus pseudoranges. A five minute sampling rate is enough for the orbit estimation. The satellite clock biases are also estimated with the same sampling although it would be more convenient to use all the available data with 30 second sampling. Computer limitations do not allow this option.

The observation file is filtered to select the passes with at least 4 observations and with a controlled noise between phase and pseudorange for every accepted pass. Phase observations of satellite gv-75 are consistently rejected because they are found to be very noisy. The orbit of this satellite is estimated only with the pseudorange and no clock bias estimations are possible.

The orbit determination is the next step. BAHN is based on the batch least squares method and has been modified to allow for the estimation of time dependent parameters. The following parameters are estimated:

- Solar radiation pressure coefficients
- State vectors

- GLONASS-GPS receiver bias
- Station positions
- Zenith path delay
- Pass biases
- Earth orientation parameters
- Station and satellite clock biases

Orbits and clocks are combined to produce the sp3 files. The accuracy exponents are set taking into consideration the phase and pseudorange residuals of the orbit determination and the orbit comparison to the overlapping fit of the previous day.

The normal equations of the terrestrial reference frame are combined to produce weekly SINEX files.

ESOC IGEX PROCESSING

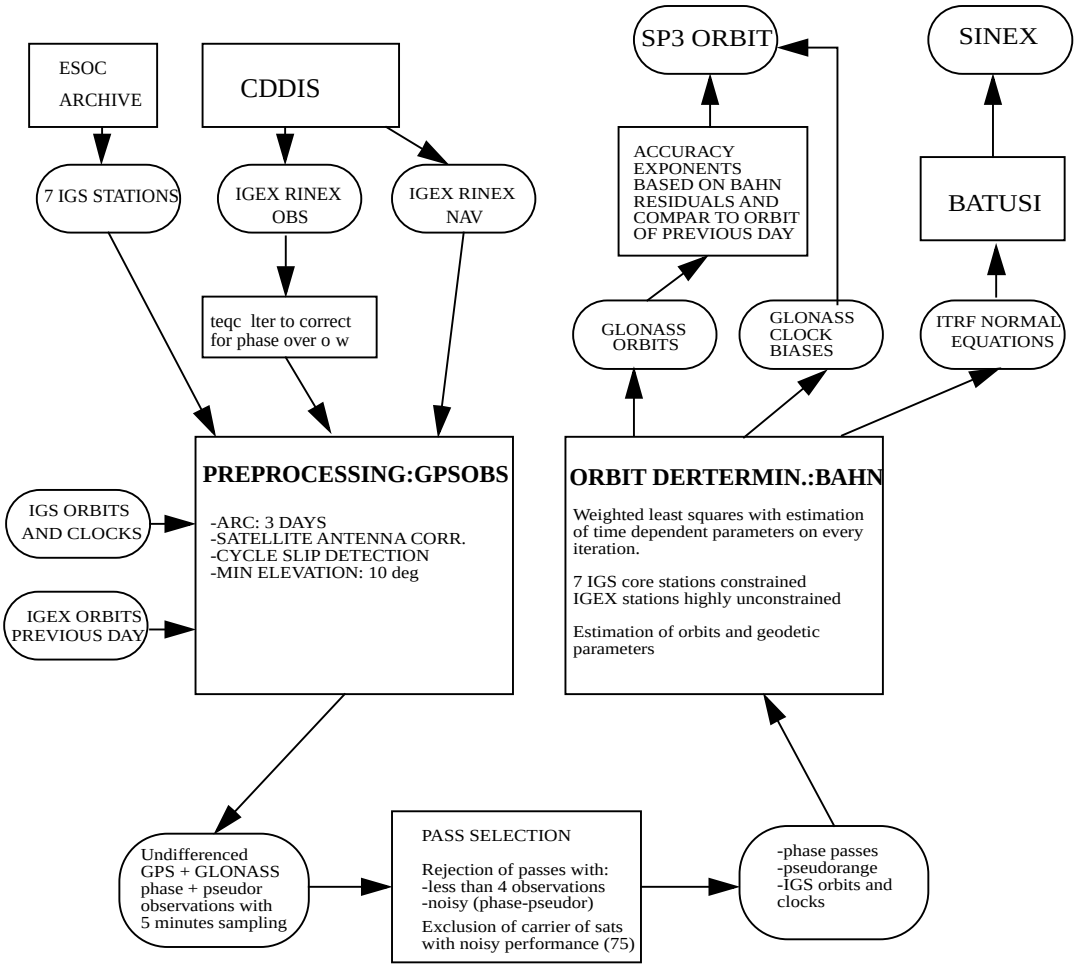

Station Network

Unfortunately the processing of the data of all the IGEX stations has not been possible. Only dual frequency receivers with GPS time tags have been considered. Single-frequency receivers do not make possible the creation of the ionospheric free combination. The inclusion of receivers working in GLONASS time reference would present conflicts for the measurement sampling times and the estimated parameter epochs.

These limitations have reduced the spectrum of receivers to the following models:

- ASHTECH Z-18
- JPS LEGACY
- 3S NAV R100
- ESA/ISN GNSS

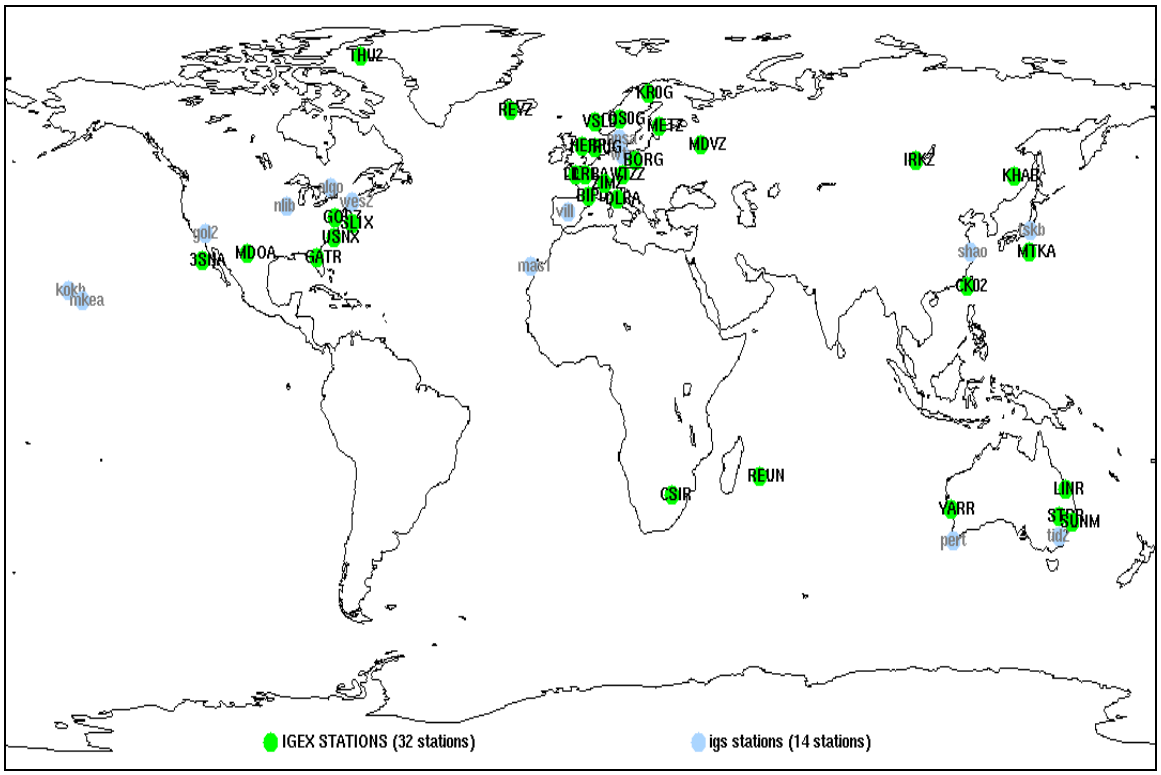

Figure 1. IGEX dual-frequency receiver network.

ESOC has been the operational data centre for the Leeds receivers during the IGEX campaign. Three receivers have contributed to the campaign from the beginning in October 98 ending the operation in August 99. The data of the following receivers was forwarded to the Global Data centres:

Table 1. Receivers at University of Leeds

4 char ID	RECEIVER	ANTENNA
LDS1	ESA/ISN	Trimble 4000SLD L1/L2 common for all receivers
LDS2	Trimble 4000SSE	
LDS3	Ashtech GG24	

Estimation of Receiver GPS-GLONASS Bias

In order to simultaneously process GPS and GLONASS data from different receivers it was necessary to estimate for each GPS-GLONASS combined receiver a inter-system bias that models the different signal path or processing delay within the antenna, cable, amplifier or receiver for the GLONASS and GPS signals.

A perturbation in the estimation of these biases is the difficulty in establishing absolute GPS and GLONASS time references due to errors caused by SA, broadcast message or our own IGS clock estimation.

After removing the common variability due to the error in the estimation of the absolute GPS and GLONASS times the biases are in most cases stable and depend mostly on the type of receiver (see Figure 2):

- Z-18 receivers have values with offsets between -55 to 40 ns and day to day variations in the range 1 to 3 ns.
- JPS Legacy receivers have lately stabilized at about -140 ns.
- The ESA/ISN receiver has a bias around -980 ns with day to day variations of about 1 ns.

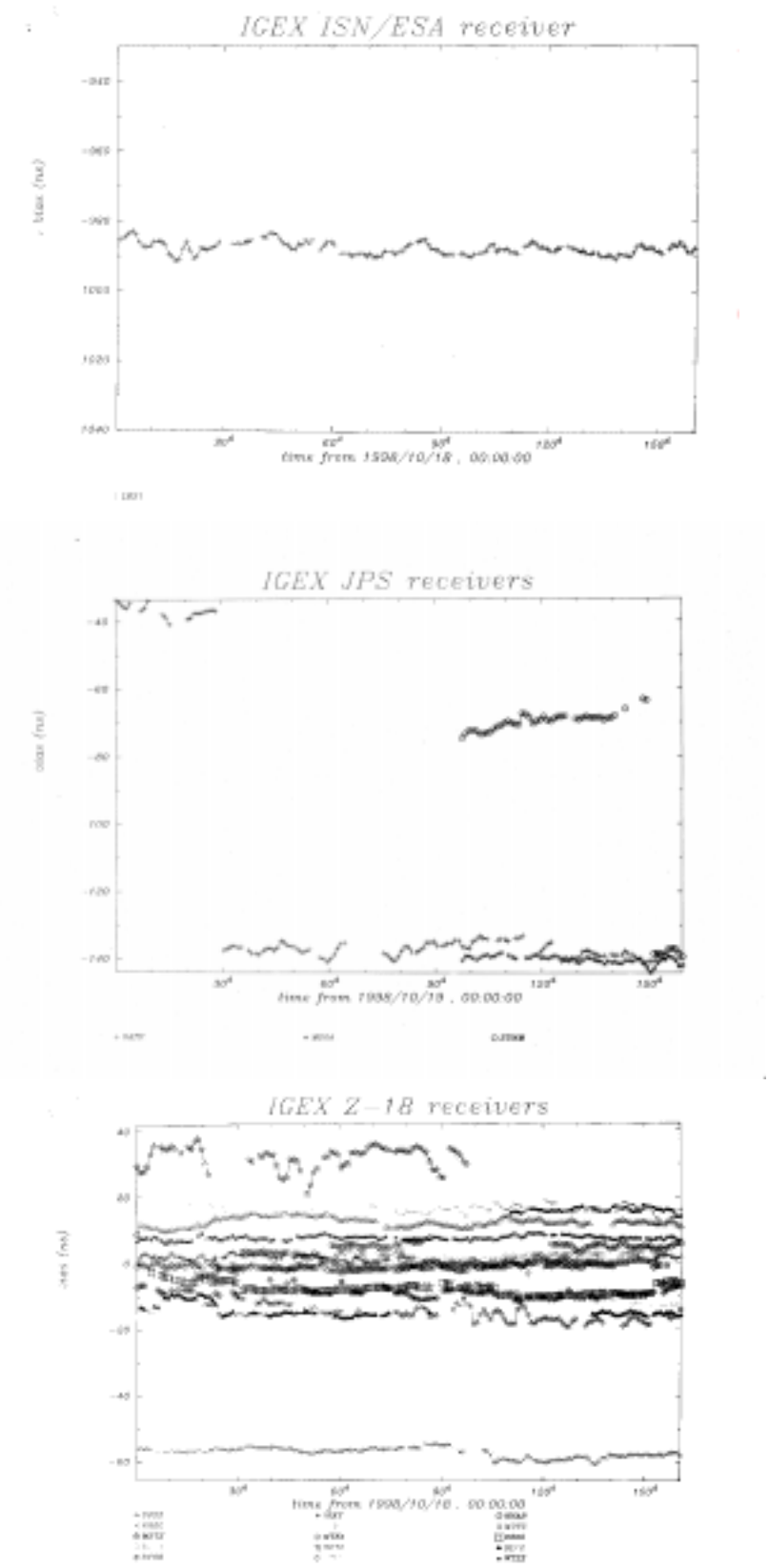

Figure 2. GPS-GLONASS receivers inter-system bias.

These models had been investigated for the IGS processing, but they were discarded because the use of the ROCK model in combination with the sine and cosine empirical accelerations proved to be equivalent. IGEX gave a second chance for the use of this implementation.

The parameterization of the model describes the forces on each of the reference frame axes as a function of the selected argument A as:

$$Fi = K (a_{i0} + a_{ic} \cos(A) + a_{is} \sin(A) + a_{ic2} \cos(2A) + a_{is2} \sin(2A))$$

where K is a factor that can be 1 or a scaling including the variation in solar radiation pressure with satellite-sun distance and an estimable global scale factor.

Several arguments and reference frames have been tested.

The most interesting arguments are:

- The solar angle (see Figure 3). It is used in the ROCK models. Useful for spacecraft oriented with the Sun direction.
- The solar anomaly. It is the orbital angle for which the origin is the point in the orbit closest to the Sun.
- True anomaly: for spacecraft in elliptic orbits
- Argument of latitude: spacecraft in near circular orbits.

Tested reference frames are:

- The ROCK model frame. Body fixed defined by the Sun and Earth directions.
- Solar frame. Defined by the Sun and the Earth and rotating in satellite fixed axes around the solar panel axis.
- Orbital frame. Defined by the position and velocity.

After several tests the selected argument is the solar anomaly, and the frame the solar one. Sine and cosine terms are only estimated in the z axis. Terms in 2A are not estimated, resulting in a 5-estimated-coefficients model: constant terms in the three axes plus sine and cosine in z. The selection of the model was based on the residuals of the orbit determination and the observability of the selected parameters.

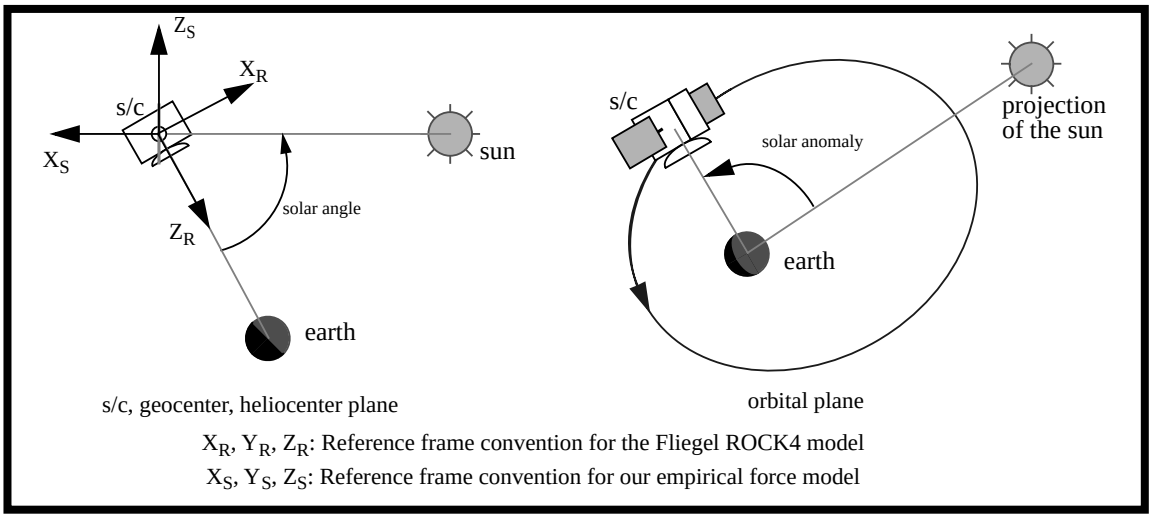

Figure 3. Solar radiation pressure reference systems and arguments.

Results

The routine processing of GLONASS data started in March 1999 with the analysis and submission of GPS week 0980, the official start of the IGEX campaign. Currently we have covered the processing of the whole campaign with the delivery of results of GPS week 1005. We are continuing the processing beyond this date as long as our internal resources allow it and a meaningful network of GLONASS receivers continues in operation.

Every week the following products are delivered to CDDIS:

- Orbit files with satellite clock bias information every 5 minutes
- Summary file
- Earth orientation parameters
- SINEX file with station positions

Orbit Comparisons

The following plot (Figure 4) shows an estimation of the orbit errors. It is the rms comparison of the orbit of a day with respect to the same fit of the overlapping arc of the previous day. This information is presented every week in the summary file.

Typical errors are about 20 centimeters except for satellites gv-66 and gv-75 which show larger errors.

The satellite clock bias plot (Figure 5) shows a similar behavior, with most of the satellites below 1 ns rms deviation.

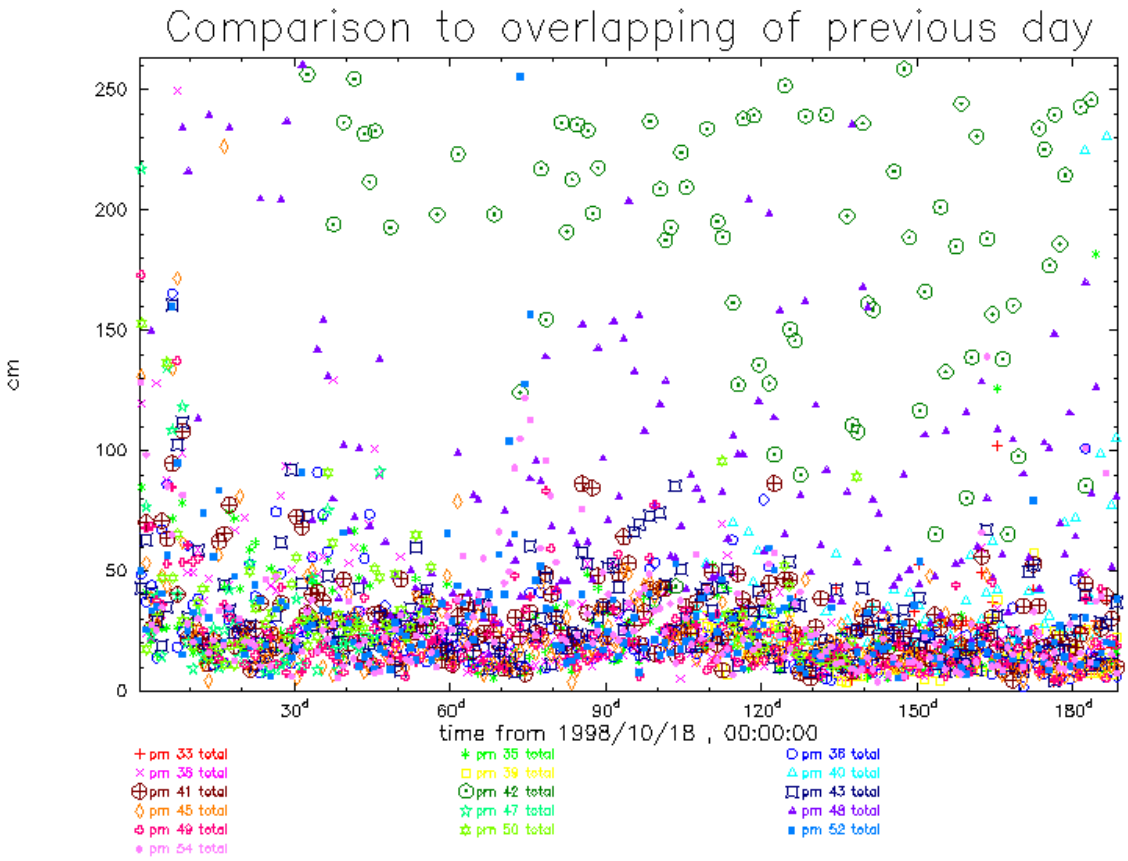

Figure 4. Orbit overlaps. Note: GLONASS almanac satellite no. = prn – 32.

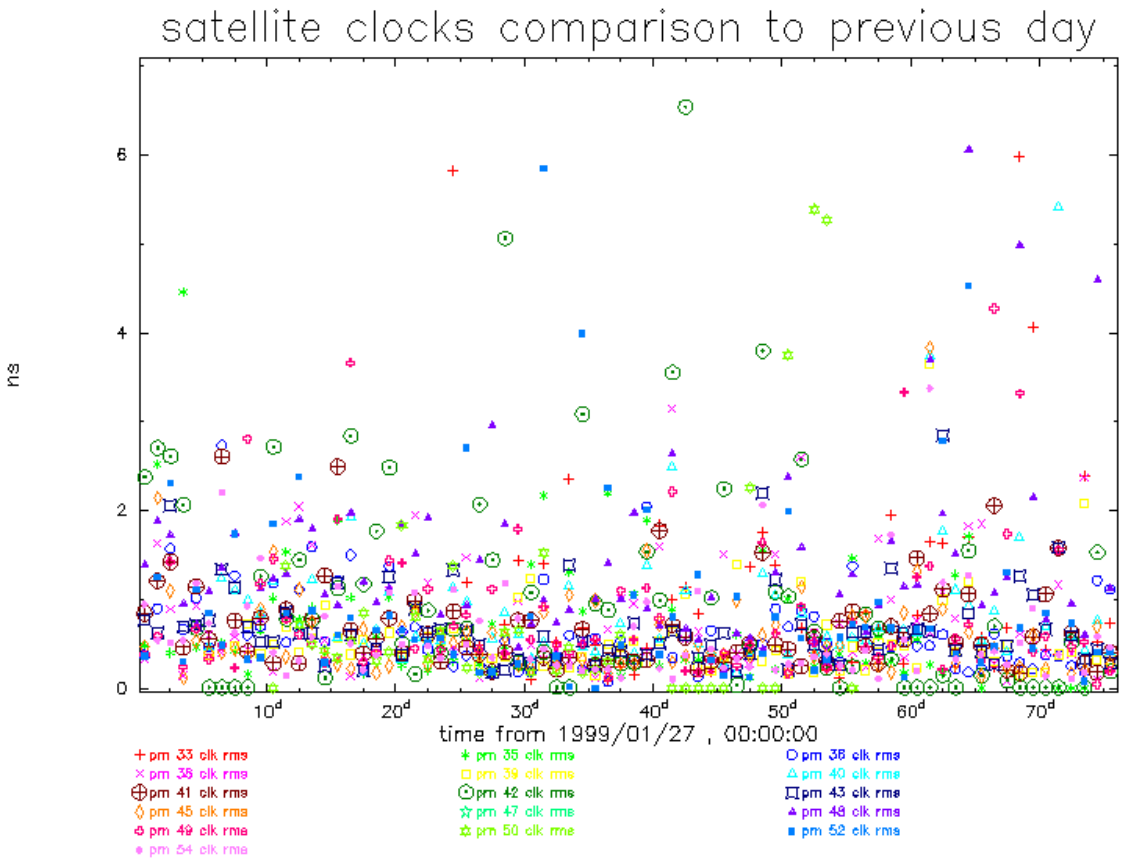

Figure 5. Daily clock comparisons. Note: GLONASS almanac satellite no. = prn - 32

Solar Radiation Pressure

The coefficients of the solar radiation pressure model are plotted for several days of the campaign. It is remarkable that:

The X term is the direct solar radiation pressure force. The value is about 150 nanoNewton for most of the satellites and about 80-90 nanoNewton for gv-64.

The Y term is the well known y bias with values in the interval [-.5,+.5] nanoNewton for most of the satellites. There are some regular variations on some satellites that could be investigated.

The Z is decomposed into constant, sine and cosine terms. The constant with values in the interval [-.5,+.5] nanoNewton. Problematic satellites like gv-66 and 75 show large variations in this term.

The cosine term is in the interval [-10,+10] nanoNewtons and the sine term in the interval [-3,3] depending on the satellite.

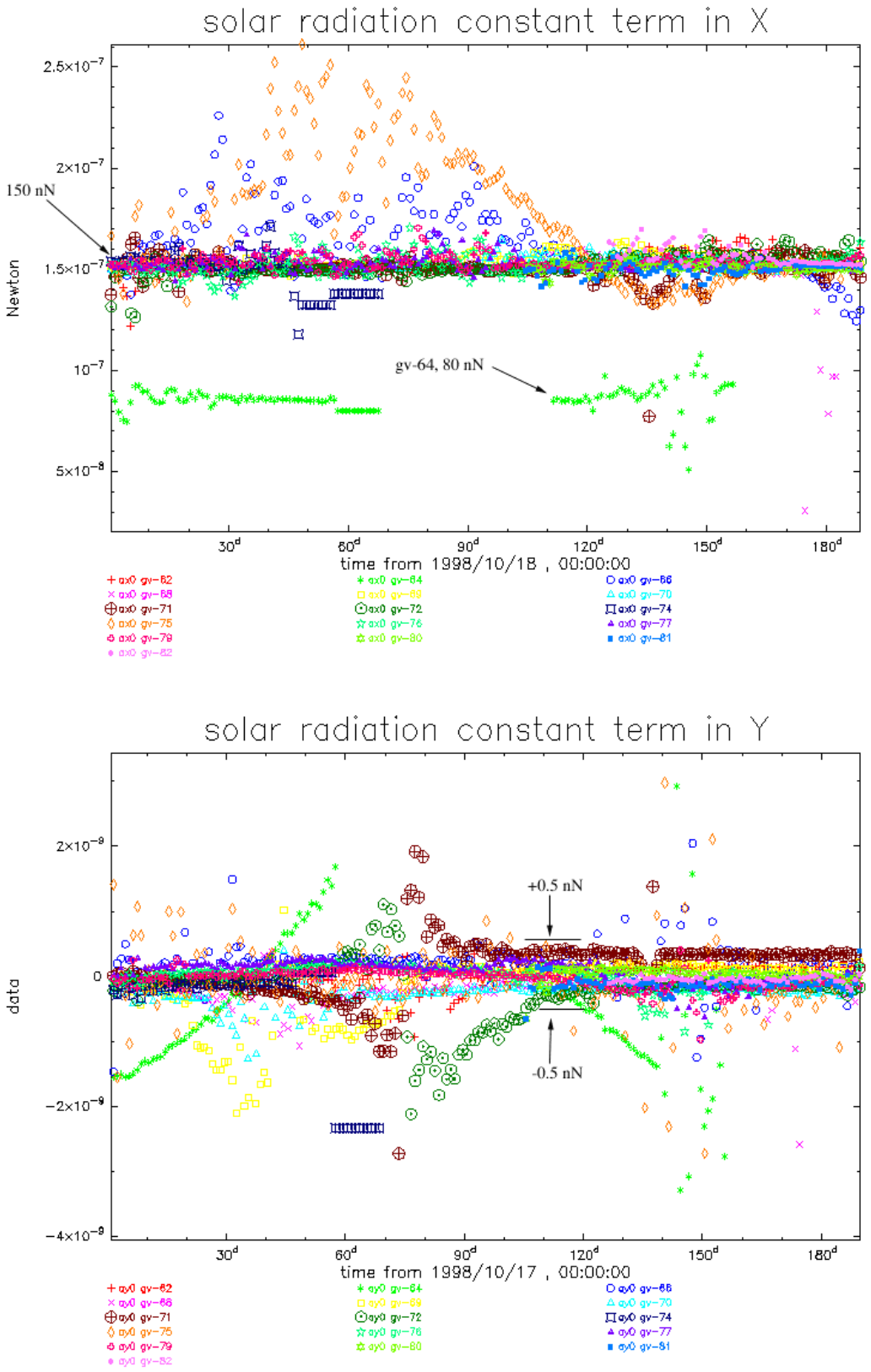

Figure 6. Solar radiation pressure constant terms in x- and y-directions.

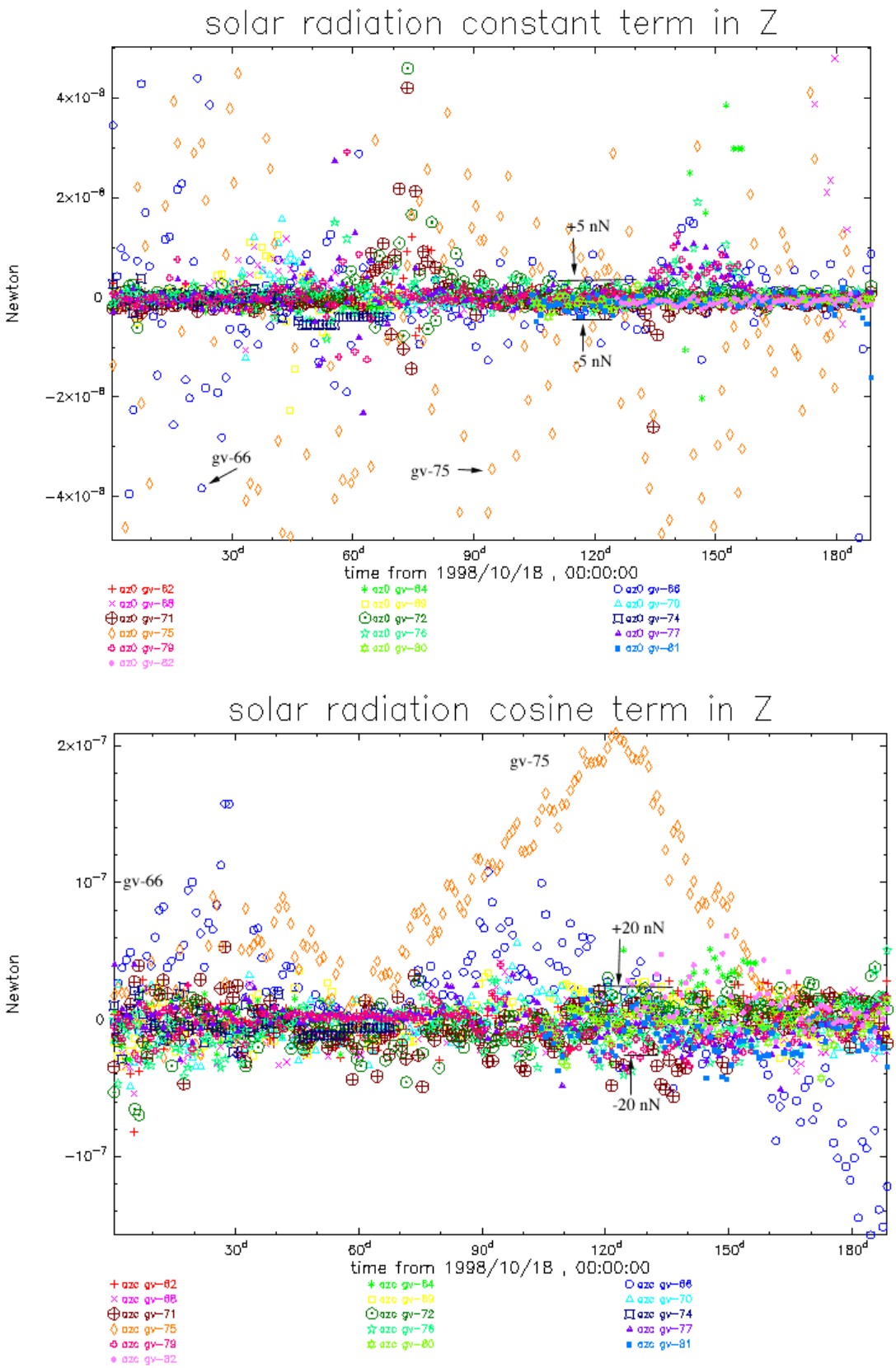

Figure 7. Solar radiation pressure constant and cosine terms in z-direction.

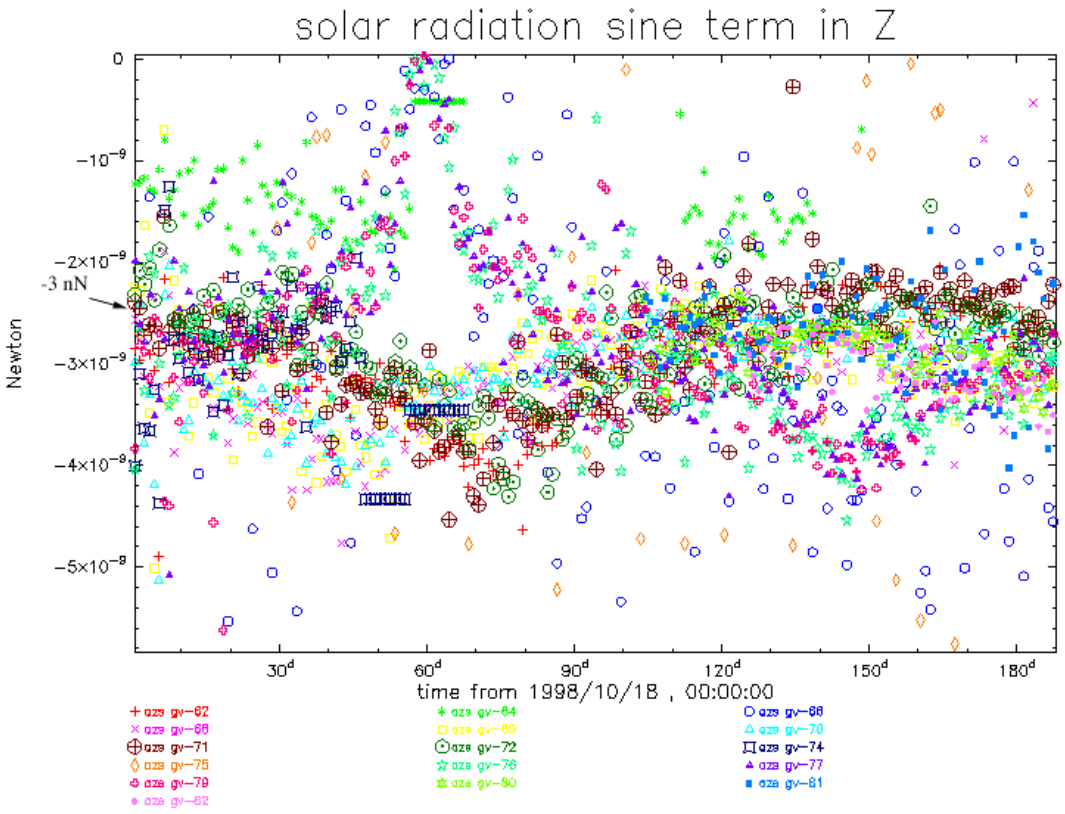

Figure 8. Solar radiation pressure sine term in z-direction.

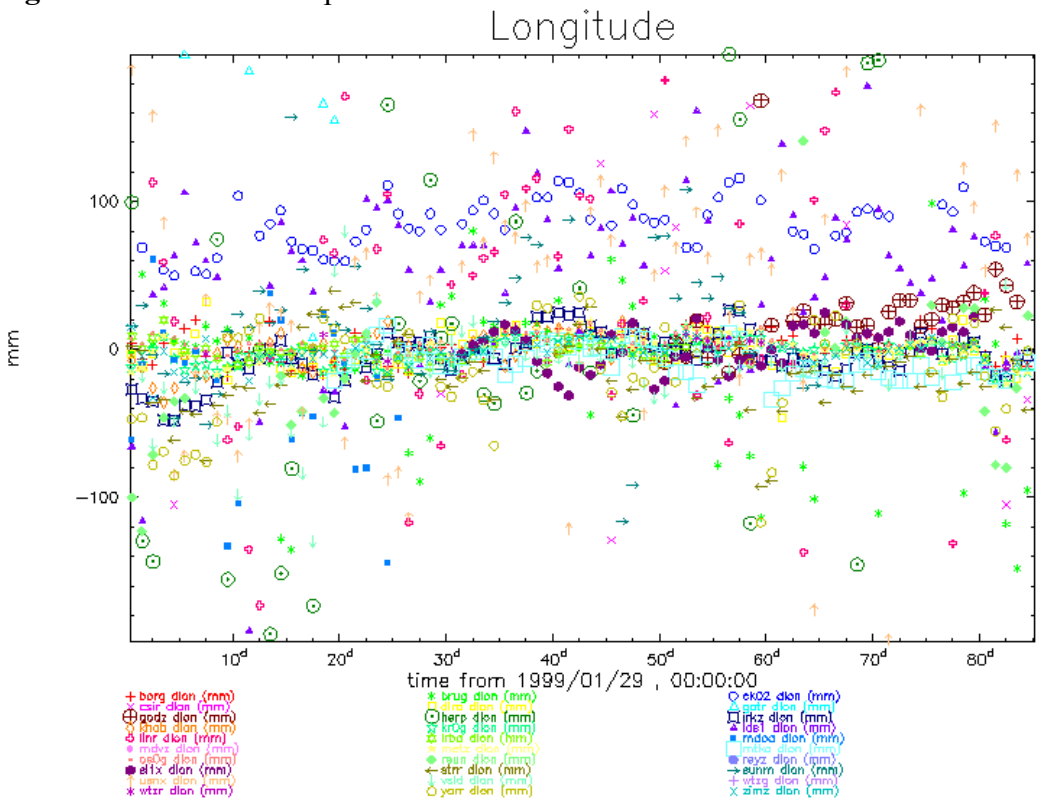

Figure 9. Computed station longitudes.

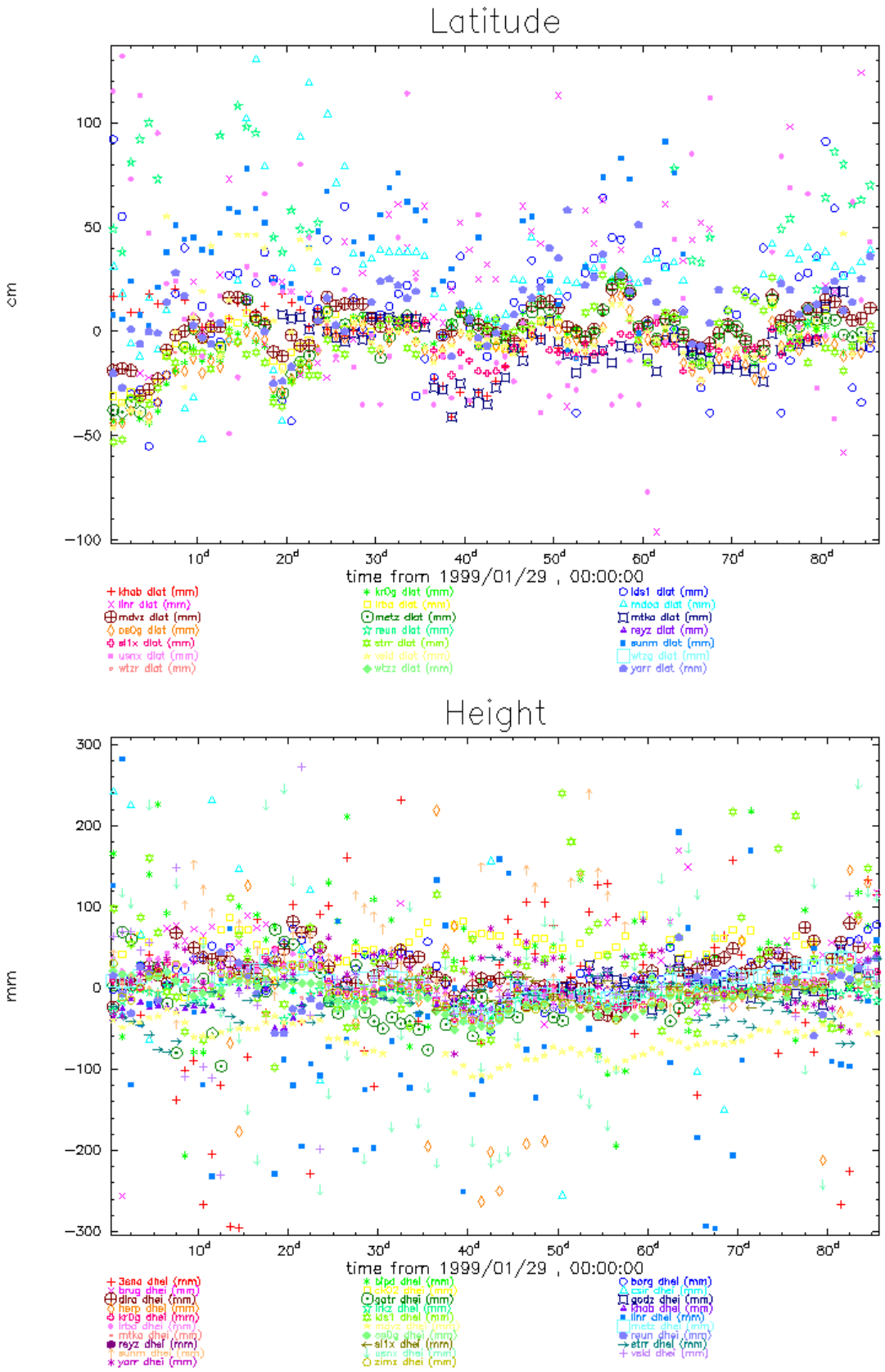

Figure 10. Computed station latitudes and heights.

Station Coordinates

One important objective of IGEX is to produce a set of GLONASS station coordinates consistent with the ITRF.

All IGEX station coordinates are very unconstrained in our processing in contrast to the 7 IGS core stations which are tightly constrained to ITRF96. This allows for the estimation of the IGEX stations coordinates in the ITRF frame. Our SINEX file has been produced every week and can be used for that purpose with the following limitations:

- Lack of available information on antenna calibration for many of the GLONASS receivers.
- Incomplete antenna information for some of the IGEX stations.
- As can be noticed in the coordinates plots (Figures 9, 10) there are fortnightly periodic variations due to the lack of ocean loading modeling.

A solution including all the official data from the IGEX campaign has been produced. The normal equations of six months of data from GPS week 0980 to 1005 have been combined in a single SINEX file estimation. Table 2 presents the results.

Table 2. IGEX Station Coordinates for EPOCH 1999.0

DOMES	Name	4-char ID	Receiver	X(m)	Y(m)	Z(m)	Sigma X (mm)	Sigma Y (mm)	Sigama Z (mm)
12361M001	Khabarovsk, Russia	KHAB	ASHTECH Z-18	-2995266.359	2990444.730	4755575.985	1	1	1
13502M008	Delft, Netherlands	VSLD	3SNAV R100	3923530.539	300596.013	5002840.911	1	1	1
40451M123	GSFC, Maryland	GODZ	ASHTECH Z-18	1130773.897	-4831253.566	3994200.353	1	1	1
12313M003	Irkutsk, Russia	IRKZ	ASHTECH Z-18	-968310.065	3794414.479	5018182.145	1	1	1
14001M005	Zimmerwald, Switzerland	ZIMZ	ASHTECH Z-18	4331292.902	567545.249	4633135.879	1	1	1
30310M001	Pretoria, South Africa	CSIR	3SNAV R100	5063684.518	2723897.108	-2754445.645	15	11	7
10202M003	Reykjavik, Iceland	REYZ	ASHTECH Z-18	2587383.843	-1043032.706	5716564.454	1	1	1
14208M002	Oberpf, Germany	DLRA	3SNAV R100	4186743.244	834902.645	4723618.614	2	1	2
49918S001	Irvine, California	3SNA	3SNAV R100	-2482980.680	-4696608.274	3517630.798	3	4	3
10422M001	Kiruna, Sweden	KROG	ASHTECH Z-18	2248123.332	865686.632	5886425.628	1	1	1
13215M001	Leeds, England	LDS1	ESA/ISN GNSS	3773063.712	-102444.078	5124373.322	3	2	3
21741M002	Tokyo, Japan	MTKA	ASHTECH Z-18	-3947762.759	3364399.879	3699428.519	1	1	1
14201M012	Wettzell, Germany	WTZG	3SNAV R100	4075588.803	931874.340	4801556.804	54	19	62
14201M014	Wettzell, Germany	WTZZ	ASHTECH Z-18	4075579.637	931853.033	4801568.976	1	1	1
10503M005	Metsahoovi, Finland	METZ	ASHTECH Z-18	2892570.021	1311843.593	5512634.462	1	1	1
12205M004	Borowiec, Poland	BORG	3SNAV R100	3738369.225	1148164.230	5021810.340	1	1	1
----------	----------	GATR	JPL Legacy	738692.576	-5498293.288	3136519.463	1	1	1
12309M004	Mendeleevo, Russia	MDVZ	ASHTECH Z-18	2845461.849	2160957.528	5265989.027	1	1	1
4044S001	MIT, USA	SLIX	ASHTECH Z-18	1513678.601	-4463031.662	4283433.528	1	1	1

Table 2. (Cont'd)

DOMES	Name	4-char ID	Receiver	X(m)	Y(m)	Z(m)	Sigma X (mm)	Sigma Y (mm)	Sigama Z (mm)
10402M004	Onsala, Sweden	OS0G	ASHTECH Z-18	3370658.678	711877.068	5349786.822	1	1	1
10094M001	BIPM, Sevres, France	BIPD	3SNAV R100	4203643.881	4203643.881	4778193.068	4	2	5
50107M006	Yarragadee, Australia	YARR	ASHTECH Z-18	-2389024.590	5043315.453	-3078534.182	1	1	1
10093M001	Normandie, France	LRBA	ASHTECH Z-18	4182176.414	109237.196	4798463.038	1	1	1
13212M009	Herstmonceux, England	HERP	3SNAV R100	4033454.679	23664.274	4924309.032	13	8	13
50119M002	Canberra, Australia	STRR	ASHTECH Z-18	-4467102.473	2683039.458	-3666949.809	1	1	1
40451S004	USNO, USA	USNX	3SNAV R100	1112158.189	-4842853.019	3985491.619	4	7	6
43001M002	Thule AFB, Greeland	THU2	ASHTECH Z-18	538093.730	-1389088.018	6180979.206	1	1	1
1310M005	Brussels, Belgium	BRUG	3SNAV R100	4027865.952	307007.347	4919504.212	2	2	2
97401M003	La Reunion	REUN	ASHTECH Z-18	3364099.320	4907944.466	-2293467.084	1	1	1
40442M008	McDonald, USA	MDOA	JPS Legacy	-1330008.101	-5328391.679	3236502.671	1	1	1
50124M001	Lindfield NML2	LINR	3SNAV R100	-4648197.941	2560483.072	-3526505.252	8	7	6
50143M001	Brisbane	SUNM	JSP Legacy	-5046793.833	2567554.742	-2926028.207	2	2	2
----------	Taiwan	CK02	ASHTECH Z-18	-2956510.331	5076009.438	246579.338	1	1	1

The reference frame is constrained to ITRF96 by using 7 IGS core stations. The transformation parameters from the original frame (ITRF96 for the constrained stations) to the one of the presented solution are given in Table 3.

Table 3. Transformation Parameters

Parameter	Estimate	Sigma	Units	estimate-equivalent-at-equator-(m)
RX	0.0000	0.0100	mas	0.0000
RY	0.0000	0.0100	mas	0.0000
RZ	-0.0020	0.0100	mas	-0.0001
TX	0.0295	0.0011	m	0.0295
TY	0.0033	0.0015	m	0.0033
TZ	-0.0514	0.0004	m	-0.0514
SC	1.3822	0.1920	ppb	0.0088

Most of the coordinates have been very accurately estimated. There are some exceptions:

WTZG. The only explanation seems to be the old model of the receiver.
HERP and LINR. The conversion to geodetic coordinates shows that the problem is the height estimation.

Conclusions

The processing of the GLONASS/IGEX data can be performed in a similar way to GPS/IGS with the following remarks:

- It is necessary to estimate a GPS-GLONASS bias for every combined receiver in order to simultaneously process GPS and GLONASS data.
- GLONASS solar radiation pressure acceleration can be modeled with a simple 5-parameter model when the reference frame and argument are properly chosen.
- Some satellites (gv-66, gv-75) show a very poor carrier phase performance.

References

Martin-Mur, T.J. (1998). Empirical Force Models for Solar Radiation Pressure, Internal ESA document, July 1998.

Dow, J., T.J. Martin-Mur, C.G. Martinez, J. Feltens, I. Romero (1999). ESOC IGS Analysis Centre, IGS Analysis Centre Workshop 1999, IGPP/SIO, La Jolla, June 8-10, 1999.

Determination of GLONASS Satellite Orbits at JPL - Approach and Results

Da Kuang, Yoaz Bar-Sever, Willy Bertiger, Kenneth Hurst and James Zumberge
Jet Propulsion Laboratory, California Institute of Technology,
4800 Oak Grove Drive, Pasadena, California 91109, USA

Abstract

We describe a scheme by which GLONASS orbit determination is performed at JPL. The undifferenced dual-frequency pseudorange and carrier phase data are processed in two steps. First, GPS tracking data are processed to determine the precise station location, receiver clock, and troposphere parameters for the dual use receivers (GPS and GLONASS). This is carried out in point positioning mode using the JPL precise GPS orbit and clock solutions. In the second step, the parameters of these stations are held fixed, and using GLONASS data alone we determine orbits of the GLONASS satellite and estimate the parameters of the GLONASS-only tracking sites. We have analyzed three months of IGEX data. We demonstrate GLONASS orbit accuracy at the 20 cm level, and station position repeatability at centimeter level.

Introduction

The International GLONASS Experiment 1998 (IGEX-98) (Slater et al., 1998) started in October of 1998 to collect GLONASS and GPS data on a globally distributed network. One of the investigation areas of this experiment is the orbit modeling and orbit determination of GLONASS satellites. We began GLONASS orbit determination at JPL using IGEX-98 data in early 1999.

The method used in this study is based on the long time development of GPS technology applications at JPL. With strategy (Lichten, 1990) and software (GIPSY/OASIS) (Wu et al., 1990) developed for high precision orbit determination using GPS tracking data, JPL has been producing precise GPS orbit and transmitter clock bias solutions on a daily basis for IGS (Zumberge et al., 1994). Besides using GPS tracking for a precise orbit determination for low-Earth orbiters (Bertiger et al., 1995), JPL also developed a precise point positioning technique (Zumberge et al., 1997) and the technique to use GPS-like tracking for high-Earth orbit determination (Wu, 1985; Haines et al., 1995). These techniques, software and products provide us a flexible tool to analyze the GLONASS data in a unique way. In principle, the GLONASS satellites are treated as individual high-Earth orbit satellites. The precise GPS orbit and transmitter clock products, generated by a separate process at JPL, are used to define the reference frame and calibrate the receiver clock and troposphere delay for the GLONASS tracking network through precise point positioning. In this way, the analysis is focused on revealing unknown features of the GLONASS tracking data and satellite force perturbations.

Approach

The GLONASS measurement models were implemented in the GIPSY-OASIS II software package in order to process the GLONASS data. We process GPS and GLONASS data, separately, in a two-step approach. In the first step, we use GPS data from the dual-use tracking sites, and the precise point positioning technique (Zumberge et al., 1997) to determine the precise location of each site, as well as the receiver clock and troposphere parameters. In this first step, the GPS orbit and transmitter clock parameters are fixed to the precise ephemerides produced by the IGS/FLINN process at JPL. The point positioning solution ties these stations to the reference frame in which the GPS ephemerides are defined (ITRF96). These stations are referred to as *fiducial* sites in this paper. In the second step, the parameters of the fiducial sites are held fixed while GLONASS data from these sites and from GLONASS-only tracking sites (or *non-fiducial* sites) are processed. In this step we simultaneously determine the precise orbits and transmitter clock biases of the GLONASS satellites, as well as the station positions, receiver clock biases and troposphere parameters of the non-fiducial sites (sites without GPS data). In addition, for each fiducial site we also estimate the differential clock bias between the GPS tracking and GLONASS tracking, modeled as a random walk process.

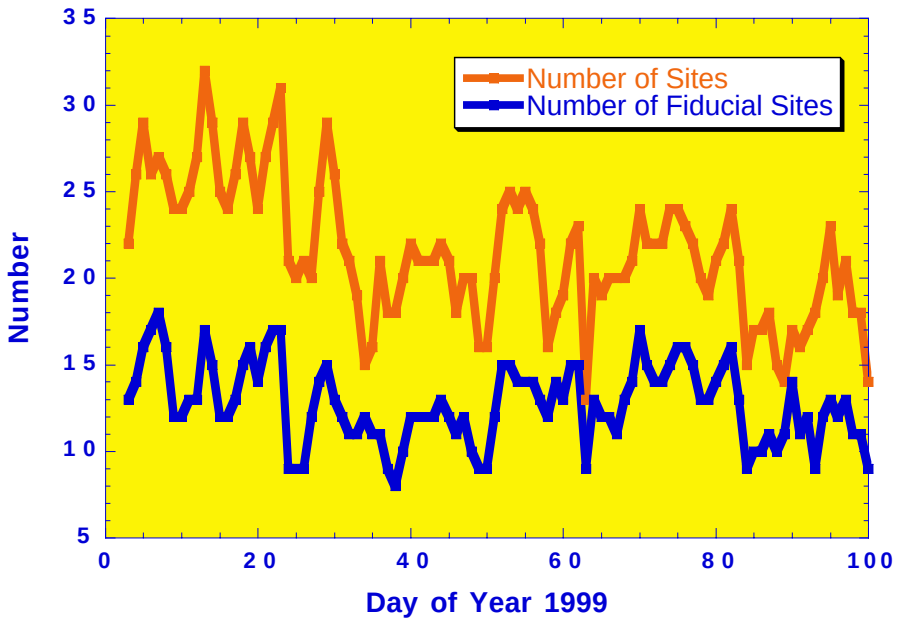

Figure 1. Number of stations used in GLONASS orbit determination.

In this study, for both GPS and GLONASS data, only the dual-frequency measurements are analyzed. Because the number of GLONASS satellites is much less than that of GPS satellites and the number of stations in the IGEX-98 (Figure 1) is less than that in the IGS network, the data strength of IGEX-98 is weak compared to that of IGS data. Three day orbit arcs are used to strengthen the data. According to the Russian Space Agency

(Revnivykh and Mitrikas, 1998) the GLONASS satellite yaw attitude is very similar to that of GPS satellites, thus GPS Block II satellite attitude and dynamic models are used in this study to approximate the solar radiation pressure force acting on the GLONASS satellites. A constant scale factor, a constant Y-Bias parameter for each orbit arc, and additional stochastic accelerations in the satellite body-fixed system are estimated to compensate for the unknown perturbing forces on the GLONASS satellite.

Results

The IGEX-98 data for early 1999 has been analyzed. The results for the first three months are presented here. Orbit precision is evaluated based on 6 hour overlap error. The middle 30-hour orbit of each 3-day arc solution is taken for evaluation, the 6 hour overlapping part of two consecutive 30-hour orbits are compared to each other after a 7-parameter transformation is performed to remove the small systematic errors. 3D RMS of the difference are computed as the orbit precision. The average of this overlap error for each satellite over the three month period is shown in Figure 2. Also shown in the plot is the average of the formal standard deviation of the orbit position error for each satellite. For most of the satellites, the average overlap error is at the 20 centimeter level. The 3 satellites, 8, 10 and 16, have significantly larger error than other satellites. These satellites have abnormally low data volumes, with satellite 8 and 16 having about one half the data points, and satellite 10 having only one tenth of data points compared to other satellites. This data weakness is also reflected in the formal errors.

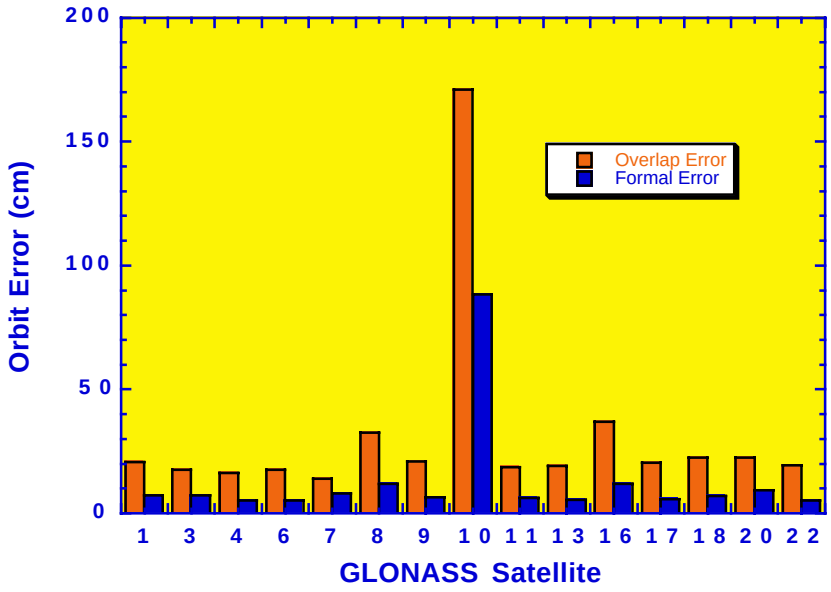

Figure 2. Average 3D orbit overlap error and formal error satellites.

The average data fit residual RMS for phase data is about the same for both GPS and GLONASS tracking data. However, the residual RMS for pseudorange data is quite

different, as shown in Table 1. Station position repeatability after small reference frame fluctuation has been removed through a 7-parameter transformation is also shown in Table 1. The day-to-day site repeatability for the GPS data solution (fiducial sites) is significantly better than that of GLONASS data solution (non-fiducial sites). The average formal error (based on 1 cm phase data noise and 1 meter range data noise) for one site position component shows a similar difference between solutions for fiducial and non-fiducial sites.

Table 1. Site Position Repeatability and Average Data Fit RMS

	formal error for site (mm)	Site Repeatability (mm)			Data Fit RMS (mm)	
		East	North	Vertical	Phase	Range
GPS	5	4	1	6	7.6	656
GLO	16	28	7	33	7.8	1218

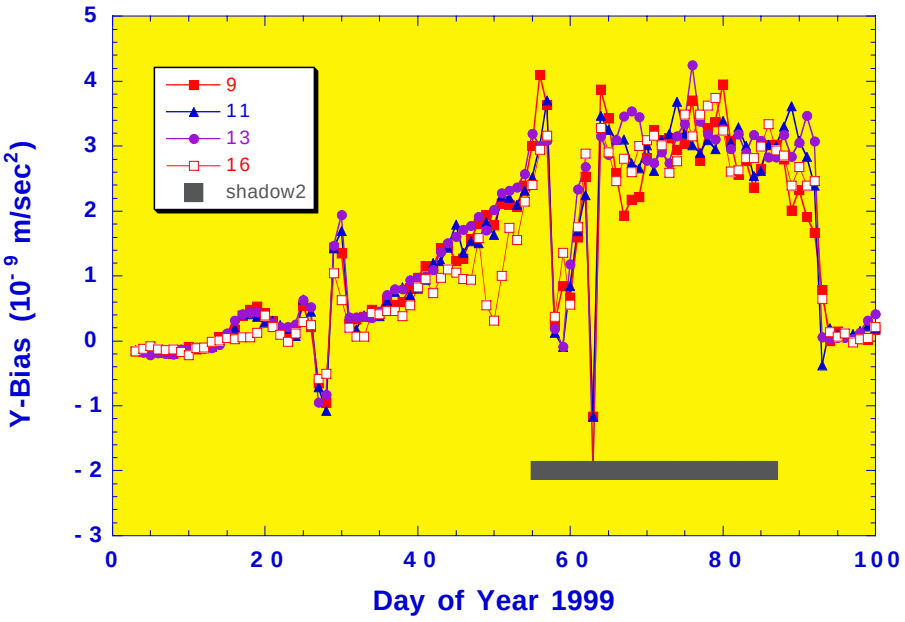

Figure 3. Estimated Y-bias parameters for satellites in orbit plane 2.

Estimated force parameters show a different pattern from what has been seen for GPS satellites. Ideally there should not be a force along the satellite body-fixed Y-axis for either GPS or GLONASS satellites, according to their structure and attitude scheme. A

small constant force along the Y-direction, the so called Y-bias, has been observed for all GPS satellites. A different pattern of Y-bias has been observed for GLONASS satellites, as shown in Figure 3. Since the nominal solar radiation pressure model is adopted from GPS satellites in this study, this Y-bias difference indicates a different feature of force acting along the Y-direction of GLONASS satellites, which can be caused by a different yaw attitude scheme or different satellite structure.

A special issue for the GPS/GLONASS receiver is the differential clock bias between GPS tracking and GLONASS tracking in dual-use receivers. Besides the clock difference between the GPS and GLONASS systems, an additional time delay difference is introduced in the receiver because it tracks the GPS and GLONASS signals at different frequencies. This receiver differential clock bias may be manufacturer-dependent, receiver-dependent, and may also drift at a level of tenths of nanosecond per day. In our process, the receiver clocks for GPS tracking at fiducial sites are synchronized to the GPS system clock through precise point positioning. The differential clock bias between GPS tracking and GLONASS tracking for the receiver is estimated as a stochastic model. Figure 4 shows the estimated differential clock bias for the Ashtech Z-18 receiver at site MDVZ. Three 3-day arc solutions are displayed; the same pattern is observed during the overlapping time period, indicating that some real signal is recovered in the process. The offset between solutions of different arcs is due to the reference clock. One receiver in the network is selected as a reference clock, whose differential clock bias is fixed to zero. The solutions exhibit 10 centimeter level drift of the differential clock bias.

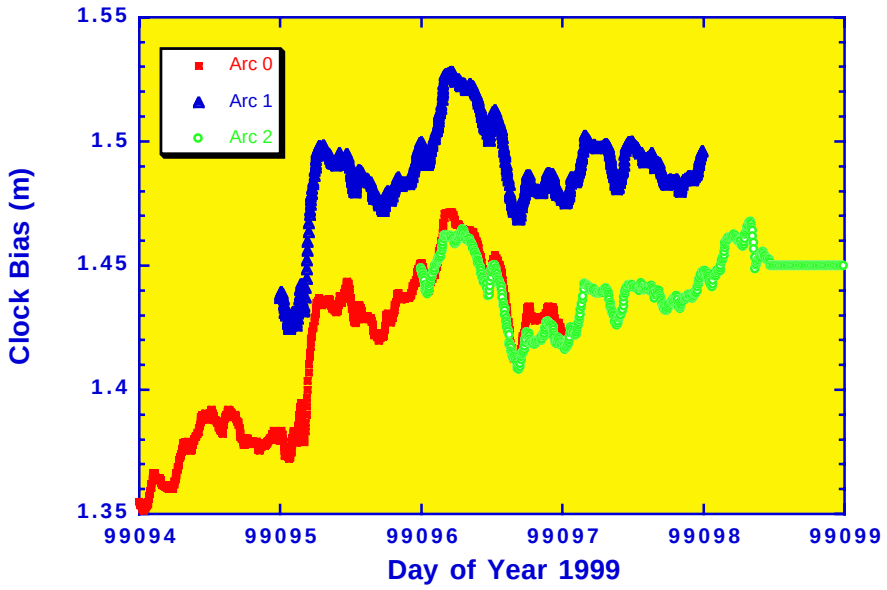

Figure 4. Differential clock bias for station MDVZ.

A by-product of the analysis is the transformation parameters between the two terrestrial reference systems, the ITRF96 system in which the precise GLONASS orbit is solved

for, and the Russian PZ-90 system in which the GLONASS broadcast ephemeris is defined. Our precise GLONASS orbit solution is compared with the broadcast orbit to solve for the 7 transformation parameters day by day. Although the accuracy of these parameters is limited by the error of the broadcast ephemerides (about 5 meters), the average of the time series over a certain period provides reasonably good information on the link between the two systems. Table 2 shows the values of the mean and standard deviation of the time series. Equation (1) explains the meaning of each term, where X, Y, Z are the coordinates in ITRF96 system and x, y, z are the coordinates in PZ-90 system.

$$\begin{bmatrix} X \\ Y \\ Z \end{bmatrix} = \begin{bmatrix} x \\ y \\ z \end{bmatrix} + \begin{bmatrix} Dx \\ Dy \\ Dz \end{bmatrix} + \begin{bmatrix} s & -Rz & Ry \\ Rz & s & -Rx \\ -Ry & Rx & s \end{bmatrix} \cdot \begin{bmatrix} x \\ y \\ z \end{bmatrix} \qquad (1)$$

Table 2. Mean and Standard Deviation of the Transformation Parameter Series

Dx (m)	Dy (m)	Dz (m)	s (ppb)	Rx (mas)	Ry (mas)	Rz (mas)
-0.139	0.027	0.088	0.16	-0.001	0.001	0.35
± 0.170	±0.175	±0.389	±5.04	±0.003	±0.003	±0.02

Summary and Discussions

A unique approach is taken to analyze the IGEX-98 data for GLONASS orbit determination. This approach does not process the combined GPS/GLONASS data, however, it provides a flexible tool to study the unknown features of GLONASS tracking data and satellite force perturbations. From the processing of three months of data in early 1999, orbit overlap evaluation demonstrated 20 centimeter level orbit precision for most of the GLONASS satellites. Repeatability of station position for non-fiducial stations, which are solved from GLONASS data only, is better than 4 centimeters. Despite the accuracy limitation of the broadcast GLONASS ephemerides, comparisons between the precise orbit solution and the broadcast orbit reveals a significant rotation around the Z-axis (about 1/3 millisecond of arc) between the ITRF96 and PZ-90 reference frames.

Based on the analysis of the three months' data, several issues need our attention. First, for the current constellation of the GLONASS satellites and the IGEX-98 data, there is insufficient strength to resolve many force parameters. At least for some of the satellites, fewer parameters and longer orbit arcs would help to obtain more robust orbit solutions. Second, real fiducial sites in the ITRF system for the GLONASS tracking network are needed. In our process so far, the so-called fiducial sites are tied to ITRF96 on a daily basis through precise point positioning with GPS, and long term stability is compromised

by the small reference system fluctuation day-to-day. A combined robust solution of station position in the ITRF system for some of these sites should be established after a certain period of IGEX-98 data has been analyzed. Besides these, the receiver differential clock bias is an interesting issue for GPS/GLONASS users. The existence of this bias affects the data processing and adds difficulties to users. For the users who explicitly double difference measurements, this clock bias does not cancel in between GPS and GLONASS differencing. For carrier phase measurement, the constant part of this bias will be absorbed into the phase ambiguity parameter and would not cause problems unless ambiguity resolution is sought. However, the temporal variation of the bias can affect high accuracy applications, if the bias drifts several centimeters during the period of a data pass. This issue, as well as a more accurate solar radiation pressure force model for GLONASS satellites, deserves more investigation.

Acknowledgment

The authors thank Pascal Willis for his help and for supplying various information about GLONASS satellites and data formats. This work was performed at the Jet Propulsion Laboratory, California Institute of Technology, under contract with the National Aeronautics and Space Administration.

Reference

Bertiger, W.I. et al., (1994). GPS Precise Tracking of Topex/Poseidon: Results and Implications, *J. Geophys. Res.*, Vol. 99(C12), pp. 24,449-24,464.

Haines, B.J., S.M. Lichten, J.M. Srinivasan (1995). GPS-like Tracking of Geosynchronous Satellites: Orbit Determination Results for TDRS and INMARSAT, AAS/AIAA Astrodynamics Specialist Conference, Paper AAS 95-372, Halifax, Nova Scotia, Aug. 14-17, 1995.

Lichten, S.M. (1990). Estimation and Filtering for High-Precision GPS Positioning Applications, *Manuscripta Geodaetica*, Vol. 15, pp. 159-176.

Revnivykh, S., V. Mitrikas (1998). GEO-ZUP Company, GLONASS S/C Mass and Dimension, IGEXmail Message No. 0086, Nov. 23, 1998.

Slater, J.A., P. Willis, W. Gurtner, C. Noll, G. Beutler, G. Hein, R.E. Neilan (1998). The International GLONASS Experiment (IGEX-98), *Proceedings ION GPS-98*, Sept. 15-18, 1998, pp. 1637-1644, Inst. of Navigation.

Wu, S.C., Y. Bar-Sever, S. Bassiri, W.I. Bertiger, G.A. Hajj, S.M. Lichten, R.P. Malla, B.K. Trinkle, J.T. Wu, J.T. Wu (1990). Topex/Poseidon Project: Global Positioning System (GPS) Precision Orbit Determination (POD) Software Design, JPL D-7275, Mar. 1990.

Wu, S.C. (1985). Differential GPS Approaches to Orbit Determination of High-Altitude Earth Satellites, in *Astrodynamics 1985*, Kaufman et al., Eds. (AAS/AIAA Astrodynamics Specialist Conference, Paper AAS 85-430), *Advances in the Astronautical Sciences*, Vol. 58, pp. 1203-1220.

Zumberge, J., R. Neilan, G. Beutler, W. Gurtner (1994). The International GPS Service for Geodynamics – Benefits to Users, *Proceedings ION GPS-94*, Salt Lake City, Sept. 20-23, 1994, pp. 1663-1666, Inst. of Navigation.

Zumberge, J.F., M.B. Heflin, D.C. Jefferson, M.M. Watkins, F.H. Webb (1997). Precise Point Positioning for the Efficient and Robust Analysis of GPS Data from Large Networks, *J. Geophys. Res*., Vol. 102, No. B3, pp. 5005-5017.

GLONASS Orbit Determination at the Center for Space Research

Richard J. Eanes, R .Steven Nerem, P.A.M Abusali, William Bamford, Kevin Key, John C. Ries, and Bob E. Schutz
Center for Space Research, The University of Texas at Austin
3925 West Braker Lane, Suite 200, Austin, Texas, 78712 USA

Abstract

In this paper we review the contributions of the Center for Space Research to the International GLONASS Experiment 98 (IGEX-98) campaign. These include 1) the temporary establishment of a GPS/GLONASS receiver at the IGS GPS site at McDonald Observatory in west Texas; 2) the evaluation of GLONASS orbits computed by different centers using Satellite Laser Ranging (SLR) data; 3) the computation of GLONASS orbits using SLR data and the CSR's UTOPIA software, and 4) the computation of GLONASS orbits using radiometric data and the Jet Propulsion Laboratory's GIPSY software. When used directly to compute range residuals relative to each center's radiometric orbit, we find the SLR data to be a very effective discriminator of the radial orbit accuracy. We also find that the mean of the SLR range residuals has a value of -5 cm, similar to what has been observed in SLR/GPS comparisons. Results from our SLR-determined GLONASS orbits shows the presence of a mean radial acceleration (positive away from Earth) of 4–5 nm/s^2. We examine whether any of this acceleration can be attributed to a "radiation rocket" force caused by the transmission of navigation signals from the satellites towards the Earth.

Introduction

The Center for Space Research at the University of Texas at Austin made several contributions to the International GLONASS Experiment 98 (IGEX-98) campaign. We temporarily established a Javad Legacy GPS/GLONASS dual-frequency receiver and single-depth choke ring antenna near the IGS GPS site at McDonald Observatory in west Texas. In addition, we have been computing GLONASS orbits using the Jet Propulsion Laboratory's GIPSY analysis software and the dual-frequency radiometric data from the global network supporting the IGEX-98 campaign. We have also analyzed satellite laser ranging (SLR) measurements to a half dozen of the GLONASS satellites to ascertain the accuracy of the GLONASS radiometric orbits, as well as for the determination of orbits based on the SLR measurements alone. It is this last contribution that is reviewed in this paper.

Radiometric Orbit Evaluation Using SLR Data

The most direct technique for evaluating the relative accuracy of the GLONASS orbits computed using the radiometric data is to compute the RMS difference of these orbits with the SLR measurements. The SLR ranges from the better stations have an absolute accuracy at the cm-level, and the station coordinates are also known to similar accuracy. Therefore, the SLR residuals can be a very effective discriminator between different orbits computed using different software packages and/or different analysis techniques. They are primarily an indicator of the radial accuracy, as the measurements are not as

sensitive to transverse and normal orbit variations for a satellite at the GLONASS altitude. Tables 1 and 2 show the weighted RMS of observed (SLR) minus computed (radiometric orbit) range residuals for GLONASS orbits computed by various IGEX analysis centers. We evaluated satellites 3, 6, 13, 16, 20, and 22, since these are the satellites that received tracking priority by the International Laser Ranging Service (ILRS) during the IGEX-98 campaign. SLR data were employed in the computation of the MCC orbits, and thus these results in Table 2 cannot be considered an unbiased estimate of orbit accuracy. In general, the best orbits (CODE and GFZ) appear to have a radial accuracy at around the 10-cm level. Exceptions to this are satellites 13 and 16, which seem to behave anomalously relative to the other satellites. Also note that the mean residual is roughly –5 cm (with the exception of satellites 13 and 16 on occasion).

Table 3 shows the same results for the IGEX combined orbit, which is a weighted average of the orbits from each IGEX analysis center. With the exception of satellites 13 and 16, the range residual RMS is less than 10 cm and the mean range residual is about –5 cm.

Table 1. Weighted RMS Residuals (cm) Using GLONASS SP3 Orbit Files from Each IGEX Center. Data from 20 SLR sites were used (CSR95L01 station coordinates) covering 1/24/99–2/20/99 (GPS weeks 994-997).

	CODE			ESA			JPL			GFZ		
SAT	# pts	Avg	rms	# pts	Avg	rms	# pts	Avg	rms	# pts	Avg	rms
3	518	-5.1	7.7	518	-9.6	19.1	517	-10.0	22.0	518	-5.4	10.0
6	570	-5.5	11.1	570	-9.1	13.2	567	-11.7	23.9	564	-6.8	11.6
13	385	3.2	10.5	385	-4.9	20.0	385	-8.9	17.8	385	-4.7	9.8
16	393	0.9	12.0	369	-6.2	41.7	393	-7.3	34.0	296	1.8	37.8
20	697	-6.3	9.4	697	-7.7	15.3	696	-9.0	21.5	697	-3.3	9.8
22	657	-8.1	10.4	657	-9.6	14.8	654	-14.9	26.1	658	-8.0	16.0

Table 2. Weighted RMS Residuals (cm) Using GLONASS SP3 Orbit Files from Each IGEX Center. Data from 20 SLR sites were used (CSR95L01 station coordinates) covering 11/1/98 – 12/19/98 (GPS weeks 982-988).

	CODE			ESA			BKG			MCC		
SAT	# pts	Avg	rms	# pts	Avg	rms	# pts	Avg	rms	# pts	Avg	rms
3	890	-2.9	9.0	890	-1.5	14.8	890	-4.6	17.1	890	-2.6	8.6
6	1173	-1.0	11.1	1173	-4.9	17.5	1173	-3.0	15.9	1173	-3.5	9.7
13	663	-5.5	33.0	663	-8.2	12.5	596	-0.3	43.3	663	-4.8	12.0
16	824	-4.5	36.3	632	-13.3	39.4	744	-1.4	42.5	841	-5.5	20.7
20	1456	-4.0	9.6	1456	-11.2	17.2	1456	-1.0	9.9	1456	-3.9	7.9
22	1488	-7.6	9.7	1488	-9.1	12.8	1488	-6.5	13.3	1488	-7.3	8.8

Table 3. Weighted RMS Residuals (cm) Using GLONASS SP3 Orbit Files for the IGEX Combined Orbit. Data from 20 SLR sites were used (CSR95L01 station coordinates) covering 11/1/98 – 12/19/98 (GPS weeks 982-988).

	IGEX		
SAT	# pts	Avg	rms
3	890	-3.2	7.5
6	1173	-2.4	9.4
13	663	-6.7	16.7
16	846	-5.8	24.0
20	1456	-3.9	7.9
22	1488	-7.3	8.8

Orbit Computations Using SLR Data

We computed orbits for GLONASS satellite 3, 6, 13, 16, 20, and 22 using the available SLR data. CSR's UTOPIA software was used for these computations. CSR97L01 station position and velocities were employed, along with the IERS C04 polar motion series. The JGM-3 gravity model was employed (Tapley et al., 1996) along with a GM value of 398600.4415 km^3/s^2. Solar and Earth radiation pressure were both modeled with a satellite reflectivity coefficient of 1.4. Because of the lack of availability of a detailed satellite model, we used values of 24 and 15 m^2 for the satellite cross-sectional area in the solar and Earth radiation pressure models, respectively. The latter value represents an approximate average of the variable cross-sectional area presented by the spacecraft towards the Earth. The mass of each satellite was assumed to be 1413 kg, and the offset

of the laser retroreflectors with respect to the center-of-mass was assumed to be 0, 0, -151 cm in the satellite-fixed xyz frame.

A 7-day arc length was used to analyze the SLR data. Over each arc, we estimated the initial position and velocity vectors, mean accelerations in the radial and transverse directions, and once/revolution accelerations (cosine and sine components) in the radial and normal directions. As shown in Figure 1, the RMS of the SLR normal point residuals was approximately 3 cm, although there was considerable variation from one week to the next. Figures 2 and 3 show the weekly values for the estimated radial once/revolution accelerations. Note that they tend to be quite coherent. The sine component tends to be the same for satellites occupying the same orbit plane, suggesting that the empirical acceleration are probably accommodating the mismodeled solar radiation pressure forces. Figure 4 shows the weekly values of the mean radial acceleration. Possible explanations for the 4.5 nm/s^2 mean of these apparent accelerations will be discussed in the next section.

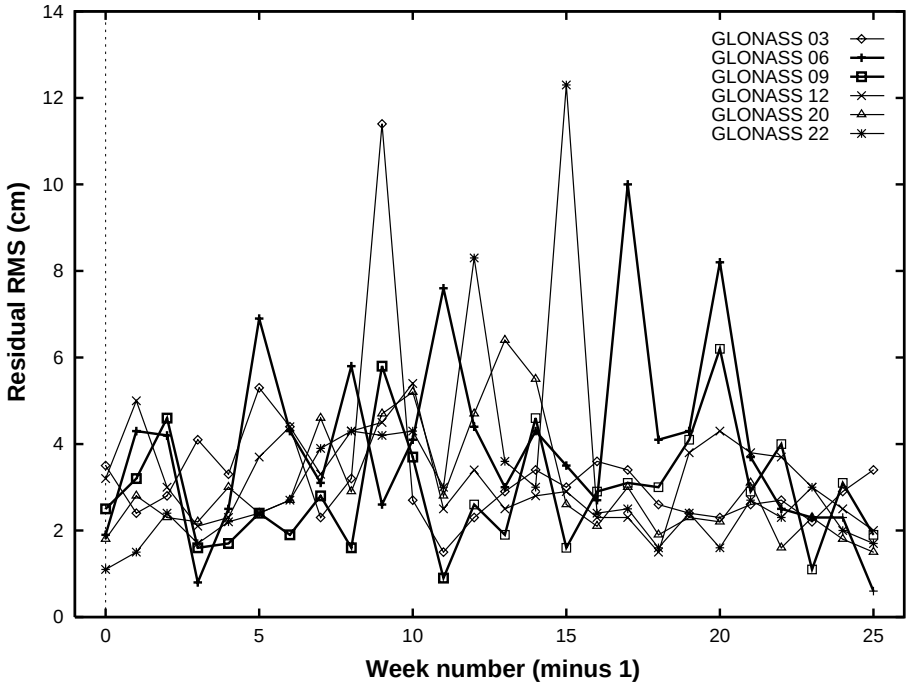

Figure 1. RMS of laser range residuals for GLONASS weekly arcs starting 13 Oct 1998.

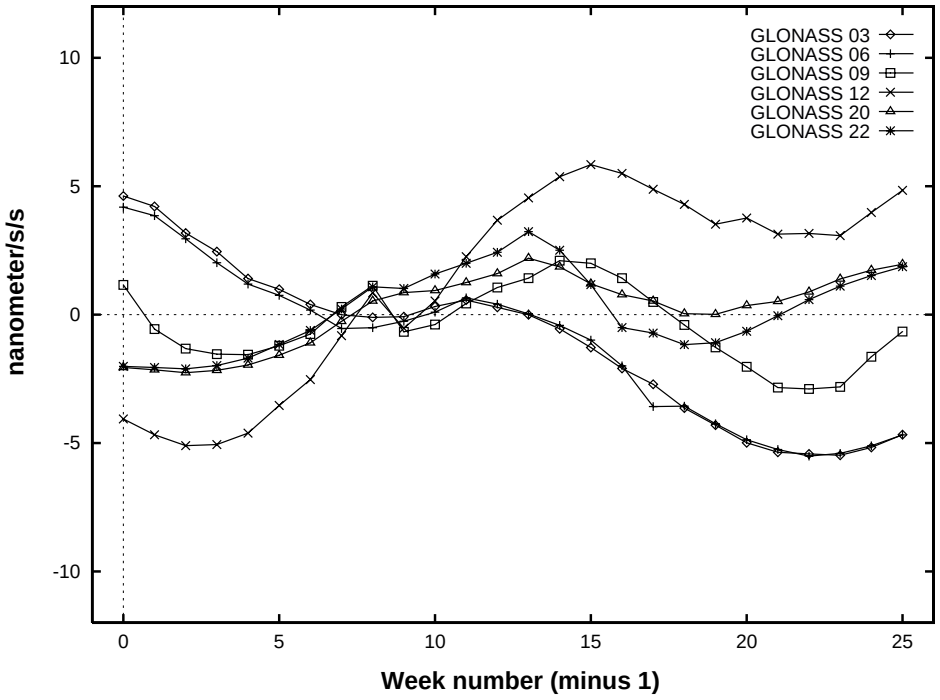

Figure 2. Cosine term of 1-cpr radial acceleration for GLONASS weekly arcs starting 13 Oct 1998.

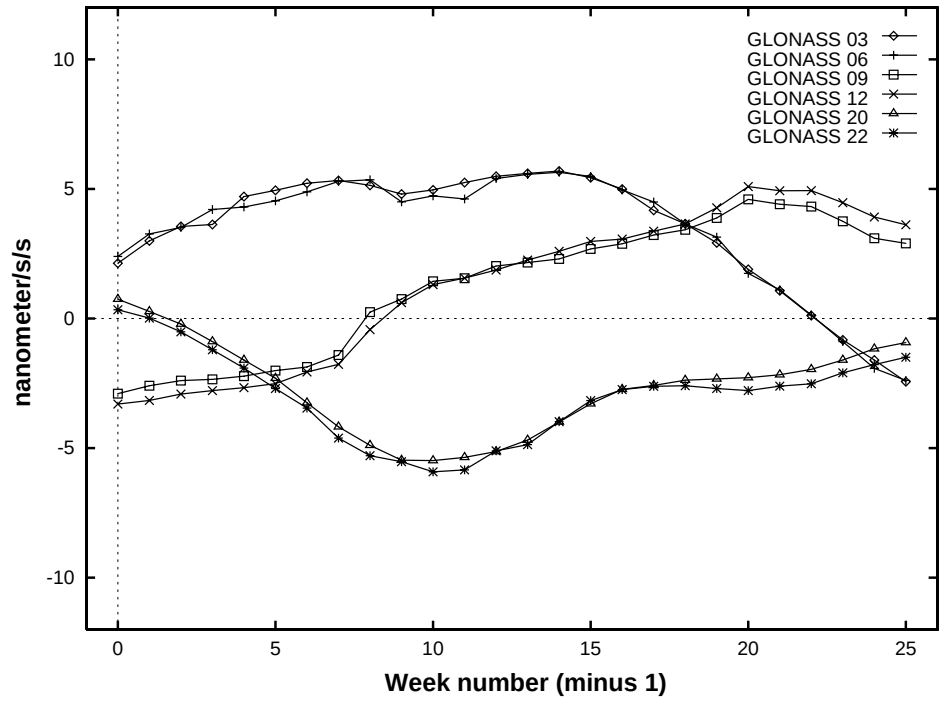

Figure 3. Sine term of 1-cpr radial acceleration for GLONASS weekly arcs starting 13 Oct 1998.

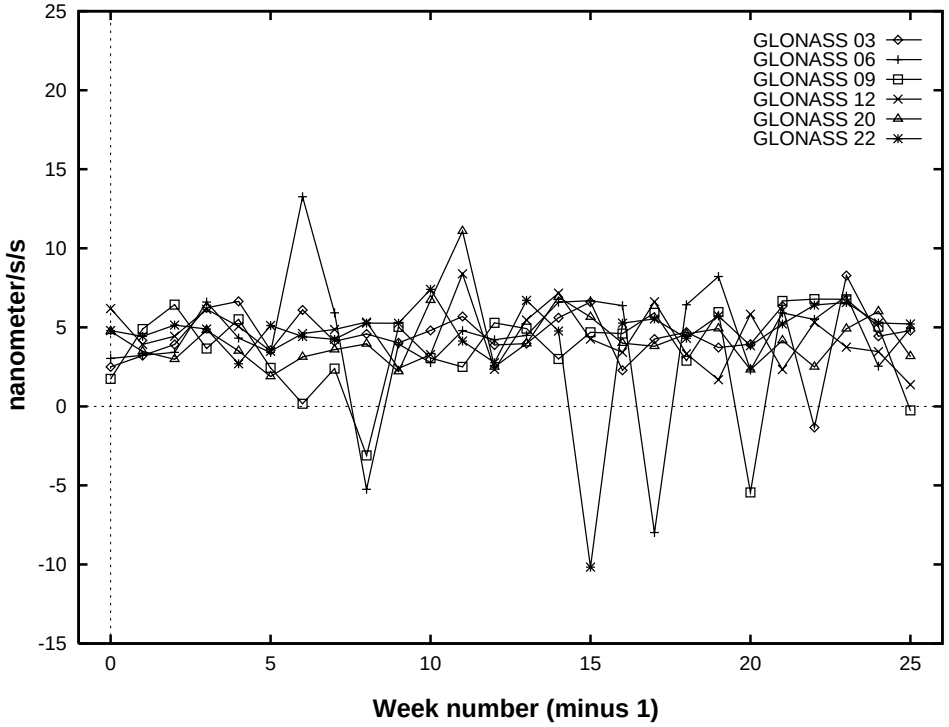

Figure 4. Mean radial acceleration for GLONASS weekly arcs starting 13 Oct 1998.

We compared the SLR GLONASS orbits with the radiometric GLONASS orbits computed by each of the IGEX analysis centers. The radial-transverse-normal RMS orbit differences were typically ~10 cm, 40 cm, and 45 cm respectively, with an overall 3-D position RMS of ~60 cm. It is difficult to use the SLR orbits to evaluate the accuracy of the radiometric orbits because the SLR orbit accuracy can be highly variable within a 7 day arc; anywhere from less than 10 cm when tracking coverage is good to over a meter when the coverage is poor. The mean radial difference of the SLR minus radiometric orbits varies considerably, but is consistently negative from center to center and week to week. The mean was approximate –7-8 cm, except for satellite 13 and 16, where the mean was a few centimeters smaller. A mean radial difference between the SLR and radiometric orbit occurs because we estimated a mean radial acceleration, and the recovered value for this acceleration is significantly different from zero.

GLONASS and GPS "Radiation Rockets"

We estimated a mean radial acceleration for the GLONASS SLR orbits because the power contained in the L-band signals being broadcast by the satellites is not insignificant. As a consequence, an outward (radial) force was probably acting on the satellites, as illustrated in Figure 5. This idea was originally suggested by (Milani et al., 1987), although their description of the resulting effect on the orbit is not what is observed in orbit determination strategies, since all the orbit elements will adjust to accommodate the tracking observations in a least squares sense. It should be noted that the radiometric data alone does not have the strength to reliably estimate a mean radial

acceleration because the estimation of other parameters (clock offsets, ambiguities, troposphere, etc.) dilutes the radial information content of the data.

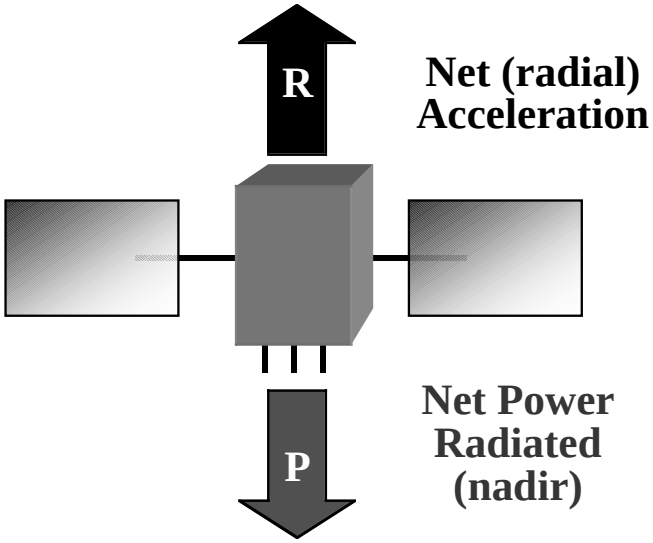

Figure 5. "Radiation Rocket" for GPS and GLONASS satellites.

We have little information on how much power is being transmitted by the GLONASS satellites, so we have used the GPS satellites as a model and assumed that the GLONASS satellites would be similar. The mean radial bias between the SLR and radiometric orbits was actually first detected on the GPS satellites (e.g. Springer et al., 1998). Table 4 shows the power being transmitted by the GPS satellites. We do not know how much power is being transmitted on the L3 or S band frequencies, but power is probably not transmitted continuously in these bands in any case. In our original analysis, we used the power values provided by (Langley, 1998), which led to a total transmit power estimate of 1092 Watts. As illustrated in Figure 5, the radial acceleration (R) on the satellite may be computed from the transmitted power (P) as R = P/(c x mass). For a 1413-kg satellite like GLONASS, the radial acceleration is 2.6 nm/s^2, whereas for a GPS satellite (1000 kg), it is 3.6 nm/s^2. This is clearly a large fraction of the observed radial acceleration on the GLONASS satellites. For GLONASS, 1 nm/s^2 is roughly equivalent to 1.2 cm of radial orbit bias. However, it was pointed out that the values given in (Langley, 1998) included the effect of antenna gain. The actual transmit power is considerably less (Aparacio et al., 1995), as shown in the last column of Table 4. This reduces the radiation rocket effect to 0.09 nm/s^2 for the GLONASS satellites, equivalent to only 0.1 cm of radial bias.

Table 4. Power Transmitted by the GPS Satellites (Langley, 1998; Aparicio et al., 1995)

	Transmitted Power		
Signals	dBW	Watts (with effect of antenna gain included)	Actual Watts
P Code on L1	23.8	240	10.7
P Code on L2	19.7	93	6.6
C/A Code on L1	28.8	759	21.9
Other (L3, S, ?)	?	?	?
Total		1092	39.2

Part of the radial biases observed in the orbits of the IGEX analysis centers may be caused by not modeling Earth radiation pressure, which contributes about 1 nm/s^2 of radial acceleration. Since Earth radiation pressure was modeled in our computations and the radiation rocket from the transmitted signals is too small, we must invoke other explanations for the remaining radial acceleration. One possibility is that the value of GM we employed is too large. If we reduce our GM value by 1-σ(0.0008 km^3/s^2) (Ries et al., 1992), this would explain 1 nm/s^2 of the observed mean radial acceleration. An error in GM much larger than this is considered to be unlikely.

Another possibility is an error in the modeled offset of the laser retroreflector array (LRA) from the satellite center-of-mass. It is impossible to evaluate the uncertainty in the location of the LRA without detailed information on the satellite dimensions and center-of-mass changes, and we have no information about the effect of the LRA design on the laser range biases. We hesitate, however, to attribute the apparent radial bias entirely to an error in the LRA location, since it is unlikely that the error would be similar for both the GPS and GLONASS satellites.

Conclusions

We have used SLR measurements and a precise set of station coordinates/velocities to evaluate the accuracy of the GLONASS radiometric orbits computed during the IGEX-98 campaign by the analysis centers. The orbits computed by the CODE and GFZ groups generally have a radial accuracy on the order of 10 cm, although the accuracy can be several times larger on occasion. The mean of the SLR range residuals is ~ -5 cm, indicating the radiometric orbits are 5 cm too high.

We have also computed GLONASS orbits independently using the SLR measurements only. We have observed a persistent 4–5 nm/s^2 outward radial acceleration that can fully explain the 5-cm bias in the SLR range residuals. It appears that the satellite broadcast signals are not large enough to be causing the observed radial acceleration after all. We might attribute a part of the apparent acceleration to an error in GM and the correction for the center-of-mass offset of the laser retroreflector array, but a source of several nm/s^2 acceleration is required to explain the rest. Failure to model Earth radiation pressure can contribute an additional 1 nm/s^2 to the apparent radial acceleration.

The relative insensitivity of GLONASS and GPS radiometric data to radial accelerations should be investigated further, as it may help explain some of the "common-mode" signals observed in time series of station positions. Further study of the forces acting on the GLONASS and GPS satellites is recommended. A carefully constructed error budget for the location of the LRA phase center for the GPS and GLONASS satellites is also essential to limit this area of uncertainty.

References

Aparicio, M., P. Brodie, L. Doyle, J. Rajan, P. Torrione (1995). GPS Satellite and Payload, in *Global Positioning System: Theory and Applications, Volume 1*, B. W. Parkinson and J. J. Spilker, Jr., Eds., pp. 209-214, American Institute for Aeronautics and Astronautics, Inc.

Langley, R.B. (1998). Propagation of the GPS Signals, in *GPS for Geodesy*, 2nd Edition, P.J.G. Teunissen, and A. Kleusberg, Eds., pp. 650, Springer-Verlag.

Milani, A., A. M. Nobili, P. Farinella (1987). *Non-Gravitational Perturbations and Satellite Geodesy*, Adam-Hilger, Bristol, England, 125 pp.

Ries, J. C., R. J. Eanes, C. K. Shum, M. M. Watkins (1992). Progress in the Determination of the Gravitational Coefficient of the Earth, *Geophys. Res. Lett.,* Vol. 19, No. 6, pp. 529–531.

Springer, T., M. Rothacher, G. Beutler (1998). GPS Orbit Biases, *Eos Trans*., Vol. 79, No. 45, p. F182.

Tapley, B. D., M. M. Watkins, J. C. Ries, G. W. Davis, R. J. Eanes, S. R. Poole, H. J. Rim, B. E. Schutz, C. K. Shum, R. S. Nerem, F. J. Lerch, J. A. Marshall, S. M. Klosko, N. K. Pavlis, R. G. Williamson (1996). The Joint Gravity Model 3, *J. Geophys. Res.*, Vol. 101, No. B12, 28,029–28,050.

GLONASS Precise Orbits as a Result of IGEX-98 Laser Tracking Campaign

Vladimir Glotov, Mikhail Zinkovski, and Vladimir Mitrika
Russian Mission Control Center
2 Pionerskaya Street, Korolyov of Moscow Region, Russian Federation

Introduction

There are different Mission Control Center (MCC) activities related to GLONASS/GPS issues. At this time the MCC is responsible for supporting GLONASS civil users in Russia. The Mission Control Center has certain technical capabilities, for example, receivers, precision clocks, and its own software for data processing (Figure 1).

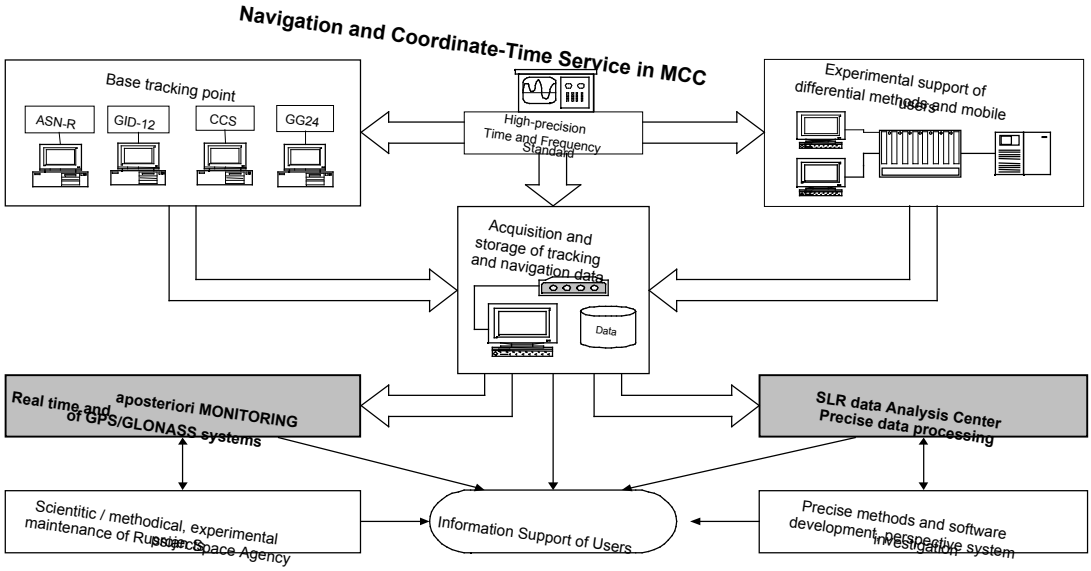

Figure 1. Technical capabilities and MCC activities related to GLONASS/GPS issues.

Recently in MCC new software was developed and real-time monitoring with a 30-second updating rate was established with a posteriori monitoring and continuous GLONASS/GPS performance analysis. Real-time monitoring data are available on-line via the Internet. The information is placed in real-time on MCC's web site with a rate of update equal to 30 sec. The following information is presented on the real-time monitoring web page:

- Satellites in view
- Estimated position
- User range error (URE) for satellites in view

Because the Mission Control Center is interested in different areas of activity related to GPS and GLONASS and has experience in SLR data analysis, MCC was a participant in the IGEX-98 campaign as an SLR Data Analysis Center for GLONASS.

The Results of the IGEX SLR Tracking Campaign

The second part of this presentation concerns the results of the IGEX SLR tracking campaign. Table 1 shows the total number of passes observed during the official duration of the IGEX-98 campaign. The results of the tracking campaign are very different for all stations. Seven stations out of the total 31 participating stations had less than 10 SLR passes each during the IGEX-98 campaign. Another seven stations (7090, 7110, 7845, 7849, 7840, 7839, 8834) provided about 70% of the SLR tracking data of the IGEX-98 campaign.

Table 1. Overview of Number of Passes Observed by SLR Stations During IGEX Campaign
(8 satellites, 17.10.98 – 30.04.99)

	1998			1999				
Station	Oct	Nov	Dec	Jan	Feb	Mar	Apr	Sums
1864			8	27	43	27	21	126
1868		4	15	5	33	20	4	81
1873	1	1						2
7080	15	54	41	45	35	23	26	239
7090	99	181	146	177	211	140	158	1112
7105	57	76	45	47	23	36	57	341
7110	79	150	153	131	144	137	59	853
7124	1	2	3	2	7	7	20	42
7210	31	23	53	49	16	38	21	231
7236	3		16	1			3	23
7237	45	54	65	60	17	20	12	273
7249		1	21	4	8		11	45
7328				1	2	8	8	19
7335					2	1	1	4
7337					2			2
7339					8	4	8	20
7548							1	1
7806							1	1
7810	13	28	32	71	28	48	2	222
7811	1	4	8	6	1	5	3	28
7820				2	21	7	3	33
7835			1					1
7836	12	21	21	18	10	15	11	108
7837	2	30	48	19	27	8	22	156
7838							4	4
7839	37	55	71	69	96	91	72	391
7840	20	61	49	86	57	58	67	398
7843	39							39
7845	41	136	106	159	72	63	21	598
7849	27	85	110	71	86	81	123	583
8834	30	46	41	53	40	88	80	378
Total	**553**	**1012**	**1053**	**1103**	**989**	**925**	**819**	**6454**

However, from a more detailed analysis of the SLR data we can see for many days there was not SLR tracking data for every satellite. For example (see Figure 2) for GLONASS-71 there were 5 days without SLR data, for GLONASS-72 there were 12 days without SLR data, and for GLONASS-62 there were 16 days without SLR data. The total for these three satellites in the third orbital plane was more than 30 days without SLR data.

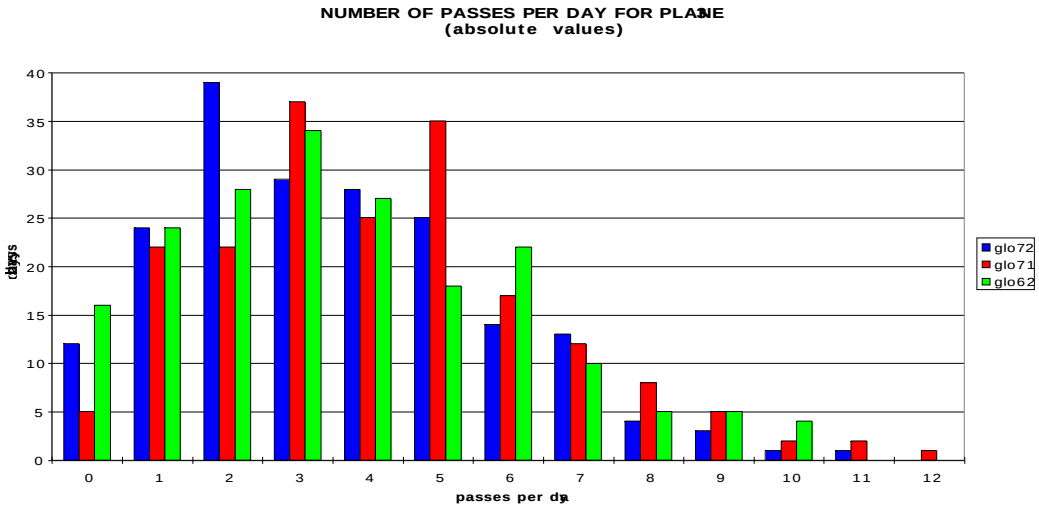

Figure 2. The results of analysis of the number of SLR passes per day for GLONASS-62, 71, 72.

The amount of SLR tracking data and the distribution of the data are very similar for all 8 satellites that were tracked by laser stations during the official IGEX-98 campaign (see Figure 3). For 8 satellites the number of days without SLR data was 89. In addition, there were more than 190 days with only one pass per day, etc. It is necessary to take into account when examining Figure 3 that the first and third orbital planes contain three satellites each (GLONASS-68, 69, 70 and GLONASS-62, 71, 72 respectively) and the second plane contains only two satellites (GLONASS – 66, 79).

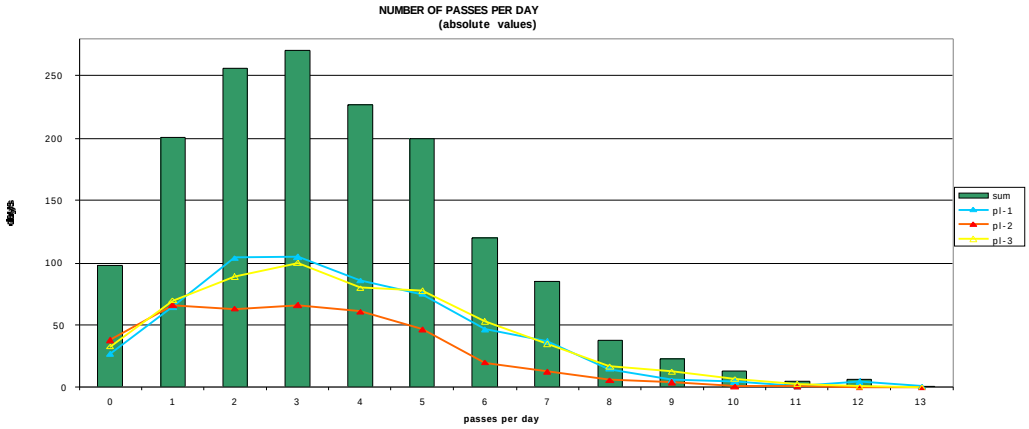

Figure 3. The results of analysis of the number of SLR passes per day for orbital planes 1, 2 and 3.

We can consider the cumulative average number of passes per day for all satellites. The number of passes per day is approximately the same for all of the satellites (see Figure 4). So for more than 50% of the days there were less than four SLR passes per day. Similar information is

provided for the number of laser measurement stations working per day. For comparison the number of SLR passes per day for ERS-1, 2 and LAGEOS-1, 2 is approximately 12-16 or more.

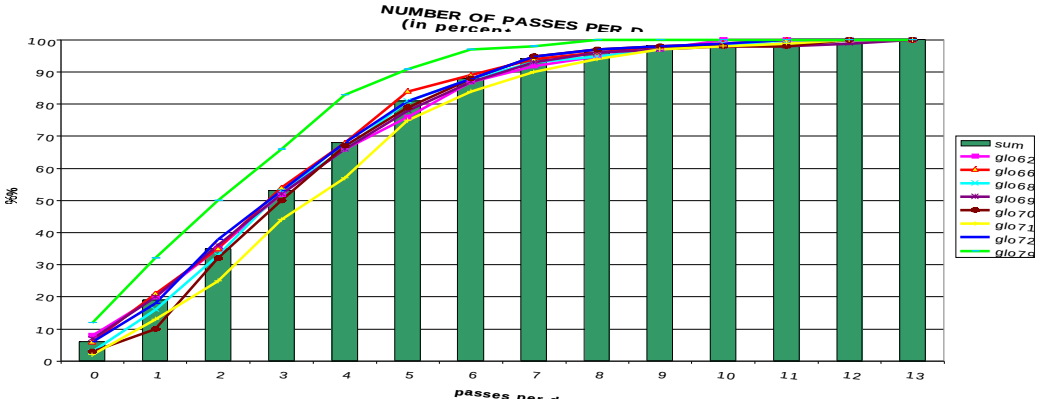

Figure 4. The cumulative number of SLR passes per day for all satellites.

Figure 5 shows the total duration of the SLR passes per day. As you can see, for more than 80% of the days the total duration of the SLR passes per day was less than four hours.

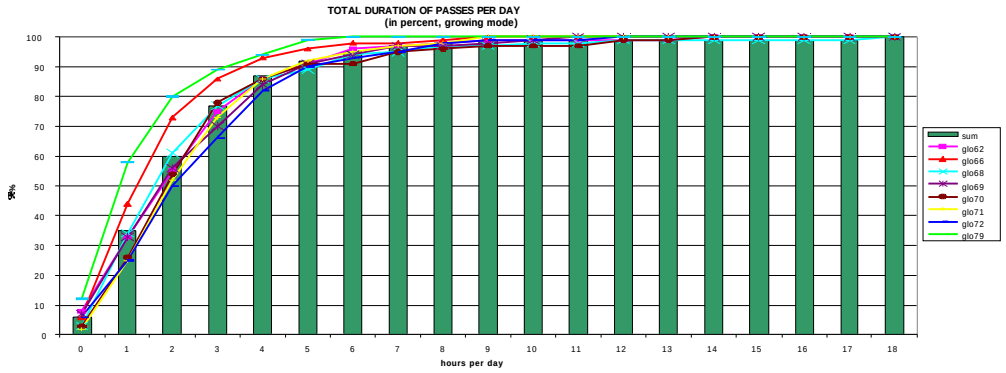

Figure 5. The total duration of the SLR passes per day for 8 GLONASS satellites.

Thus there were many days during the official IGEX-98 campaign when there were a small number of SLR passes per day for each satellite. It is necessary to take this into account during laser orbit analysis. The accuracy of the SLR orbit varies depending on the amount of SLR data and the distribution of the data.

The Determination of the Laser Orbits

The results of the orbital determinations in the Mission Control Center were formatted in the SP3 format and transmitted to CDDIS throughout the entire IGEX-98 campaign. The models that were used during the campaign had been verified by the experience of the Mission Control Center in the processing of SLR data in the past. These models generally followed the recommendations of IERS, with the exception of the direct and reflected solar pressure models,

which were developed by the Center in 1995 and 1996. The orbits of all of the satellites were solved independently during 8-day arcs. Neighboring solutions were independent because each arc started eight days after the beginning of the previous arc. This provided for monitoring of the accuracy of the orbital determinations by means of comparison of neighboring solutions.

Figure 6 shows statistics for GLONASS SLR data residuals for the typical satellite in one of the three orbital planes. Each point corresponds to one tracking pass for one station. The mathematical expectation of the residuals (the red points) were as a rule plus or minus 10 centimeters, and RMS (blue points) were approximately from two to five centimeters.

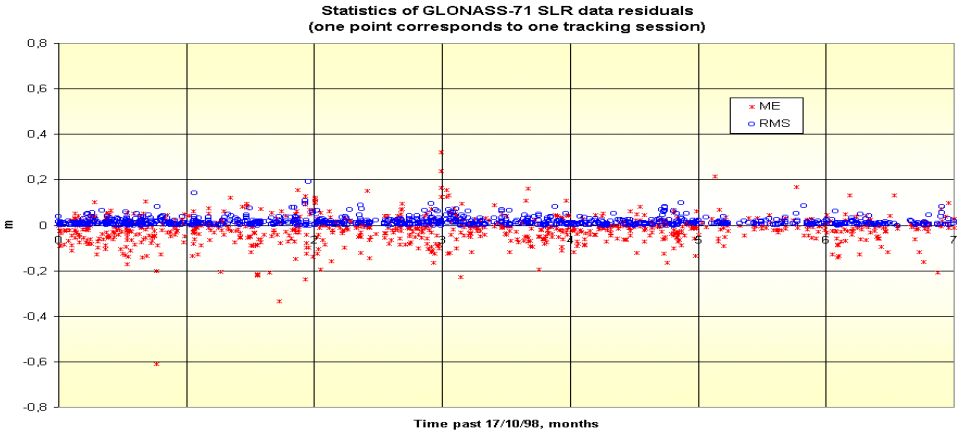

Figure 6. The statistics for GLONASS-71 SLR data residuals (third orbital plane).

In the other papers presented in this workshop, there is detailed information concerning MCC laser orbit accuracy in the comparison with other Centers' computed SLR orbits and receiver-based orbits.

The analysis of the accuracy of the SLR orbits in MCC additionally was based on the comparison of sequential independent orbits with predictions for either one half-day or two days. Figure 7 shows the RMS of the mean range difference between consecutive independent orbits. You can see that the results for different satellites are very similar.

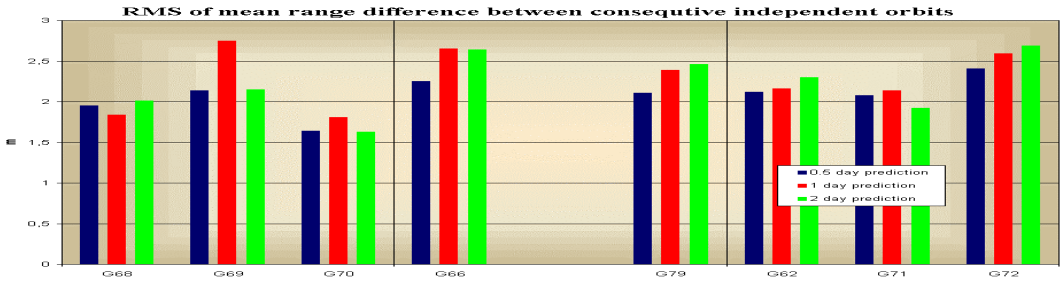

Figure 7. The estimation of accuracy of laser orbit predictions.

Figure 8 shows that in approximately 40 percent of the solutions the total difference between consequent independent orbits with one-half day predictions was less than one meter; the

difference for radial errors was less than 10 centimeters for approximately 70 percent of all cases. In this analysis we used approximately 90 percent of our orbit determination results, because certain results were not useable.

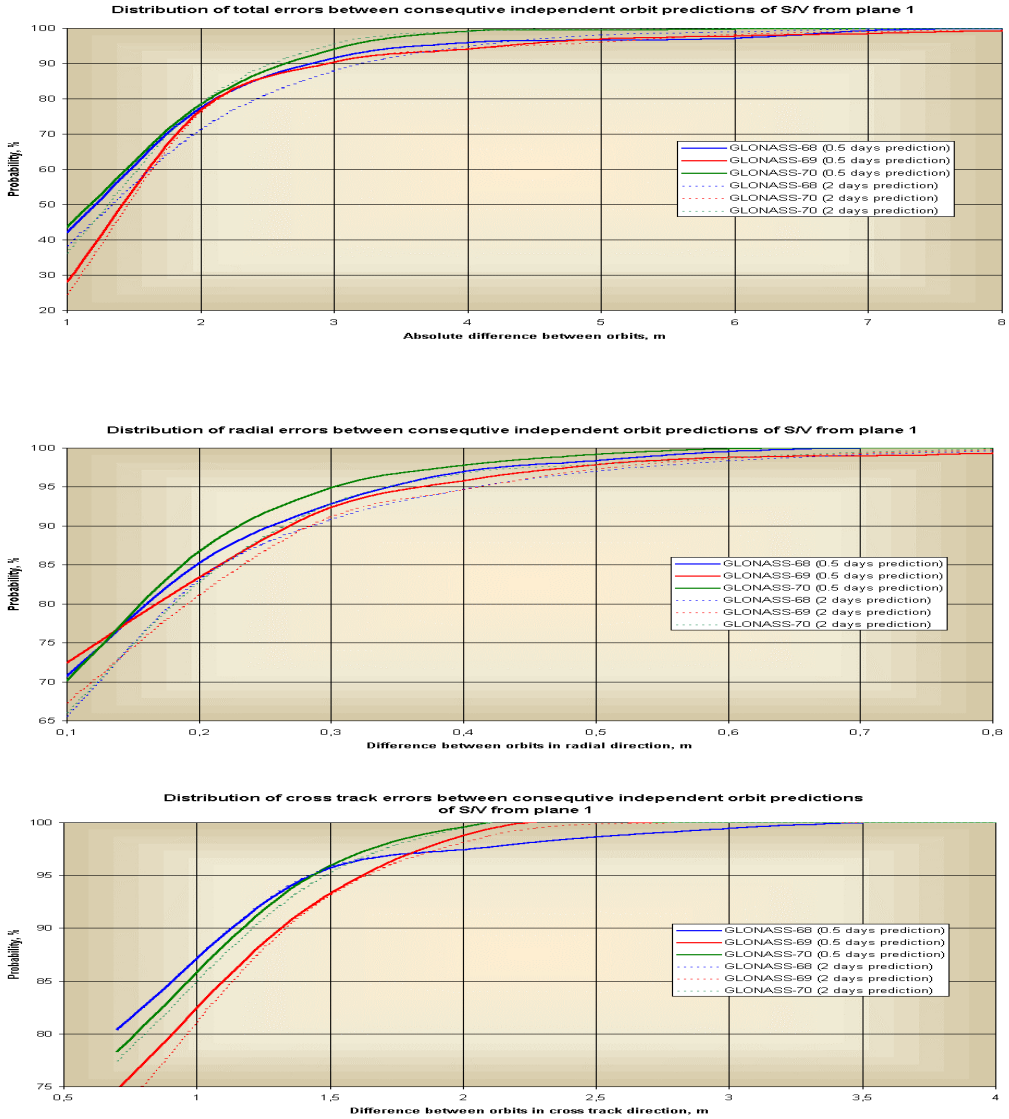

Figure 8. Distribution of errors between consequent independent orbit predictions of satellite vehicles from plane 1.

Conclusion

From 17 October 1998 to 27 April l999, there were 193 SLR tracking days for each of eight satellites. In all, there were a total of 1544 tracking days. For approximately 60% of the days there were less than four passes per day. The accuracy of the SLR orbits and the "phase" orbits for GLONASS is very close. The Mission Control Center is interested in the continuation of SLR orbit analysis in some future research context.

SLR GLONASS Orbit Determination

Ramesh Govind, John Dawson and Geoff Luton
Australian Surveying and Land Information Group
P.O. Box 2, Belconnen ACT 2616, Australia

Abstract

The intense observation campaign during IGEX-98 provided a data set that was used to compare and calibrate SLR- and microwave-determined GLONASS satellite orbits. Orbit determination of the GLONASS satellites was undertaken using the SLR data observed from November 1998 to March 1999. The resulting trajectories generated from this estimation process are compared to those produced by the Centre for Orbit Determination in Europe (CODE) IGS Analysis Centre using the microwave data. The results of these comparisons are presented and conclusions given in the form of differences in the satellite trajectories (radial, along- and cross-track) and a set of transformation parameters between these two orbit types. The precision of the estimated set of station coordinates (SSC) -- over the five monthly solutions -- is given in the form of their repeatability. The estimated SSC are compared to the ITRF97.

SLR Data

Five months of GLONASS SLR data (November 1998 to March 1999) observed to satellites 62, 65, 66, 68, 69, 70, 71, 72 and 79 during the IGEX-98 campaign were processed. Figure 1 shows the distribution of the 25 SLR stations that observed GLONASS during the IGEX-98 campaign.

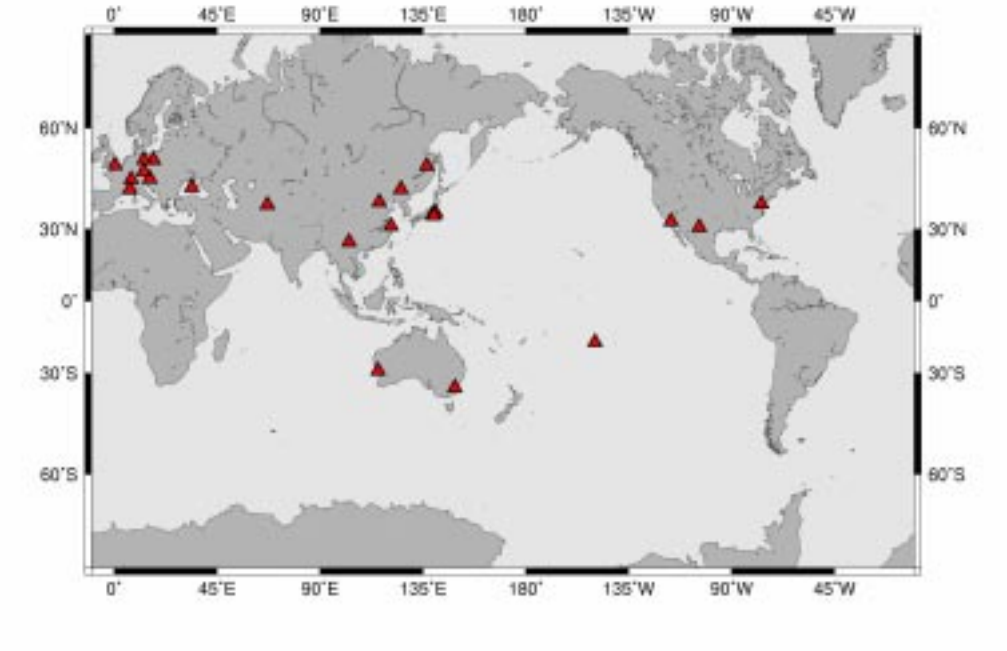

Figure 1. Distribution of observing IGEX-98 SLR stations.

Computation Standards

The IERS Conventions 1996 (IERS, 1996) were closely followed. In addition, the following parameters were used for the reference frame modeling and the satellite orbit modeling. The a priori set of station coordinates were those determined in previous solutions for Lageos-1 and Lageos-2. Since no specific Solar Radiation Pressure (SRP) Model for GLONASS was available, the ROCK IV GPS Block IIR SRP models (Fliegel and Gallini, 1992) were adopted as a priori and a SRP scale factor was estimated.

A Priori Reference Frame – (SSC)	AUSLIG* Hybrid CSR96l01/ITRF
Direct Solar Radiation Pressure Model	ROCK IV (GPS Block II)
Centre of Mass Correction / Attitude	Observation Correction applied -1510, 0, 0 mm

The following global and arc parameters were estimated for each monthly arc (for all satellites):

Global
- Station Coordinates
- EOP

Orbit
- 30 day arc
- 1 SRP scale factor
- pass by pass range bias
- pass by pass time bias
- general acceleration
  - constant
  - periodic 1/rev
  - every 5 days

* Australian Surveying and Land Information Group (AUSLIG)

Results and Analysis

Figures 2, 3 and 4 show the differences between the AUSLIG-determined SLR-based satellite trajectories and the Centre for Orbit Determination in Europe's (CODE) microwave-based orbit trajectories. These differences are shown in the radial, along- and cross-track components. The mean and rms of the differences in these components for GLONASS satellites 4, 3, 9, 16 and 6 are shown in table 1. Table 2 shows the set of transformation parameters between the AUSLIG SLR orbits and the CODE microwave orbits. Table 3 lists the month-to-month repeatability of the estimated SLR station coordinates. Table 4 gives the comparison between the estimated station coordinates and the ITRF97 – after transformation.

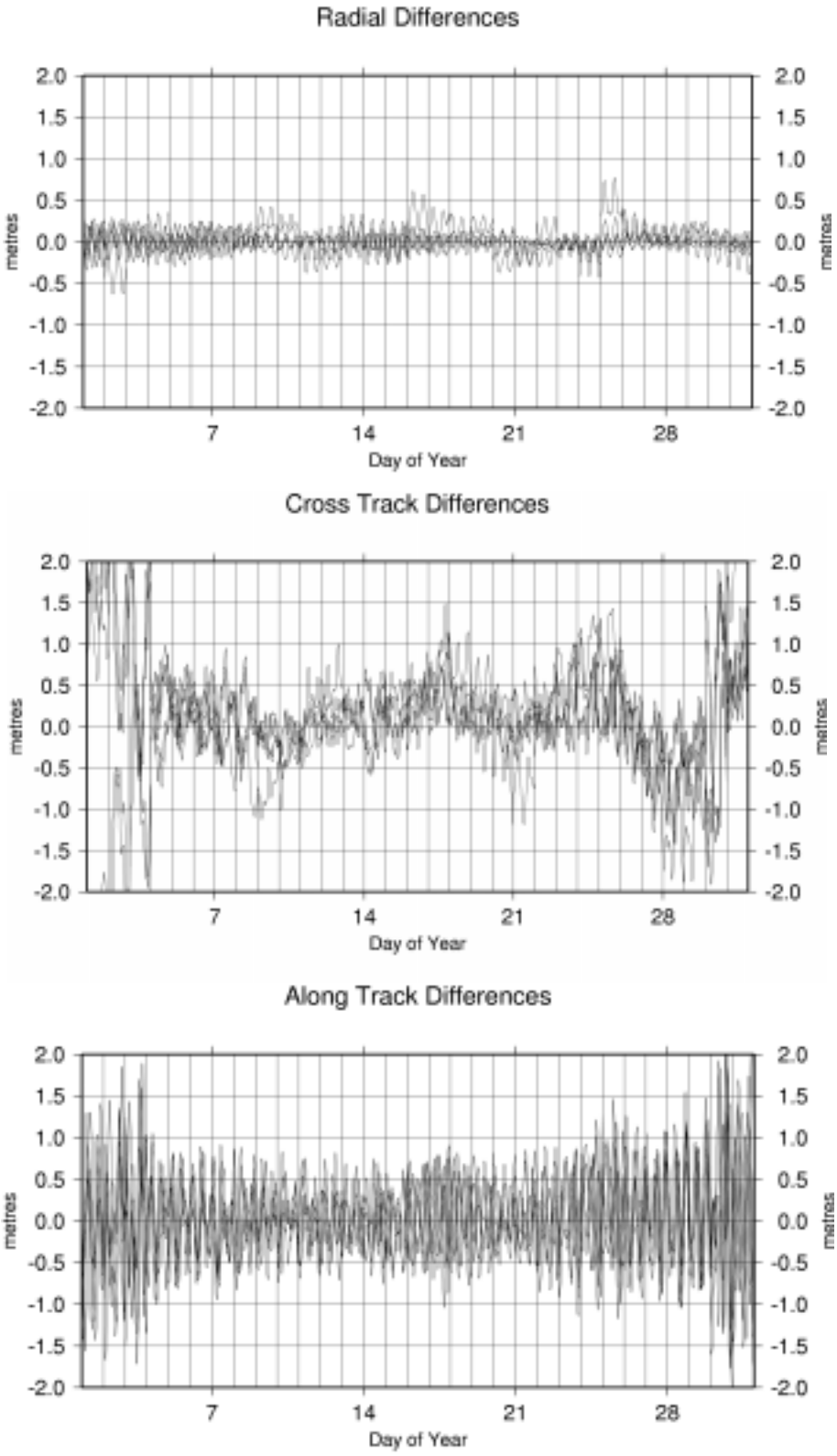

Figures 2, 3 and 4. AUSLIG SLR vs. CODE Microwave-Based Orbits --Trajectory Differences for January 1999.

Table 1. Trajectory Differences – AUSLIG SLR vs. CODE Microwave-Based Orbits for January 1999

		dX	dY	dZ	dDIFF	dCLOCK	dRADIAL	dLONG	dCROSS	N
R04	MEAN	0.004	0.004	-0.051	0.687		-0.004	0.246	0.044	2977
R04	RMS	0.536	0.498	0.454	0.497		0.084	0.641	0.569	2977
R03	MEAN	0.004	0.007	-0.049	0.593		-0.005	0.179	0.054	2977
R03	RMS	0.424	0.414	0.409	0.416		0.060	0.520	0.495	2977
R09	MEAN	-0.011	-0.014	0.015	0.694		0.013	-0.110	-0.020	2977
R09	RMS	0.512	0.425	0.554	0.500		0.137	0.722	0.458	2977
R16	MEAN	-0.005	-0.027	-0.015	0.741		0.037	-0.108	-0.011	2977
R16	RMS	0.584	0.511	0.603	0.567		0.220	0.821	0.492	2977
R06	MEAN	-0.003	-0.010	0.052	0.868		-0.007	0.286	0.051	2977
R06	RMS	0.608	0.652	0.656	0.639		0.113	0.955	0.548	2977

	dX	dY	dZ	dDIFF	dRADIAL	dLONG	dCROSS
MEAN	-0.002	-0.008	-0.009	0.717	0.007	0.099	0.024
RMS	0.537	0.507	0.543	0.529	0.135	0.747	0.514

Table 2. Transformation Parameters – AUSLIG SLR Orbit vs. CODE Microwave-Based Orbits

Scale	:	2.6782e-10 (+/- 4.76e-09) parts	0.27 (+/- 4.76) ppb
Rotation X	:	2.1815e-09 (+/- 5.66e-09) rad	0.45 (+/- 1.17) mas
Rotation Y	:	-6.2558e-09 (+/- 5.66e-09) rad	-1.29 (+/- 1.17) mas
Rotation Z	:	1.1637e-08 (+/- 2.18e-11) rad	2.40 (+/- 1.28) mas
Translation X	:	-0.003 (+/- 0.000) m	-0.25 (+/- 12.13) cm
Translation Y	:	-0.008 (+/- 0.000) m	-0.78 (+/- 12.13) cm
Translation Z	:	-0.010 (+/- 0.000) m	-1.02 (+/- 12.13) cm

Table 3. Month-to-Month Repeatability for Estimated SSC

STATION	PTCODE	TECH	#SOLN	X	Y	Z (mm-rms)	E	N	(mm-rms)	01234
1864	A	L	3	21	52	39	21	59	28	-P-PP
1868	A	L	4	-	-	-	-	-	-	-PPPP
1873	A	L	1	-	-	-	-	-	-	P----
7080	A	L	4	10	16	16	14	19	10	PPPP-
7090	A	L	4	17	5	2	14		7	8 PPPP-
7105	A	L	1	-	-	-	-	-	-	---P-
7105	A	L	3	-	-	-	-	-	-	PPP--
7110	A	L	4	6	21	14	6	23	10	PPPP-
7124	A	L	5	45	37	29	41	30	41	PPPPP
7237	A	L	5	29	38	35	34	45	18	PPPPP
7249	A	L	4	43	43	61	34	21	76	PPPP-
7328	A	L	2	31	23	3	3	25	29	---PP
7335	A	L	2	0	23	27	18	14	28	---PP
7337	A	L	1	-	-	-	-	-	-	---P-
7339	A	L	2	10	18	36	20	27	24	---PP
7810	A	L	4	8	3	8	3	7	10	PPPP-
7811	A	L	3	17	29	14	23	19	21	PPP--
7820	A	L	2	-	-	-	-	-	-	---PP
7835	A	L	1	-	-	-	-	-	-	-P---
7836	A	L	4	19	9	28	12		62	PPPP-
7837	A	L	5	47	36	37	49	38	32	PPPPP
7839	A	L	4	7	6	5	7	2	8	PPPP-
7840	A	L	4	8	6	10	6	8	10	PPPP-
7845	A	L	5	20	31	14	30	14	21	PPPPP
7849	A	L	5	30	26	49	22	40	43	PPPPP
8834	A	L	4	3	6	10	6	4	10	PPPP-
RMS				24	26	28	23	26	29	

Table 4. Comparison of Estimated SSC with ITRF97

	ID	PTCODE	DOMES	T	dX(mm)	dY(mm)	dZ(mm)	dE(mm)	dN(mm)	dU(mm)
1	7080	A	40442M006	L	-27.9	-97.5	-9.5	-3.5	-59.9	82.3
2	7090	A	50107M001	L	-81.1	24.2	10.3	62.9	36.5	44.4
3	7105	A	40451M105	L	-11.9	-111.1	-16.5	-36.9	-79.2	71.6
4	7110	A	40497M001	L	-28.1	-102.0	-16.5	20.2	-70.2	78.2
5	7810	A	14001S001	L	-1.4	-14.7	21.0	-14.4	16.8	13.1
6	7811	A	12205S001	L	36.9	-25.2	36.2	-34.9	0.1	45.7
7	7836	A	14106S009	L	0.0	0.0	0.0	0.0	0.0	0.0
8	7837	A	21605S001	L	0.0	-52.2	26.1	27.0	45.4	-24.8
9	7839	A	11001S002	L	17.4	-21.9	-5.5	-25.8	-11.8	3.4
10	7840	A	13212S001	L	5.0	-43.2	-5.4	-43.2	-7.1	-1.2
11	8834	A	14201S018	L	30.0	4.8	22.7	-2.0	-8.1	37.0
	RMS				31.4	59.4	18.5	30.8	41.3	47.0

Future Work

At the time of the computations, there was no readily available solar radiation pressure model for the GLONASS satellites. The orbit determination computations were therefore based on a GPS solar radiation pressure model as an initial guess. It is therefore proposed to continue to experiment with other empirically determined GLONASS solar radiation models – monitoring any improvement in the orbits.

The next stage is to undertake the analysis of the GLONASS microwave data and make direct comparisons between the two measurement types – with a view to combining them.

References

Fliegel, H. F., T.E. Gallini (1992). Global Positioning System Radiation Force Model for Geodetic Applications, *J. Geophys. Res*., Vol. 97, No. B1, pp. 559-568.

IERS (1996). IERS Conventions, IERS Technical Note 21, D.D. McCarthy (ed.), Observatoire de Paris, July 1996.

Combined GLONASS Orbits

Robert Weber and Elisabeth Fragner
Institute of Geodesy and Geophysics
University of Technology, Vienna
Gusshausstrasse 27-29, A-1040 Vienna, Austria

Abstract

IGEX-98, a worldwide GLONASS observation campaign, was scheduled for a six-month period starting in October 1998. About 75 organizations agreed to contribute to this Experiment and most of them are in fact suntil active within IGEX. For details about organizational aspects of the campaign, the tracking network as well as the data flow and the comprehensive list of the mission goals we refer to (Willis and Slater, 1999; Noll et al., 1999; Slater et al., 1999).

The estimation of GLONASS satellite orbits at the 1m accuracy level or even better was identified as one of the principal aims of the campaign. Besides five institutions that provided orbital information for selected weeks, six IGEX Analysis Centers calculated precise satellite ephemerides more or less regularly over the duration of the whole experiment. This paper deals in principal with the consistency and quality of these ephemerides and highlights the fundamentals of the orbit combination strategy.

Introduction

An important role for the success of IGEX falls to the Analysis Center (AC) working groups. Several groups agreed to process the IGEX data and until the end of June 1999 at least six ACs were able to deliver (more or less regularly) precise GLONASS orbits and station coordinate solutions. The products of BKG (Federal Bureau for Cartography und Geodesy, Germany), CODE (University of Berne, Switzerland), ESOC (European Space Operations Center) and MCC (Mission Control Moscow) cover the whole duration of the basic field experiment. Due to the fact that the MCC solution is solely based on laser distance measurements, the delivered ephemerides are restricted to the number of satellites tracked by the International Laser Ranging Service (ILRS) (9 satellites from October 98 until April 99 and 3 satellites afterwards). GFZ (Geoforschungszentrum, Potsdam, Germany) stopped processing GLONASS orbits in GPS Week 1002, but recently the JPL (Jet Propulsion Laboratory,USA) started calculating ephemerides covering all the weeks in 1999 (since GPS Week 991).

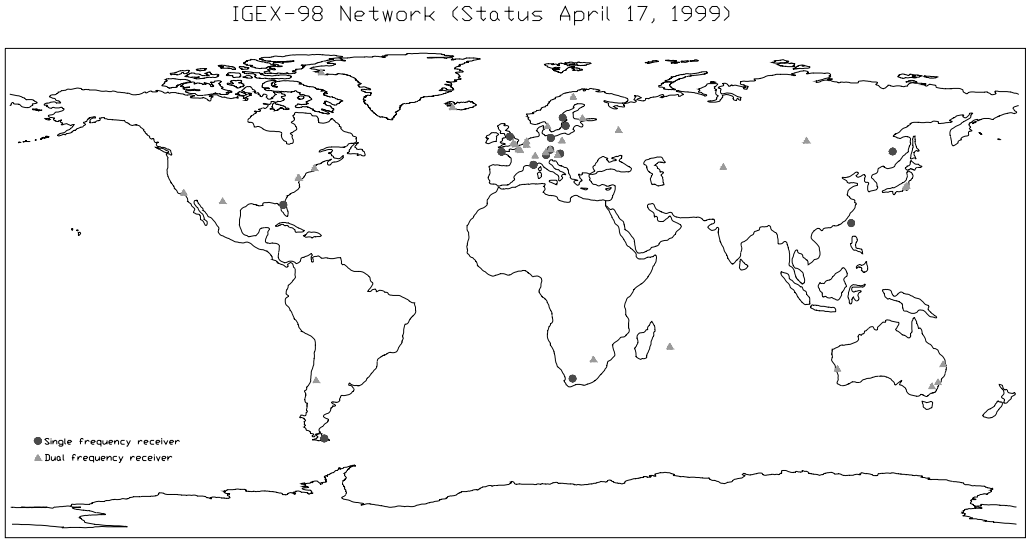

Figure 1. IGEX-98 global tracking network on April 17, 1999.

Figure 1 shows the status of the global tracking network on April 17. The distribution of the sites is of course not comparable to the current IGS/GPS network but is in a way similar to the IGS network in 1992.

Orbit Combination Strategy

Although the ACs base their computation on different data types (microwave phase and code data, laser ranges), different basic variables (zero and double differences), different parameterization of the force field and different arc-lengths (3 days up to 8 days), all of them were able to estimate GLONASS orbits well below the 1 meter accuracy level and consistent at about 30cm from the start. Figure 2 shows the results of a 7-day arc evaluation. Each satellite has been characterized by a state vector and 9 solar radiation pressure parameters. Similar to the GPS, the solar radiation pressure is the major error source in the orbit modeling. Thus we will discuss the applied parameterization in detail later. The symbols in Figure 2 denote the median value of the coordinate rms calculated from the daily center solutions with respect to the long arc.

In April 1999 it was decided to process a combined GLONASS orbit, based on the individual precise center solutions. The advantage of such a combination is the increased reliability of the orbits. Moreover all satellites included in at least one center solution are considered (Beutler et al., 1995).

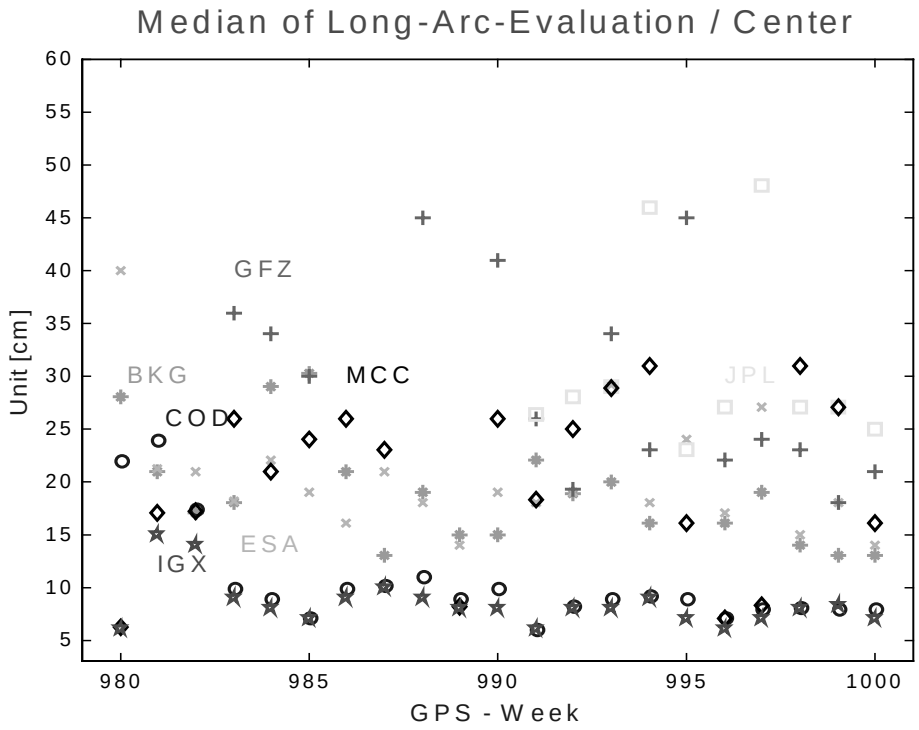

Figure 2. Median values (in centimeters) of coordinate rms values calculated from the daily center solutions with respect to the long arc (week nos. 980-1000).

First of all we have to obtain weights (weight per satellite and center) characterizing the weekly satellite performance within the center solutions. Thus the satellite positions are input (pseudo-observations) to establish seven-day arcs and afterwards the weights are calculated from the post-fit residuals of this long arc evaluation. After applying small center-specific reference frame corrections, the combined IGEX solution (labelled IGX in Figure 2) is finally calculated as a weighted mean of the available center satellite positions. The Earth Orientation Parameters are fixed to the values of the final IGS combination of the week. Contrary to the IGS-GPS combination the satellite clocks currently given in the IGX SP3 files are broadcast values.

The IGX precise ephemerides as well as a weekly report can be retrieved from the global IGEX data centers (e.g., CDDIS; igex/ products directory). The summary file contains comprehensive information on the quality and consistency of the individual center solutions. For example, the seven parameters of a spatial Helmert transformation, performed daily, with respect to the combined orbit and the center specific rms of this transformation (see Figure 3) are listed.

It has to be mentioned that our combination model gives preferential treatment to orbit submissions based on increased arc-lengths. This fact is evident in Figure 3 for CODE (five day arcs; labelled with circles) and MCC (eight day arcs; labelled with squares). The remarkable variations in the rms numbers of the MCC can be explained by the varying amount of available laser tracking data.

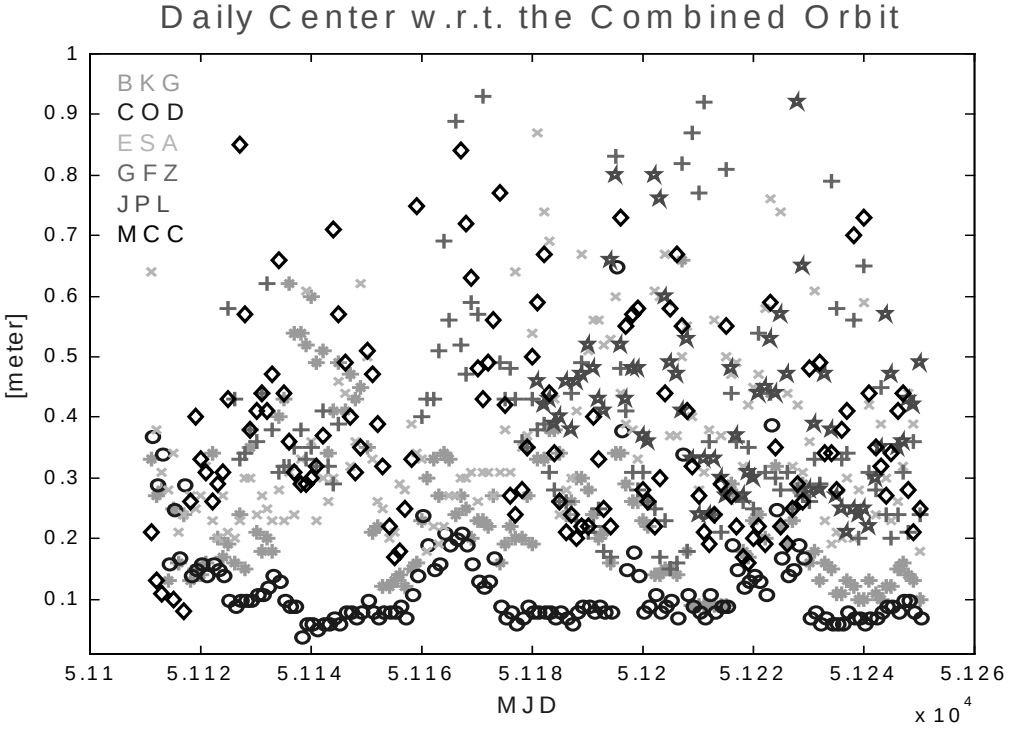

Figure 3. Period GPS Week 980 – Week 1000.

Another interesting point concerns the stability of the reference frames of the different center submissions, characterized for instance by the time series of the rotation angles of the Helmert transformation. The small rotations plotted in Figures 4a to 4d are daily mean values of all GLONASS satellite orbits calculated by the specific center. Therefore few peaks may be caused by one or the other outlier but a qualitative interpretation is suntil instructive. Note, that the scale in all graphics given below is identical and the period covered is again Week 980 to Week 1000. We have chosen for discussion the BKG, ESA, GFZ and MCC submissions in the subsequent examples.

The first plot is related to the BKG ephemerides. Rotations around the x- and y-axes show a very smooth behaviour (this is also true for the remaining 5 individual center solutions). Of particular interest are the rotations around the z-axis. There are no remarkable peaks visible in Figure 4a which is on the other hand a clear indication for the high weight of the BKG submission in the combination process.

The ESA graphic (Figure 4b) shows a similar behavior with a somewhat increased scatter. In contrast, Figure 4c demonstrates very impressively modeling deficiences before Week 988 (=MJD 51160). It is supposed that this problem was related to an inadequate modeling of the solar radiation pressure within the first weeks of the campaign.

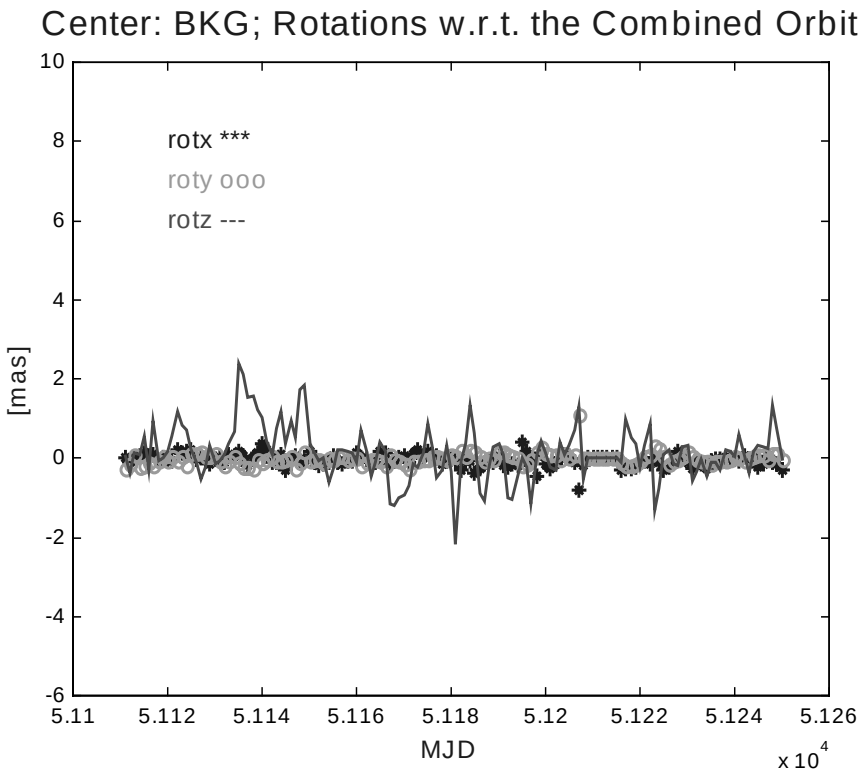

Figure 4a. BKG. Daily mean values of Helmert transformation rotation angles of all GLONASS satellites.

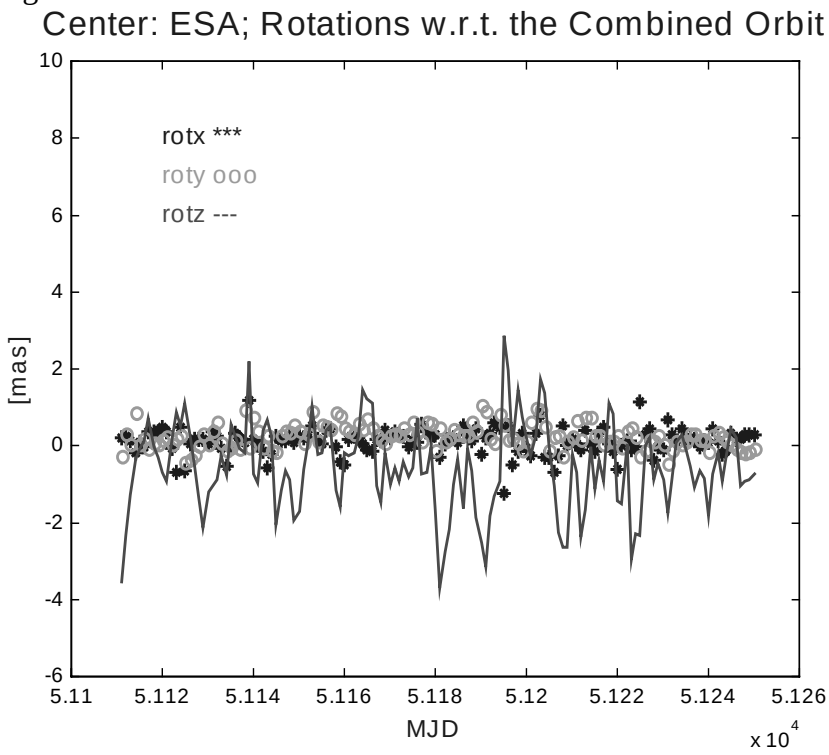

Figure 4b. ESA. Daily mean values of Helmert transformation rotation angles of all GLONASS satellites.

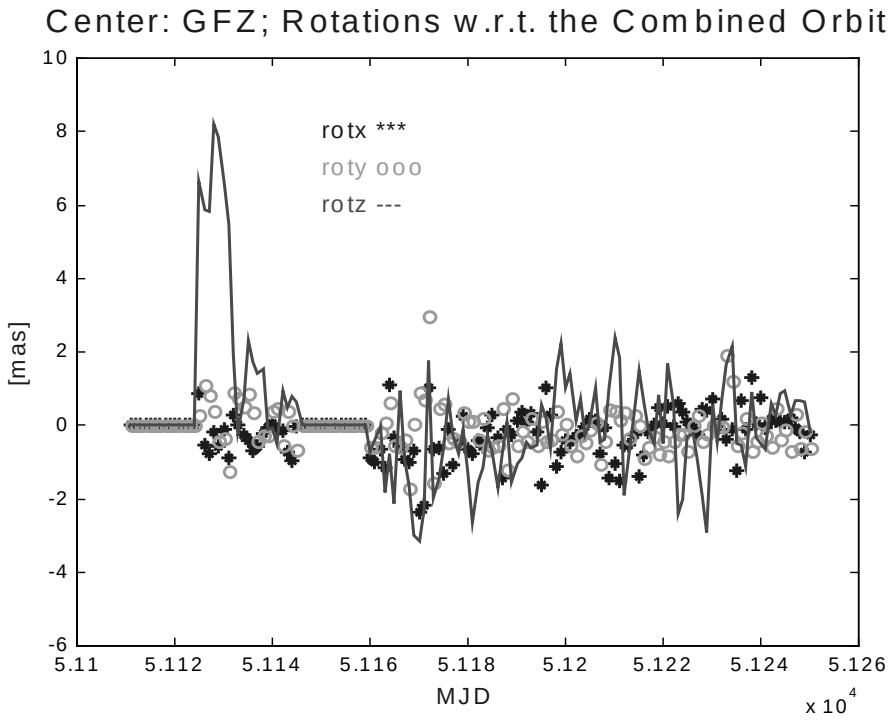

Figure 4c. GFZ. Daily mean values of Helmert transformation rotation angles of all GLONASS satellites.

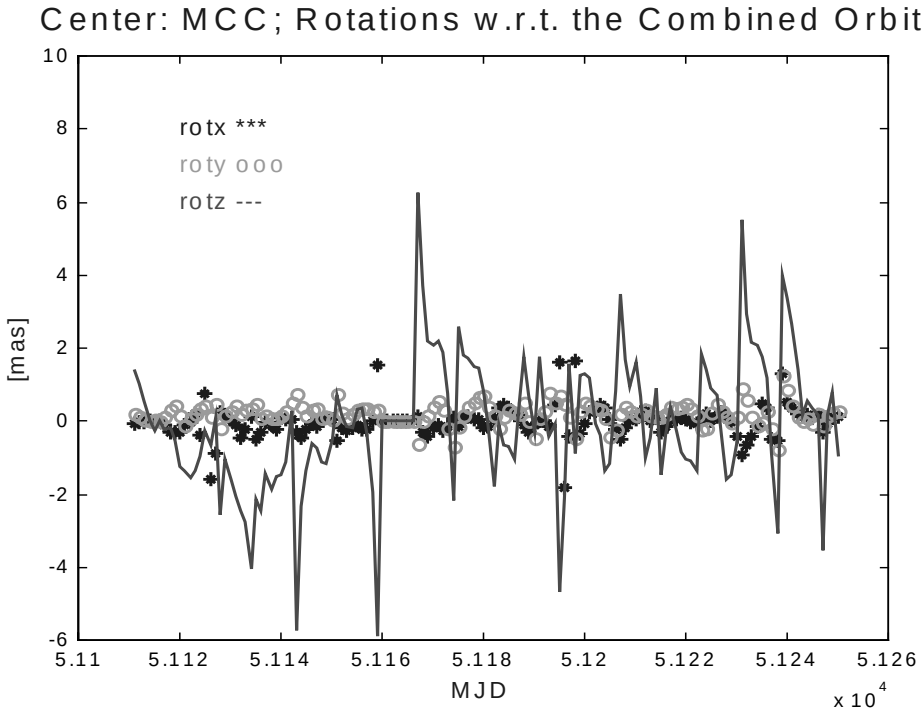

Figure 4d. MCC. Daily mean values of Helmert transformation rotation angles of all GLONASS satellites.

Very significant peaks can be identified in Figure 4d. The most prominent jumps of the z-rotation show up with an 8-day period, which coincides exactly with the arc-length of the MCC orbit solutions.

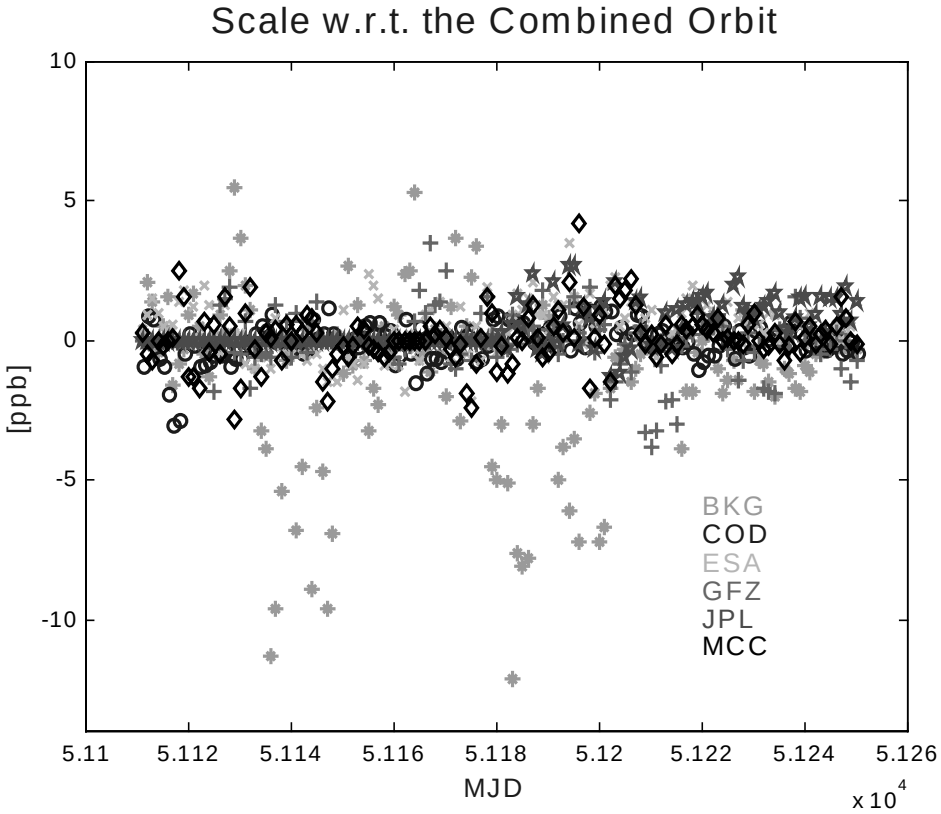

Figure 5. Value of the scale parameter computed by the ACs relative to the combined orbit scale parameter.

Figure 5 demonstrates the behaviour of the scale parameter with respect to the combined orbit. Scale factors vary from –3 to +3ppb for most of the daily center solutions. Only the BKG submissions show some outliers (up to 12 ppb) until the end of Week 993, which may be caused by a lack of ´fixed´ stations in the GLONASS solution (Habrich, private communication).

Radiation Pressure Model

The IGS processing allowed investigation various parameterizations of the solar radiation pressure. Besides the well-known ROCK-models, purely empirical models with 2, 5 or up to 9 parameters are available, sometimes used in combination with stochastic accelerations in the body-fixed system.

The acceleration a_{rpr} due to the solar radiation pressure may be modelled as

$$a_{rpr} = a_{Rock} + D(u)\cdot \vec{e}_D + Y(u)\cdot \vec{e}_Y + X(u)\cdot \vec{e}_X$$

with

$$D(u) = a_{D0} + a_{DC} \cdot \cos(u) + a_{DS} \cdot \sin(u)$$
$$Y(u) = a_{Y0} + a_{YC} \cdot \cos(u) + a_{YS} \cdot \sin(u)$$
$$X(u) = a_{X0} + a_{XC} \cdot \cos(u) + a_{XS} \cdot \sin(u)$$

and

a_{Rock}	the standard models ROCK4/42
$\vec{e}_D$	the unit vector Sun - Satellite
$\vec{e}_Y$	the unit vector pointing along the spacecraft's solar panels axis
$\vec{e}_X$	the unit vector in direction $\vec{e}_X = \vec{e}_Y \times \vec{e}_D$
u	the argument of latitude of the satellite
a_{i0}	the constant terms in the three axis
a_{iC}, a_{iS}	the periodic coefficients in the three axis

Note, that the Y-direction of this system corresponds to the Y-direction of the body fixed coordinate system (convention for the Fliegel ROCK models; argument: solar angle).

It is obvious that similar models are in use to describe solar radiation pressure for GLONASS satellites. For example, the ESA/ESOC Analysis Center estimates the three constant terms and the periodic terms in X-direction (Garcia et al., 1999). The authors selected the solar angle as the argument which is the argument of latitude corrected for the latitude of the sun in the orbital plane (see also, Rothacher et al., 1995). At the JPL Analysis Center the solar radiation pressure force is modelled by a scale factor, a constant Y-bias and stochastic accelerations (Da Kuang et al., 1999).

The complete set of 9 model coefficients has been estimated to establish Center-Specific seven-day arcs and to obtain weights as described in the next section. Although the resulting IGX-orbit originates from a weighted mean (not from a dynamical fit), it satisfies the equation of motion under the assumption that the sum of the Center weights equals 1. Therefore we used this parameterization to validate the combined (IGX) orbit. The behaviour of the constant direct term and the traditional Y-bias are shown in Figures 6 and 7 respectively. Furthermore the diagrams distinguish between satellites in the three orbital planes (plane I: solid; plane II: dotted; plane III: dashed).

First of all we recognize a similar behaviour for all satellites in the same plane except for Slot 18 (GLONASS Nr. 758). The direct solar radiation pressure acceleration is usually around $110 \cdot 10^{-9}\, m/s^2$, the Y-bias is in the order of $0.2 \cdot 10^{-9}\, m/s^2$. The latter is significantly smaller than the corresponding value for GPS-satellites. The constant term in X-direction (not shown) is larger by a factor of two than the Y-bias. Very interesting in Figure 6a is the distinct peak at Week 988 indicated by all satellites of plane II. To explain this jump we give in addition the variations of the rms of a_{D0}.

The vertical axis in Figure 6b varies from [0 to $1 \cdot 10^{-9}\, m/s^2$]. Obviously, a_{D0} is very poorly determined for plane II satellites. The Y-bias shows a complete contrary course. Compared to planes I and III, this value is very well determined for satellites in plane II

around Week 988. Twelve weeks later the rms seems to increase considerably (Week 998-Week 1000). The vertical axis of Figure 7b varies from 0 to $0.02 \cdot 10^{-9}\, m/s^2$.

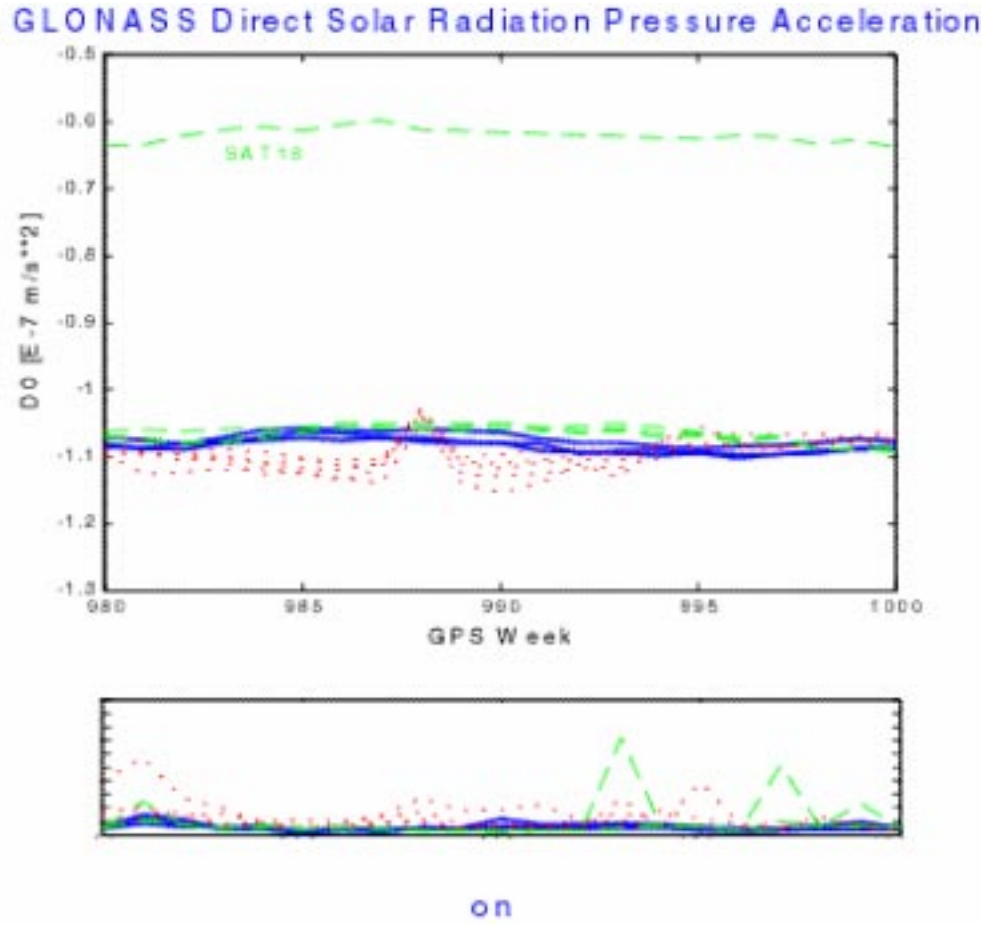

Figures 6a,b. a_{D0}; rms (a_{D0})

We have to introduce the angle β, denoting the elevation of the sun above (or below) the orbital plane. β can vary between $\pm(i + 23.45^o)$ where i stands for the inclination of the satellite's orbit. Calculating β for Week 988 we find that the elevation of the sun above plane II became approximately 88^o. According to (Rothacher et al., 1995) in the case of $\beta \to \pi/2$ a perturbation parallel to the sun-satellite direction is a constant out-of-plane acceleration which can easily be verified by the residuals of the long arc evaluation. The perturbation due to the Y-bias, which is determined very well, is a constant along-track acceleration (the sign depending on the position of the sun).

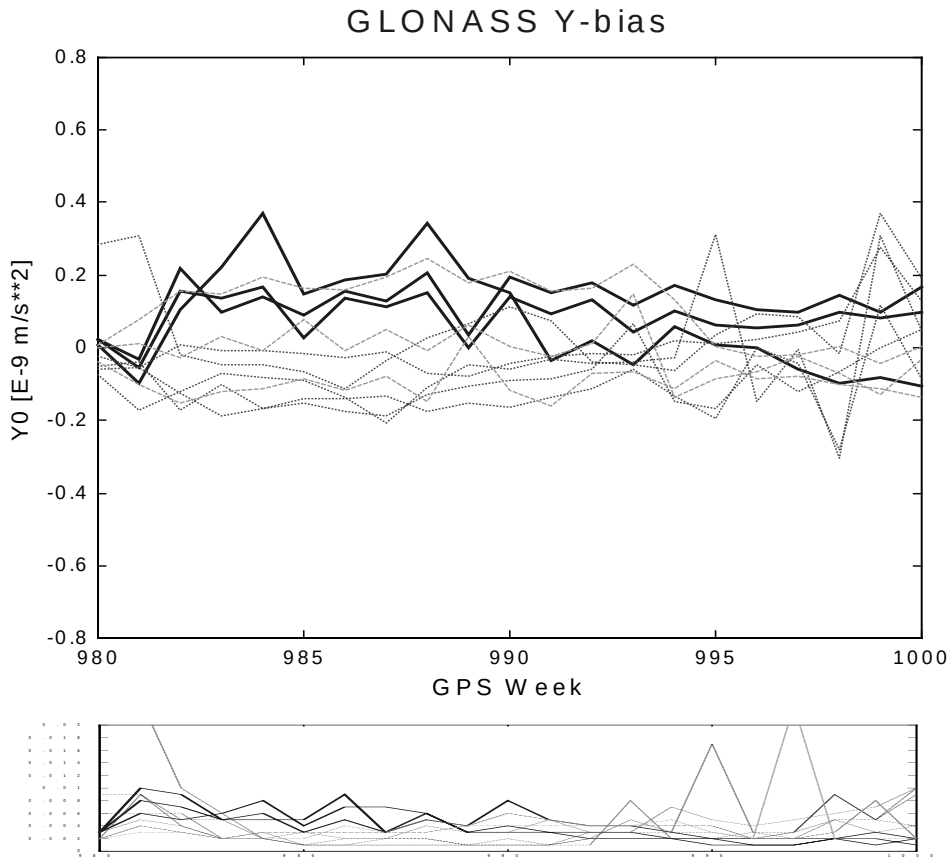

Figures 7a,b. a_{Y0} ; rms (a_{Y0})

In the case of $\beta \to 0$ (eclipse) a perturbation in the sun-satellite direction causes oscillations of the radial and along-track component. A perturbation due to the Y-bias consists of an along-track and an out-of-plane component. Plane II gets into the eclipse phase in Week 1001.

Figures 8 and 9 describe the variations of the periodic terms in the X-direction. Again the time just before and after Week 988 is of particular interest. Large (but worse determined) fluctuations of the estimates dominate the graphic. The vertical axes of figures 8b and 9b vary from 0 to $4 \cdot 10^{-9}\, m/s^2$. Excluding plane II from our considerations, variations of about $3 \cdot 10^{-9}\, m/s^2$ are visible between satellites within the same orbital plane.

The discussed situation in Week 988, documented in the weekly summary file of the Combined GLONASS Orbits, led to a considerable degradation of the orbit quality in all Center submissions for all plane II satellites. Refined models have to be investigated to overcome this difficult (half a year periodic) geometry .

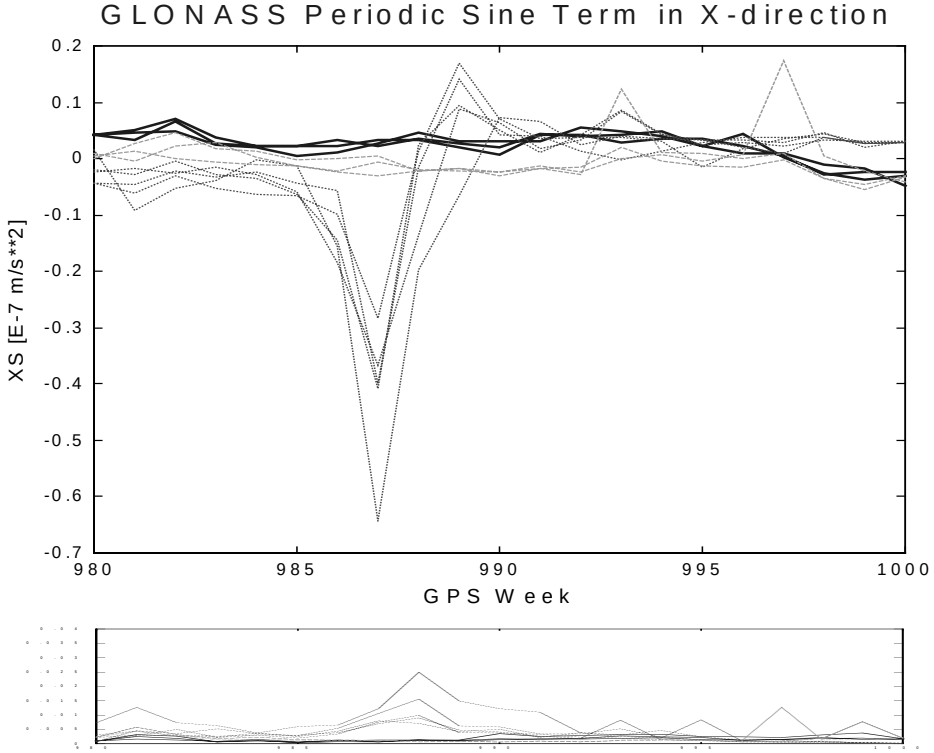

Figures 8a,b. a_{XS} ; rms (a_{XS})

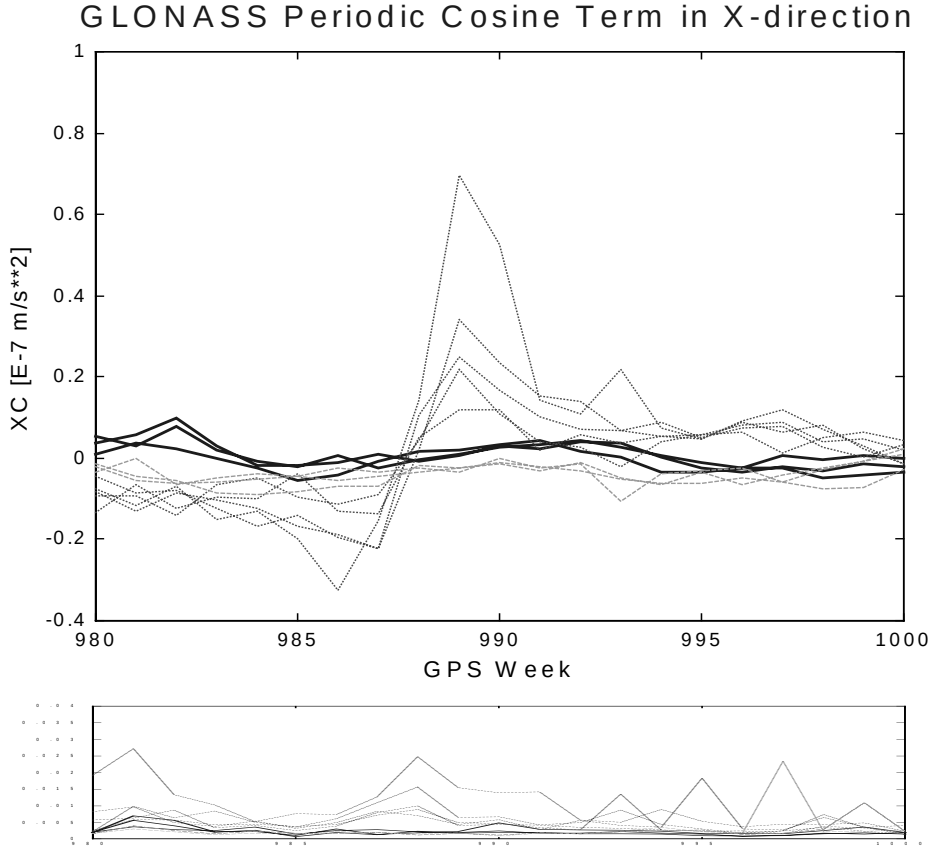

Figures 9a,b. a_{XC} ; rms (a_{XC})

Improved Weighting Scheme

As mentioned, the weighting scheme in use favors Center solutions based on increased arc-lengths (5 or more days). (Springer and Beutler, 1993) presented a scheme which obtains the combined orbits as daily weighted averages of the satellite positions computed by different Analysis Centers. Daily Center and satellite-specific weights are required. The (slightly changed) principles of this algorithm can be characterized as follows:

Again, the orbits will be combined in the ITRF system. The effect of less precise orbit estimates can be reduced by applying Center-specific weights which have to be determined every day for all processing Centers. Therefore an unweighted mean for each satellite position $\vec{x}_s^{(1)}$ has to be computed and Center (Center i , Center Weight / Day p_i) and satellite-specific (Satellite s , Satellite Weight / Center / Day p_{si}) weights are calculated from the rms errors of a Helmert transformation between $\vec{x}_s^{(1)}$ and the individual Center solutions $\vec{x}_{si}$.

$$\vec{x}_s^{(1)} = \frac{\sum_{i=1}^{n} \vec{x}_{si}}{n} \qquad T_7(\vec{x}_s^{(1)} \Leftrightarrow \vec{x}_{si}) \;\Rightarrow\; p_i = \frac{1}{\sigma_i^2},\; p_{si} = \frac{1}{\sigma_{si}^2}$$

The Center-specific weights are used to compute a weighted mean for each satellite position and another Helmert transformation is performed between $\vec{x}_s^{(2)}$ and the Center solutions (this time weighted, using the satellite-specific weights).

$$\vec{x}_s^{(2)} = \frac{\sum_{i=1}^{n} p_i \vec{x}_{si}}{\sum_{i=1}^{n} p_i} \qquad T_7(\vec{x}_s^{(2)} \Leftrightarrow p_{si}\vec{x}_{si}) \;\Rightarrow\; \Delta\vec{x}_i, R_i, m_i$$

This step results in a shift vector, a scale factor and 3 rotations (per Center) used to calculate the weighted (p_i) IGX orbit $\vec{x}_s^{(3)}$.

$$\vec{x}_s^{(3)} = \frac{\sum_{i=1}^{n} p_i m_i R_i (\vec{x}_{si} + \Delta\vec{x}_i)}{\sum_{i=1}^{n} p_i}$$

Summary and Outlook

We may summarize, that IGEX Analysis Center solutions, comprising precise orbits for 11-15 active GLONASS satellites (note that 3 more satellites were launched in December 1998), are consistent at the 20-30 cm level. An improvement of that orbit quality is actually hindered to a certain extent by the low number and sparse distribution of tracking sites.

Starting in Week 1006 the calculation of combined GLONASS Orbits will be based on a different strategy. Similar to the GPS orbit combination of the IGS, the new model calculates daily satellite- and Center-specific weights from the deviation of the Center submissions from the unweighted mean orbit. This reduces the heavy dependence on the long-arc performance. Moreover, it is a first step towards the integration of GLONASS into IGS operations and programs.

An improved timeliness in the availability of the combined IGX orbits (available within 3 weeks of observation), to provide substantial contributions to the ITRF, and the computation of precise clock information are the stated objectives for the first months of the upcoming GLONASS Pilot Service.

References

Beutler, G., J. Kouba, T. Springer (1995). Combining the Orbits of the IGS Analysis Centers, *Bulletin Geodesique*, Vol. 69, pp. 200-222.

García, C., T. Martin-Mur, J. Dow, I. Romero (1999). GLONASS Data Analysis at ESA/ESOC, *Proceedings IGEX-98 Workshop,* Nashville, Sept. 13-14, 1999, JPL.

Kuang, D., Y. Bar-Sever, W. Bertiger, K. Hurst, J. Zumberge (1999). Determination of GLONASS Satellite Orbits at JPL – Approach and Results, *Proceedings IGEX-98 Workshop,* Nashville, Sept. 13-14, 1999, JPL.

Noll, C., M. Rothacher, G. Beutler, L. Mervart (1995). The Perturbation of the Orbital Elements of GPS Satellites Through Direct Radiation Pressure, in *IGS Workshop Proceedings on Special Topics and New Directions,* G.Gendt and G. Dick, Eds., pp. 152-166, Geoforschungszentrum, Potsdam, Germany.

Slater, J.A., P. Willis, G. Beutler, W. Gurtner, W. Lewandowski, C. Noll, R. Weber, R.E. Neilan, G. Hein (1999). The International GLONASS Experiment (IGEX-98): Organization, Preliminary Results and Future Plans, in *Proceedings ION GPS-99*, Nashville, Sept. 13-14, 1999, pp. 2293-2302, Inst. of Navigation.

Springer, T., G. Beutler (1993). Towards an Official IGS Orbit by Combining the Results of All IGS Processing Centers, in *Proceedings 1993 IGS Workshop*, pp. 242-250, Berne, Switzerland.

Springer, T., G. Beutler, M. Rothacher (1998). A New Radiation Pressure Model for the GPS Satellites, in *Proceedings IGS 1998 Analyis Center Workshop*, J. Dow, J. Kouba and T. Springer, Eds., pp. 89-106, ESOC, Darmstadt, Germany.

Weber, R. (1999). Report on the Status of the International GLONASS Experiment (IGEX), in *Proceedings IGS 1999 Analysis Center Workshop*, SIO, La Jolla, California.

Willis, P., J. Slater (1999). International GLONASS Experiment, in *IGS Annual Report 1998*, pp. 38-39, IGS Central Bureau, JPL, Pasadena, California.

Comparison of Precise SLR Orbits of the GLONASS Satellites with Microwave Orbits

Graham Appleby, Toshimichi Otsubo[1] and Andrew Sinclair
NERC Satellite Laser Ranging Facility
Monks Wood, Abbots Ripton, Cambridgeshire PE17 2LS, UK

[1] On leave from Communications Research Laboratory, Tokyo, Japan.

Abstract

In this paper we describe our analyses of satellite laser ranging (SLR) data to the GLONASS satellites obtained by the global tracking network during the IGEX-98 main and extended campaigns. We look in some detail at the measurement process to the spacecraft, and conclude that detailed treatment is required of the retroreflector array correction in order accurately to refer the range measurements to the centre-of-mass (CoM) of the satellites, and to avoid producing orbital information biased with respect to the true orbit. We compare our orbital arcs to published microwave-based orbits, and show that those orbits appear to be accurate radially to about 20cm.

Orbit Determination

For this investigation we analysed laser range observations taken by the global tracking network, during the period January to July 1999 to the three GLONASS satellites, GLONASS-70 (slot 4), GLONASS-72 (slot 22) and GLONASS-79 (slot 9). These three satellites were chosen by the IGEX-98 steering committee for continued laser tracking following the end of the main campaign on April 30, 1999. From that date we found that significantly more laser range data for each satellite was generated by the network, presumably in response to the reduced workload relative to the original nine satellites. For our comparison of SLR-derived orbits with microwave-derived orbits, we concentrate on this period of enhanced tracking.

Our force model follows closely the IERS Conventions (IERS, 1996), and uses the JGM-3 gravity field model (Tapley et al., 1996), truncated to degree and order 10, ITRF96 tracking station coordinates and velocities and IERS Earth rotation parameters. Our solar radiation force computation takes account only of the solar panels, assumed oriented normal to the direction to the Sun. The computations were carried out using the SATAN package (Sinclair and Appleby, 1988). During the adjustment of each orbital arc we solved for satellite initial state vector, empirical along-track acceleration, a single scaling factor (coefficient) for the solar radiation force and empirical, once-per-revolution, along-track accelerations. The latter terms tend to absorb deficiencies particularly in our non-gravitational force model, such as the neglect of photon thrust from heated elements of the spacecraft, and solar radiation forces from parts other than the solar arrays. In order to compare during this preliminary stage of the analysis the measured laser range distances with the computed distance of the centre-of-mass of the satellite, we used the value of 151cm for the distance from mass centre to the phase centre of the retroreflector array

(Russian Space Agency, 1999). The satellites were assumed nominally oriented such that the vector from their mass centres through the centre of the retroreflector array intercepts the centre of the Earth. For this stage of the analysis we fit orbital arcs of duration seven days to the laser range data, beginning on each day of the period. In this way we obtain daily estimates of our satellite force-model parameters, and can also monitor the consistency of our solutions. For the three satellites we obtain post-fit residual RMS values of about 6-10cm.

Solutions

Among the parameters of interest derived from these solutions are smoothed daily estimates of the solar radiation coefficient, time series of which are given in Figure 1 for GLONASS-70 and GLONASS-79. The results for GLONASS-72 were very similar to those of GLONASS-70, and are not shown here. The results for GLONASS-70 are seen to be fairly smooth and featureless, with a long-term variation due probably to model deficiencies as the orbital plane rotates relative to the Sun. However, the results for GLONASS-79 show a more dramatic, 40-day excursion from the smoothly varying series of values. A possible explanation for this anomalous period, which does not coincide with an eclipse season for the satellite, is that the solar panels were at that time not aligned optimally with the Sun, which may indicate an attitude control problem.

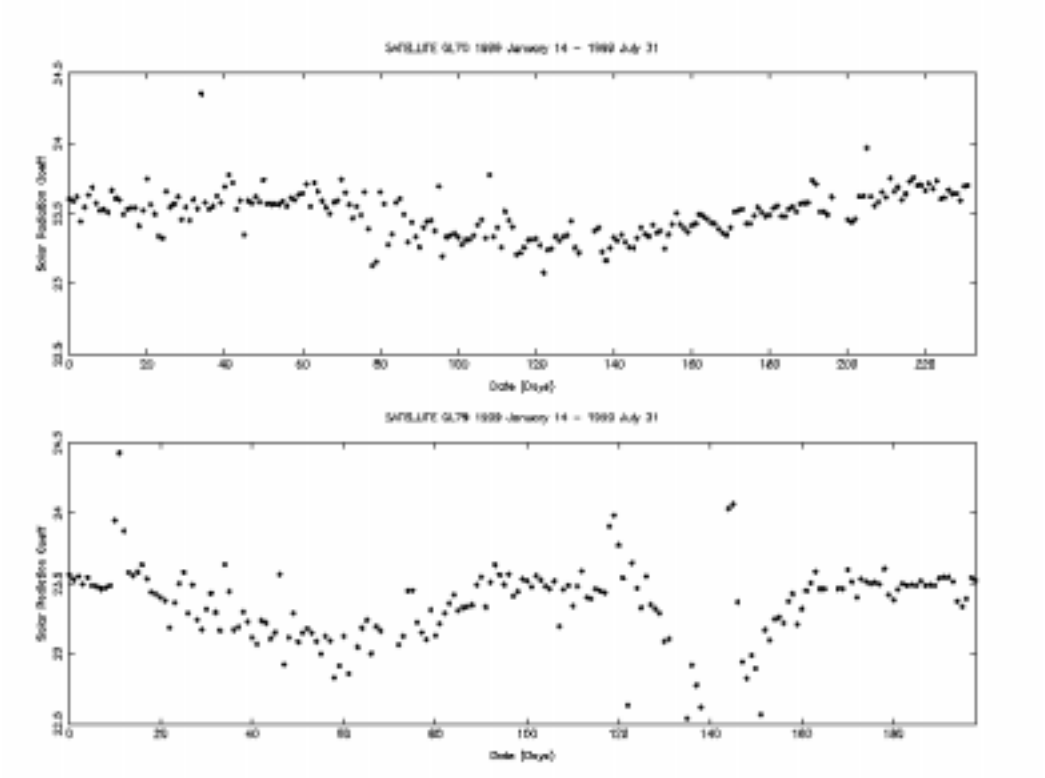

Figure 1. Smoothed daily estimates of solar radiation coefficients for GLONASS70 and –79.

Post-Fit Range Residuals

We found that on average the post-fit range residuals from our 7-day orbital arcs for many of the tracking stations were consistently and significantly biased towards negative values. On further investigation it became clear that the magnitude of the bias depended on the type of ranging system making the measurements. The systems that are designed to work at high levels of return, which include the NASA tracking stations, consistently produced mean values of about -3 cm, whereas for systems working at or close to single-photon levels of return the residual mean values were close to zero. For example, for the high-power systems MOBLAS 4 at site 7110, Monument Peak and MOBLAS 5 at site 7090, Yaragadee, the means of the range residuals over the period May 1 to July 31,1999 were -2.5 ±0.2 cm and -3.0 ±0.2 cm, respectively. By contrast, the mean value for the 7840 Herstmonceux system, which works strictly at the single-photon level, was -0.9 cm. In view of our previous experience with system-dependent range bias induced by the extended nature of retroreflector arrays, the so-called satellite signature effects (Otsubo et al., 1999; Appleby, 1993), a fuller investigation seemed warranted.

The GLONASS Retroreflector Arrays

The GLONASS retroreflector array is a planar array consisting of 396 fused quartz cube-corners, arranged over a region of size 101 by 101cm. The exact arrangement of the cube-corners has recently been provided to the laser community by Dr. Vladimir Vassilyev of the Russian Space Agency (Kunimori, 1999), and confirms that they are arranged pseudo-randomly over the nadir-facing base of the spacecraft, and positioned around various radio antennae. As stated previously, the phase centre of the array is at a distance of 151cm from the CoM of each satellite. For the following discussion, we assume this general pseudo-random arrangement of the cube-corners. A more detailed study taking into account the position of each one will be made in the future.

Array-Induced Range Bias

An SLR system capable of detecting single-photons reflected from the array will, in the course of many such events during an observing session, receive photons that have been reflected from many of the cube-corners of the array, and will therefore 'map' the spatial distribution of the array. By contrast, a system capable of receiving a large number of photons from each transmitted laser pulse will tend preferentially to detect photons from the leading edge of the return pulse. Therefore, for such a system, most measurements will be to the part of the array closest to the system at the time of the observation. We therefore have the potential for a system-dependent bias, which will vary depending upon the geometrical circumstances during the ranging measurements; if the satellite appears close to the zenith such that the laser pulse illuminates the array at near-normal incidence, the system-dependent bias will be minimised. If however, the satellite is at a low elevation above the horizon, say at 40^o, then the angle of incidence will be greater than 10^o. In this configuration the outer regions of the planar array will be closer to the ranging system by up to10cm compared to the centre regions. The single-photon systems will continue to obtain returns from all regions of the array, and thus on average measure

the distance to the centre of the array. But the multi-photon systems will tend to measure short, by up to 10cm in this example. The effect is illustrated in Figure 2, which traces the path of a laser pulse striking the array of half-diameter R at an angle ϕ from normal. In the diagram, ray 'O' shows the measured range to the part of the array nearest the tracking station, whilst ray 'C' shows the computed distance from the station to the centre of the array. The difference 'Observed range minus Computed range' is then - Δx, where Δx is given simply by R Sin ϕ.

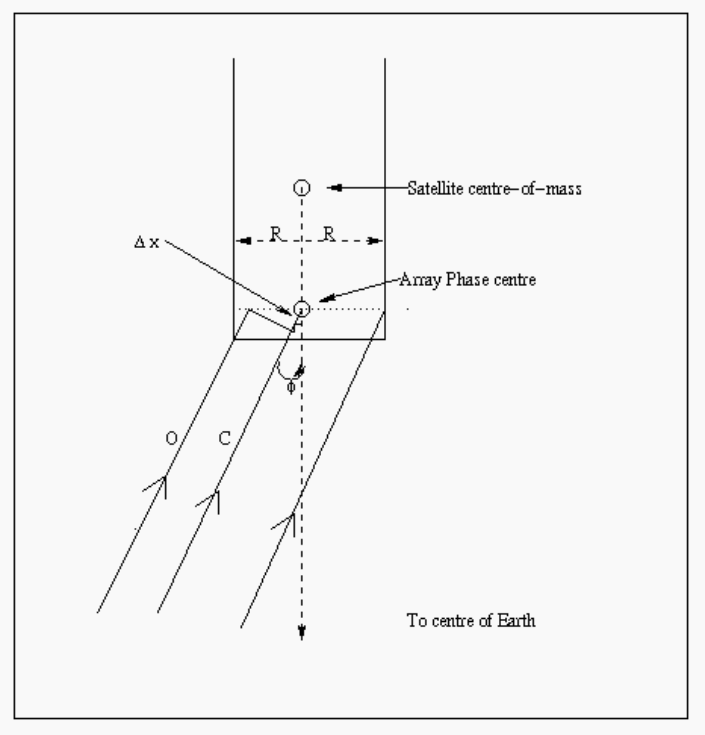

Figure 2. Schematic of laser range measurement process to flat array on GLONASS

Experimental Evidence

We can examine and experimentally verify the reality of this effect by using the versatility of the Herstmonceux ranging system. In standard mode, whereby the return energy is kept at the single photon level, we might expect the precision of observations made when the satellite is near to the zenith to be similar to that for observations to a flat calibration target board. For observations away from the zenith, we expect to see an increase in observational scatter (decrease in range precision) as a function of decreasing satellite elevation, as the planar array presents a 'deeper' reflective surface. This is indeed the case, the range precision varying during a pass from about 15mm at high elevation to 80mm at low elevation. The effect is shown in Figure 3, where each point in the scatter plot represents a single range measurement to GLONASS-79, from which has been subtracted a fitted smoothing function such that the mean over all such residual values for the pass is close to zero. The residuals are clearly more scattered (RMS=76mm) at the

beginning and end of the time period, when the satellite elevation was about 35°, and much less so (RMS=25mm) during the central period of the pass, when the elevation reached 76°.

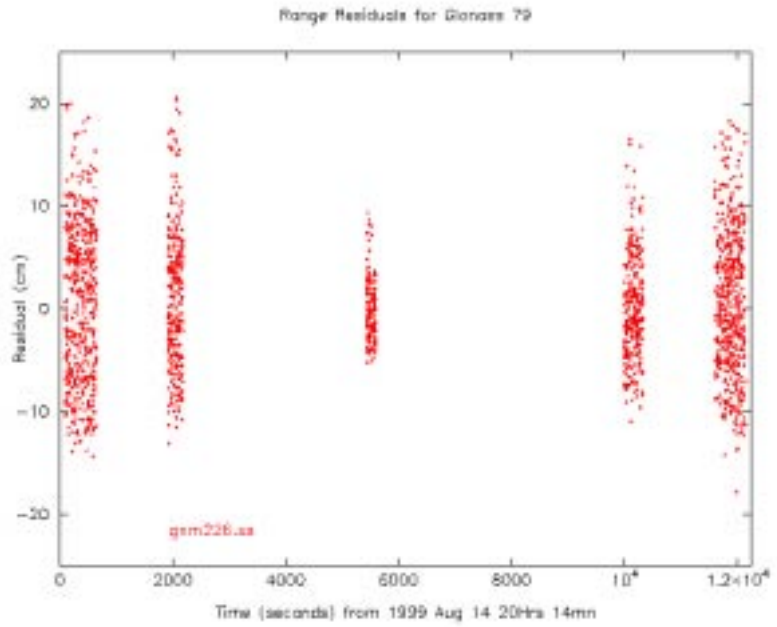

Figure 3. Range residuals from a pass of GLONASS-79 observed at 7840 Herstmonceux.

Having demonstrated that the planar array causes a variation of the scatter in range residuals for a single-photon system, we can now experimentally verify our hypothesis that multi-photon systems systematically measure ranges shorter than the distance to the centre of the array. The system at Herstmonceux was used to make range measurements to GLONASS-72 and at intervals during the pass the return energy was switched from single to multi-photon, using filters in the receive path. It was found that, relative to the measurements made at single-photon levels, the mean range deduced from the higher-energy observations was up to 4cm shorter, the magnitude of the effect depending upon the altitude of the satellite, and hence on angle ϕ. Correspondingly, the observational scatter was less for the multi-photon data as the influence of the effective array size on the error budget decreased.

Discussion

It is this mechanism that we propose to explain the consistently negative range residuals for the multi-photon systems, and near-zero mean values for the single-photon systems in our 7-day global arcs. Given the dominance of multi-photon systems in the global network, we also suggest that this effect might at least partially explain the reported radial offset of some 5cm between microwave-based orbits of the GLONASS satellites

and direct laser range measurements (Ineichen et al., 1999). We note that for our method of orbit determination, whereby we solve for the orbital state vector and various empirical parameters, a mean range bias of several centimetres cannot all be absorbed by the solution, and is reflected in a non-zero residual mean. Were we to solve for additional parameters that would allow a change in the scale of the system, such as a correction to GM or a series of system range-bias values, the solution would adjust such that the range residuals did have zero mean. This emphasises the need both to minimise system range bias, and also to understand fully the interaction between each ranging system and the satellite retroreflector arrays.

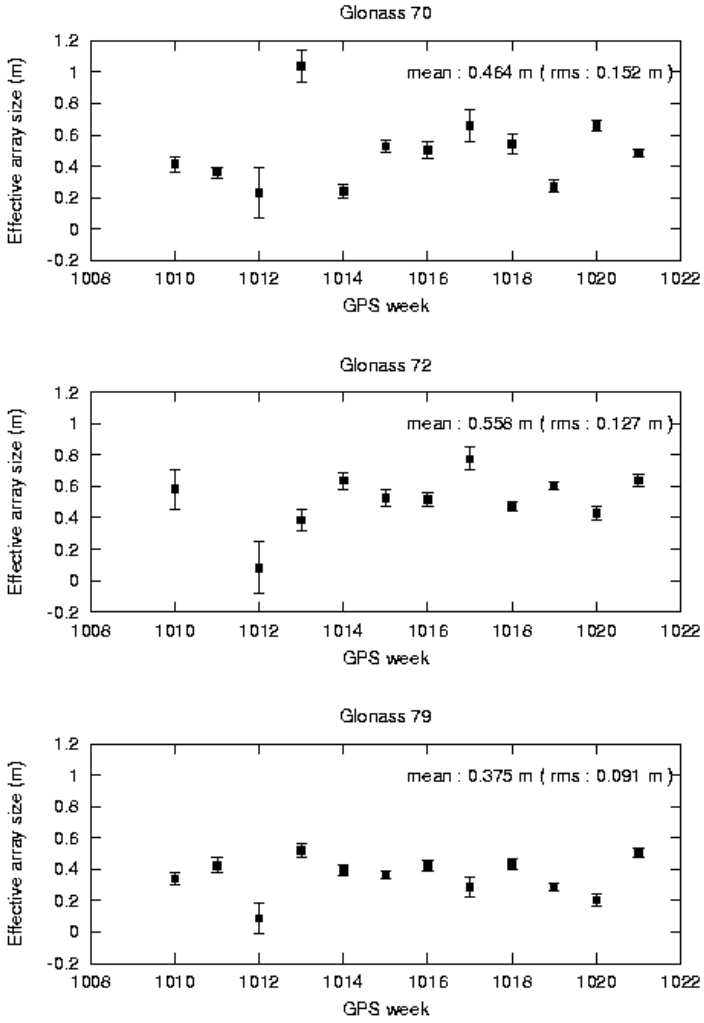

Figure 4. Individual estimates of effective sizes of retroreflector arrays on three satellites.

Solutions for Effective Array Size

With this insight into the expected system-dependent array-effects, we now use our 7-day orbital arc determinations to solve for a further parameter, the effective array size. For each arc and for each of the three satellites, we used observations from the multi-photon

systems to estimate the average distance of the observational point from the centre of the arrays on the assumption that those systems tend to range to the outer regions of the arrays. We find that the post-fit range residuals are now close to zero.

Our array-size estimates are shown in Figure 4 for the period May-July, 1999 where individual 7-day results and their RMS error bars are plotted for each satellite against the date expressed as GPS week.

If our hypothesis is true that multi-photon systems preferentially range to the outer regions of the retroreflector, our estimates of effective array sizes using that data should be close to half the size of the planar array, that is about 50cm. The individual results for GLONASS-70 and -72 are somewhat scattered, with mean values of 46cm and 56cm respectively and RMS errors of about 15cm. The results for GLONASS-79 are more consistent between each solution, and the mean value of 38cm is not significantly less than the results from the other two satellites. We consider that the overall mean for the effective array size of 46cm (RMS 12cm) is in good agreement with the true size of the array, given the following two limitations of this study. In the derivation of the solutions we have no information on the 'azimuthal' attitudes of the planar arrays, and thus our results are averaged over all the orientations that happen to be presented. For instance, should an observation be made to a corner of the array, its linear distance to the array centre would be more than 70cm. In comparing our result to the known size of the arrays, we also have assumed that the multi-photon systems always effectively range to the part of the array closest to the station. At times when the two-way link is less than maximal, this may not be true, and observations from 'deeper' within the array may be obtained. However, in the absence of accurate information on either of these points, we consider that our method of solving for effective array size is the best way to allow for this effect. Certainly, if no allowance is made for the array size, it is likely that biased orbital information will result.

Comparison with CODE Microwave Precise Orbits

We now use our SLR-derived orbits to investigate the quality of the microwave orbits of the three satellites available routinely from the Centre for Orbit Determination in Europe (CODE), located in Berne, Switzerland. The CODE precise orbits are available in SP3 Format, and give the coordinates of the satellites at 15-minute intervals referred to the Greenwich meridian and true equator of date, with respect to the GPS timescale. The CODE daily orbits are determined from the mid-day of a 5-day orbit, for which post-fit residual RMS values are usually better that 20 cm (Ineichen et al., 1999). From our best-fit orbit we generate 15-minute geocentric ephemerides in the J2000 reference frame and with UTC time argument. We convert the SLR positions and velocities to the terrestrial frame, and at UTC times corresponding to the CODE epochs such that a direct comparison can be made between the independent sets of rectangular coordinates. We then resolve the differences between the coordinates into along-track, across-track and radial directions.

Results

We have carried out this analysis for the three satellites for the period May 16 to July 10, 1999.

A typical example of the results is given in Figure 5, where the 15-minute differences between the SLR and CODE orbits for GLONASS-72 (Slot 22) are plotted for the 7-day period of a single SLR orbital arc, determined for the period May 16-22, 1999. The clear once-per-revolution periodic signatures in the differences are typical of orbit comparisons, and indicate small differences between the orbital reference frames. The results imply that maximum differences between the orbits are of order 1m, the radial components agreeing to better than 30cm. The mean differences in the radial and across-track components are close to zero, but the along-track differences appear to have a systematic negative bias. Interestingly, the comparisons show small daily discontinuities at the level of a few centimeters between the orbits. Since the continuous 7-day SLR orbit cannot introduce such discontinuities, we interpret them as indicating an excellent level of agreement of a few centimeters between the daily CODE orbits, which are essentially independent from one day to another.

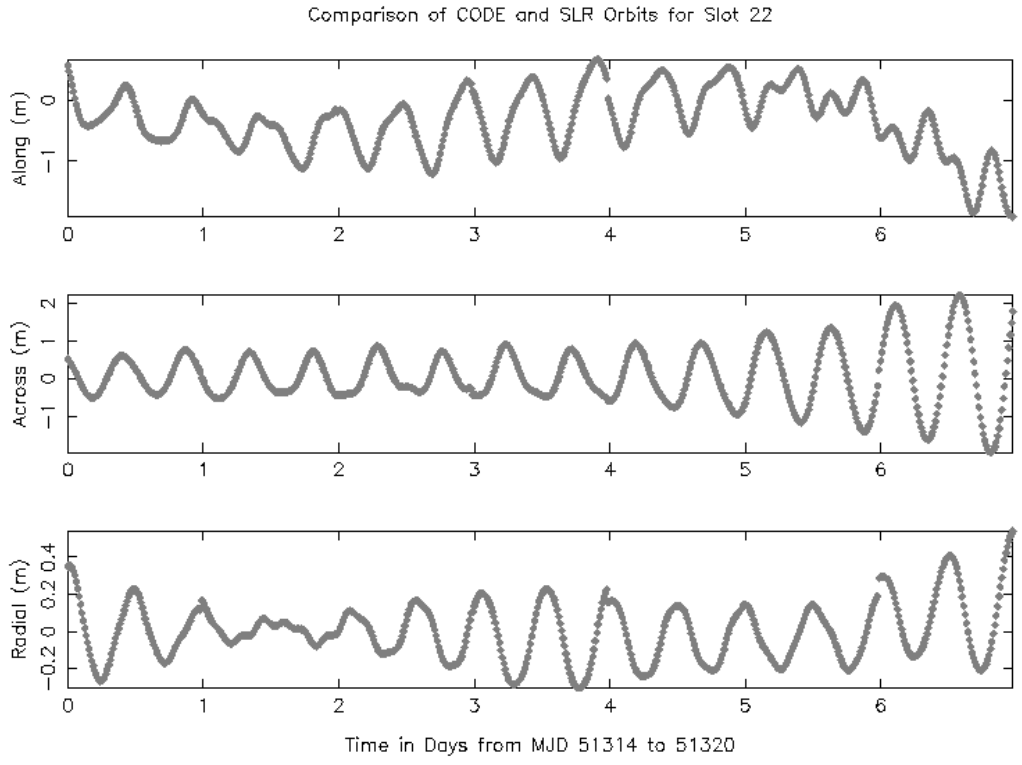

Figure 5. Comparison of SLR-derived and microwave (CODE) orbits for GLONASS-72.

Numerical results for all three satellites are shown in Table 1, where we give for each 7-day SLR orbital arc the mean and RMS values in metres of the components of the

differences from the daily CODE orbits. Also given in the Table for each satellite for the whole period are the mean values of differences in along-track (A/L), across-track (A/C) and radial (Rad) directions. Most of these overall mean values are close to zero, but with some indication that the along-track differences for GLONASS-70 (slot 4) have a negative bias. The RMS values of the differences confirm the earlier indication that the CODE and SLR orbits agree at the 1m level in along- and across-track directions, and at the 20cm level in the radial direction.

Table 1. Comparisons between 7-day SLR Orbits and CODE Precise Orbits

GLONASS-70(Slot 4)

Date	A/L	rms	A/C	rms	Rad	rms
990516	0.134	1.194	0.060	0.254	-0.015	0.183
990530	-2.093	2.160	-0.131	2.667	-0.023	0.413
990606	-0.630	0.909	0.085	2.152	-0.035	0.211
990613	0.503	0.823	0.067	0.667	-0.003	0.161
990620	-0.445	0.885	-0.088	1.059	0.043	0.106
990627	-0.311	0.472	-0.054	1.375	0.046	0.112
990704	-0.603	1.383	0.065	1.582	0.019	0.199
Mean	-0.492	1.440	0.001	1.595	0.005	0.222

GLONASS-72(Slot 22)

Date	A/L	rms	A/C	rms	Rad	rms
990516	-0.727	0.662	0.149	1.551	0.007	0.244
990530	1.023	1.249	-0.166	1.972	0.033	0.150
990606	0.660	0.927	0.083	1.257	-0.056	0.132
990613	0.946	1.662	-0.034	0.769	-0.051	0.288
990620	-0.707	1.532	0.028	1.401	0.002	0.277
990627	-0.283	0.416	0.043	1.379	-0.005	0.119
990704	-1.142	1.305	-0.118	1.695	-0.061	0.278
Mean	-0.033	1.445	-0.002	1.477	-0.019	0.227

GLONASS-79(Slot 9)

Date	A/L	rms	A/C	rms	Rad	rms
990516	-0.165	0.379	-0.104	0.766	-0.038	0.126
990530	-0.169	0.973	0.146	2.009	0.072	0.380
990606	0.181	0.739	-0.071	1.460	-0.122	0.376
990613	0.357	0.822	-0.080	0.916	-0.007	0.388
990620	-0.137	0.453	0.127	0.845	0.094	0.232
990627	0.070	0.364	0.023	1.602	0.075	0.213
990704	-0.608	0.816	-0.030	1.813	-0.016	0.136
Mean	-0.067	0.746	0.002	1.425	0.008	0.294

Conclusion

The main results of this investigation may be summarised as follows.

The International GLONASS Experiment IGEX-98 has resulted in a valuable data set of SLR observations for analysis. We have analysed observations obtained principally

during the extended campaign, and find that they may be fit to a precision of 6-10cm RMS for a 7-day orbital arc.

The large planar retroreflector arrays on the satellites can induce ranging-system-dependent measurement bias at the level of several centimeters. The presence of this bias may to some degree explain the reported radial offsets between laser-based and microwave-based orbits. Proper treatment of the array bias requires further information on the arrangement of the corner-cube reflectors, and a knowledge of the attitude of the array during the ranging process.

The daily microwave orbits computed by the Centre for Orbit Determination in Europe fit our laser-based orbits to better than 20cm RMS radially, and at the level of one metre in along-track and across-track directions. The degree of continuity between successive daily CODE orbits appears to be at the level of a few cm.

Acknowledgements

The NERC Satellite Laser Ranging Facility at Herstmonceux and Monks Wood, UK, is operated by the Natural Environment Research Council, which funds the Facility in collaboration with the British National Space Centre and the UK Ministry of Defence. We thank Philip Gibbs from the operational team at Herstmonceux for carrying out the non-standard ranging experiments.

References

Appleby, G.M (1993) Satellite Signatures in SLR Observations, *Proceedings 8th International Workshop on Laser Ranging Instrumentation*, NASA Conf. Publ. 3214.

IERS (1996). IERS Conventions, IERS Technical Note 21, D.D. McCarthy (ed.), Observatoire de Paris.

Ineichen, D., M. Rothacher, T. Springer, G. Beutler (1999). Results of CODE as an Analysis Centre of the IGEX-98 Campaign, *Proceedings IGEX-98 Workshop*, Nashville, Sept. 13-14, 1999, JPL.

Kunimori, H (1999). Private Communication.

Otsubo, T., J. Amagai, H. Kunimori (1999). The Centre-of-Mass Correction of the Geodetic Satellite AJISAI for Single-Photon Laser Ranging, *IEEE Transactions on Geoscience and Remote Sensing,* Vol. 34, No. 2, pp. 2011-2018.

Russian Space Agency (1999). Communication to the IGEX-98 participants.

Sinclair, A.T., G.M. Appleby (1988). SATAN: Programs for Determination and Analysis of Satellite Orbits from SLR Data, SLR Technical Note 8, Royal Greenwich Observatory, Cambridge, UK.

Tapley, B.D., M.M. Watkins, J.C. Ries, G.W. Davis, R.J. Eanes, S.R. Poole, H.J. Rim, B.E. Schutz, C.K. Shum, R.S. Nerem, F.J. Lerch, J.A. Marshal, S.M. Klosko, N.K. Pavlis, R.G. Williamson (1996). The Joint Gravity Model 3, *Journal of Geophysical Research*, Vol. 101, No. B12, pp. 28029-28050.